Studies on inhibitors of tumor-associated enzymes from marine sponges

（カイメン由来のがん関連酵素阻害物質に関する研究）

A Dissertation Submitted to the Graduate School of Agricultural and Life Sciences
The University of Tokyo in Partial Fulfillment of Requirements for
The Degree of Doctor of Philosophy

January 2013

Laboratory of Aquatic Natural Products Chemistry
Graduate School of Agricultural and Life Sciences
The University of Tokyo

Supervisor: Professor Shigeki Matsunaga

By
Yasufumi Imae

Acknowledgments

I would like to express my heartfelt appreciation to my supervisor, Professor Shigeki Matsunaga, for giving me the chance to join the Laboratory of Aquatic Natural Products Chemistry and to study on this subject as well as suitable advice and encouragement. I also wish to express my appreciation to Associate Professor Shigeru Okada and Assistant Professor Kentaro Takada for their dedicated support and appropriate advice.

I am greatly indebted to Professor Shohei Sakuda, Professor Shuichi Asakawa, and Professor Hideki Ushio for their valuable suggestions.

I would like to thank Dr. Kazuo Furihata of the University of Tokyo for his kind assistance in measuring NMR spectra. I also thank Dr. Yuji Ise of the University of Tokyo for his identification of the sponges.

I sincerely appreciate Dr. Minoru Yoshida, Dr. Akihiro Ito, and Dr. Satoko Maeda of Chemical Genetics Laboratory of RIKEN for lecturing me the methods for purification and inhibitory assay of HDAC1, and for providing me the HDAC1-overexpressing HeLa cells.

I would like to thank the officers and the crew of T/S Toyoshio-maru of Hiroshima University for their assistance in collecting the sponge *Jaspis* sp. I acknowledge Professor Kanji Hori of Hiroshima University for the arrangement of the cruise. I also thank Professor Osamu Arakawa, Mr. Hiroshi Yoshimura, Mr. Yasuhiro Morii, and the crew of T/S Nagasaki-maru of Nagasaki University for their assistance in collecting the sponge *Stelletta* sp.

I am much obliged to the members of the Laboratory of Aquatic Natural Products Chemistry for their generous support. In particular I wish to express my appreciation to Dr. Shuhei Murayama for teaching me general laboratory techniques.

Finally, I am deeply grateful to my family and friends for their great support on my life. Words cannot describe my gratitude.

Table of Contents

Introduction

1. Impacts of Marine Natural Products on Drug Discovery

Around half of the drugs approved for clinical use between 1981 and 2006 are natural products or analogs inspired by them.[1] Despite this successful record, pharmaceutical companies have sought drug candidates not in natural products but in libraries of synthetic compounds.[2,3] This trend is mainly attributed to the difficulties in discovering new natural products with appropriate property as drugs.[3] Many of the promising natural products are obtained in limited quantities, resulting in adversities in isolation, structure elucidation, and mechanism of action studies. Natural products often have complicated structures with lots of chiral centers, which does not only make it difficult to determine the structures, but hamper supply and manufacturing by chemical synthesis. In addition, screenings using crude extracts of natural organisms require dereplication of known compounds which cannot be patented.[3] However, recent improvements in analysis technologies and synthesis techniques have overcome the obstacles.[4,5] With easier access to natural products, drug discovery scientists have reassessed the structural and functional diversity. And now natural products, in particular those from marine organisms, are in their "renaissance" in drug discovery.[2,6] Several drugs originated from marine natural products have been approved in the past few years;[5] for example, ziconotide, trabectedin, and eribulin.

Ziconotide (1)

Ziconotide (also known as ω-conotoxin), a peptide originally discovered in a

tropical cone snail *Conus magus*, was the first marine-derived compound approved in the U.S. in 2004 for the management of severe and chronic pain.[7] Ziconotide potently inhibits the transmission of nerve signals by blocking the N-type voltage-sensitive calcium channels specifically.[8]

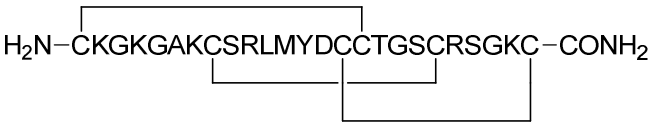

Ziconotide (**1**)

Trabectedin (2)

Trabectedin (or ecteinascidin 743) is a marine natural product isolated from the tunicate *Ecteinascidia turbinate*.[9] Trabectedin is the first marine anticancer drug, which were approved in the European Union in 2007 for the treatment of soft tissue sarcoma.[10] The mode of action has been thought to be covalent modification of DNA, resulting in cell apoptosis.[11]

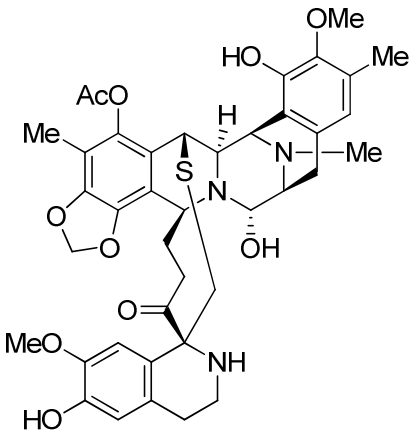

Trabectedin (**2**)

Eribulin (3)

Halichondrin B, isolated from the marine sponge *Halichondria okadai*,[12] was structurally simplified and pharmaceutically optimized to be eribulin.[13] Eribulin mesylate was approved by the U.S. Food and Drug Administration (FDA) in 2010 for the treatment of metastatic breast cancer.[5] Eribulin triggers apoptosis of cancer cells by irreversible disruption of microtubules.[14]

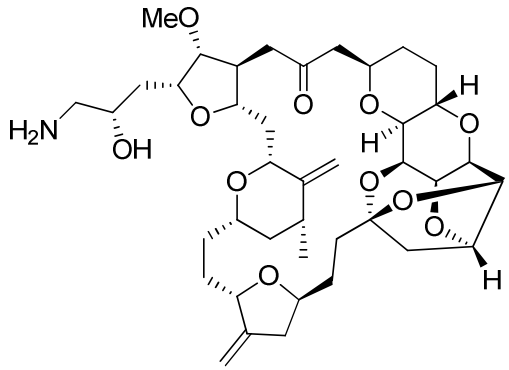

Eribulin (**3**)

Along with the compounds mentioned above, a large number of compounds originated from marine natural products are currently in the clinical pipeline or investigated preclinically as drug candidates,[5] indicating that marine organisms have still been promising sources of drug discovery.

2. Targeting Tumor-Associated Enzymes

Recent advances in molecular biology have revealed the pathways and gene expression underlying carcinogenesis and cancer phenotype. The knowledge have developed a new field of cancer therapy termed molecular-targeted therapy.[15]

Molecular-targeted therapy refers to a type of medication by attacking specific molecular targets such as enzymes or receptors which are overexpressed or highly activated only in tumor cells.[16] Molecular-targeted therapy is, thus, expected to be more effective and less harmful than other therapies using cytotoxic agents which can cause deleterious effects on normal cells.[15] Drugs for molecular-targeted therapy are discovered and developed via target-based screenings, not via phenotypic screenings. 23% of the new first-in-class drugs and 51% of the follower drugs approved between 1999 and 2008 are discovered through target-based screenings,[17] suggesting the efficacy of the strategy of this therapy. No marine natural products or derivatives thereof discovered via target-based screenings have been approved for clinical use.[5] However, the efficacy of the screenings,[17] together with the impacts of marine natural products on drug discovery, suggests a high possibility that target-based screenings using extracts of marine organisms will lead discoveries of novel drug candidates. In this study on seeking new antitumor agents in marine sponges, we focused two molecular targets associated with tumorigenesis, tumor invasion, and metastasis: cathepsin B and histone deacetylase 1 (HDAC1).

2.1. Cathepsin B

Cathepsin B occupies a central node of the proteolytic signal amplification network in mammals.[18] This lysosomal cysteine protease has been documented to be highly upregulated in tumor cells and to play a pivotal role in tumor invasion and metastasis.[19] Cathepsin B is secreted on the tumor cell surface and degrades components of extracellular matrix such as fibronectin in tumor invasion.[20] Cathepsin B also assists

the progress of metastasis by cleaving E-cadherin, a cell adhension protein.[21] In addition to degrading structural proteins, cathepsin B directly activates other proteases such as matrix metalloproteases, which facilitate tumor invasion and metastasis as well.[22] These contributions of cathepsin B for tumor invasion and metastasis, together with the diminution of invasive nature of metastatic tumor cells in the gene knockout and knockdown experiments of this enzyme,[21,23] justify cathepsin B to be a target for anticancer therapy.[19c]

2.2. Histone Deacetylase 1 (HDAC1)

Acetylation and deacetylation of histone proteins are regulated by histone acetyltransferases (HATs) and histone deacetylases (HDACs), respectively.[24] HATs mediate the acetylation of the ε-amino group of the specific lysine residues in the histone *N*-terminal domain.[24a] This modification neutralizes the positive charge on histones and leads DNA transcription.[24a] HDACs remove the acetyl groups to allow interactions between negatively charged DNA and histone proteins, which results in repression of transcription.[24b] Eighteen HDACs have been identified in the human genome and grouped into four classes based on the functions and structures; Zn^{2+}-dependent (class I, II, and IV) and NAD-dependent (class III).[25] HDAC1 is the first identified HDAC and a member of class I HDAC family.[26] The overexpression of HDAC1 has been correlated with abnormal proliferation of tumor cells,[27] dysfunction of the apoptosis pathways,[28] and acquired resistance to chemotherapy.[29] It has also documented that HDAC1 knockdown results in cell cycle arrest,[30] selective apoptosis of tumor cells,[28,30] and inhibition of tumor cell proliferation.[27c,30,31] These observations

indicate that HDAC inhibitors are potential candidates of anticancer drugs.[32] Two HDAC inhibitors have been approved for clinical use, one of which is naturally occurring.

Vorinostat (4)

Vorinostat, or suberoylanilide hydroxamic acid (SAHA), is a synthetic HDAC inhibitor.[33] Vorinostat was the first HDAC inhibitor to be approved by FDA for the treatment of cutaneous T cell lymphoma (CTCL) in 2006.[32d,33] The HDAC inhibitory activity of vorinostat was attributed to the hydroxamic acid, which chelates the zinc ion in the active-site pocket of HDACs to block their activity.[34]

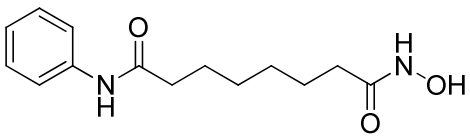

Volinostat (**4**)

Romidepsin (5)

Romidepsin was isolated from the fermentation broth of *Chromobacterium violaceum* as a cytotoxic agent against several human and murine cancer cell lines.[35] Romidepsin demonstrated growth inhibition against tumor cells by arresting the cell cycle at G_1 and G_2/M phases,[36] and exhibited inhibitory activity against HDAC1 and HDAC2.[37] Romidepsin is a stable prodrug; the disulfide bond is reduced inside the cells and the resulting sulfhydryl group interacts with the zinc ion in the active-site pocket of HDACs.[38] Romidepsin was approved by FDA for treating CTCL in 2009.[32d]

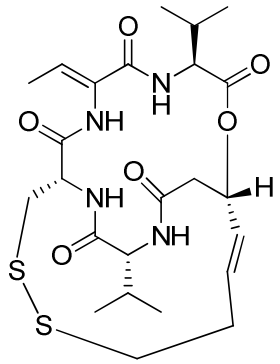

Romidepsin (**5**)

In this study, a search for new inhibitors against tumor-associated enzymes from marine sponges was carried out.

Chapter I describes the isolation, structure elucidation, and cathepsin B inhibitory activity of novel isoquinoline alkaloids jasisoquinolines A and B. Chapter II reports the isolation, structure elucidation of a new lipopeptide ciliatamide D, and the detailed investigation of the configuration of its congener. Chapter III illustrates the isolation, planar structures, stereochemical study, and HDAC1 inhibitory activity of four new compounds.

This study was partly published and submitted for publication.

1. Imae, Y.; Takada, K.; Murayama, S.; Okada, S.; Ise, Y.; Matsunaga, S. “Jasisoquinolines A and B, Architecturally New Isoquinolines from a Marine Sponge *Jaspis* sp.” *Org*. *Lett*. **2011**, *13*, 4798–4801.
2. Imae, Y.; Takada, K.; Okada, S.; Ise, Y.; Yoshimura, H.; Morii, Y.; Matsunaga, S. “Isolation of Ciliatamide D from a Marine Sponge *Stelletta* sp. and a Reinvestigation of the Configuration of Ciliatamide A” *J*. *Nat*. *Prod*. (under review).

Chapter I

Jasisoquinolines A and B, Architecturally New Isoquinolines, from a Marine Sponge *Jaspis* sp.

1. Introduction

In the screening of the extracts of marine sponges for cathepsin B inhibitors, the extract of the marine sponge *Jaspis* sp. collected at Oshimashinsone (Figure 1-1) exhibited potent inhibitory activity. Bioassay-guided fractionation of the extract furnished two architecturally new isoquinolines, jasisoquinolines A (**1-1**) and B (**1-2**), together with known sponge alkaloids schulzeines A (**1-3**) and C (**1-4**).[39,40] Their structures were determined by a combination of spectroscopic analyses and chemical methods. This chapter describes the isolation, structure elucidation, and the enzyme inhibitory activity of the compounds.

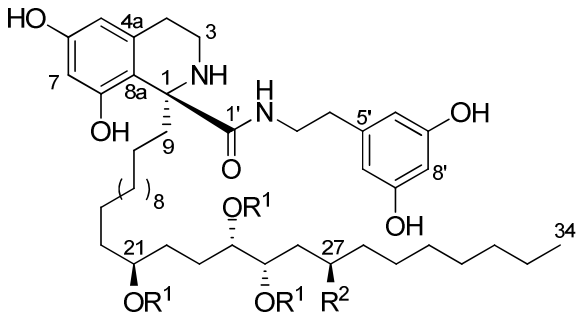

1-1 (R^1 = SO_3Na, R^2 = Me)
1-2 (R^1 = SO_3Na, R^2 = H)

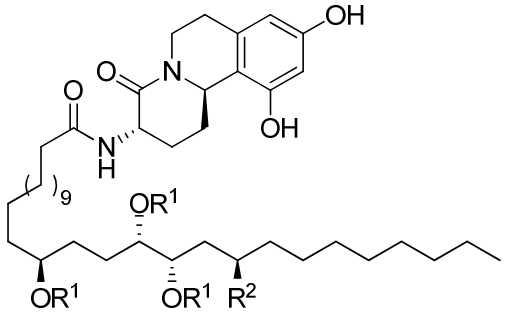

1-3 (R^1 = SO_3Na, R^2 = Me)
1-4 (R^1 = SO_3Na, R^2 = H)

2. Results and Discussion

2.1. Extraction and Isolation

The MeOH and EtOH extracts of the marine sponge (400 g, wet weight) were combined and subjected to solvent partitioning, silica gel column chromatography, ODS flash chromatography, and RP-HPLC sequentially (Figure 1-2) to afford jasisoquinoline A (**1-1**, 2.0 mg) and jasisoquinoline B (**1-2**, 0.7 mg), together with the known schulzeines A (**1-3**, 4.0 mg) and C (**1-4**, 1.5 mg).[39,40]

Figure 1-1. *Jaspis* sp. collected at Oshimashinsone.

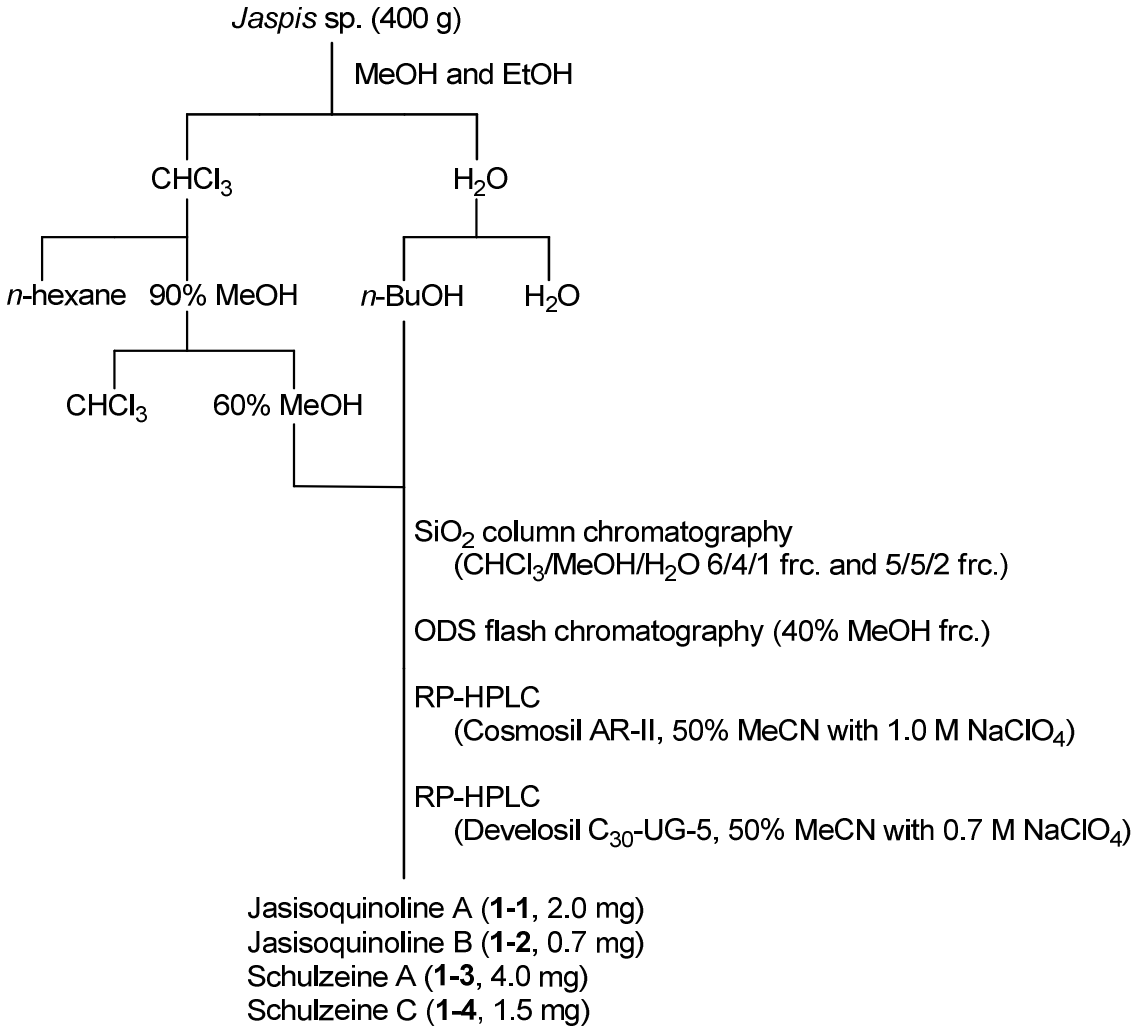

Figure 1-2. Isolation procedure of jasisoquinolines and schulzeines.

2.2. Structure Elucidation

Jasisoquinoline A (**1-1**) had a molecular formula of $C_{45}H_{71}O_{17}N_2S_3Na_3$ as determined by HRFABMS. Two fragment ion peaks due to desulfation (*m*/*z* 951 and 849) in the negative FABMS suggested the presence of three sulfate groups, because the latter ion was presumed to contain one negatively charged sulfate group.[41] An analysis of the ^{1}H NMR data in combination with the HSQC spectrum showed the presence of

five aromatic protons, three oxygenated methines, two nitrogenous methylenes, one doublet methyl, one triplet methyl, and a large methylene envelope (Table 1-1 and 1-2). One aromatic resonance integrated for 2H (δ 6.10, H-6' and H-10') was *meta*-coupled to another aromatic signal (δ 6.12, H-8'), suggesting the presence of a 5-substituted resorcinol. In the HMBC spectrum these aromatic protons were correlated to oxygenated aromatic carbons (δ 159.4, C-7' and C-9') and a carbon at δ 142.1 (C-5'); the latter was connected to a 2-substituted ethyl group. The substituent was shown to be a nitrogen on the basis of the ^{1}H and ^{13}C chemical shift data (δ_C 41.9, C-3'; δ_H 3.51 and 3.43, H_2-3'; Figure 1-3a, substructure **A**). The remaining aromatic signals were *meta*-coupled to each other. Interpretation of the COSY and HMBC data demonstrated the presence of a 4,5-disubstituted resorcinol moiety. This resorcinol moiety was also linked to a 2-substituted ethyl group, the substituent being assigned as a nitrogen on the basis of the ^{1}H and ^{13}C chemical shifts of the methylene group (δ_C 40.9, δ_H 3.39 and 3.03, substructure **B**). Substructure **C** encompassed three oxymethines, one branched methyl, and six methylenes. The planar structure of this moiety, which was identical to a partial structure of schulzeine A (**1-3**), was assigned by analysis of 2D NMR data (Figure 1-3a). The coincidence of the ^{1}H and ^{13}C chemical shifts suggested the identity of the relative configurations of these units.

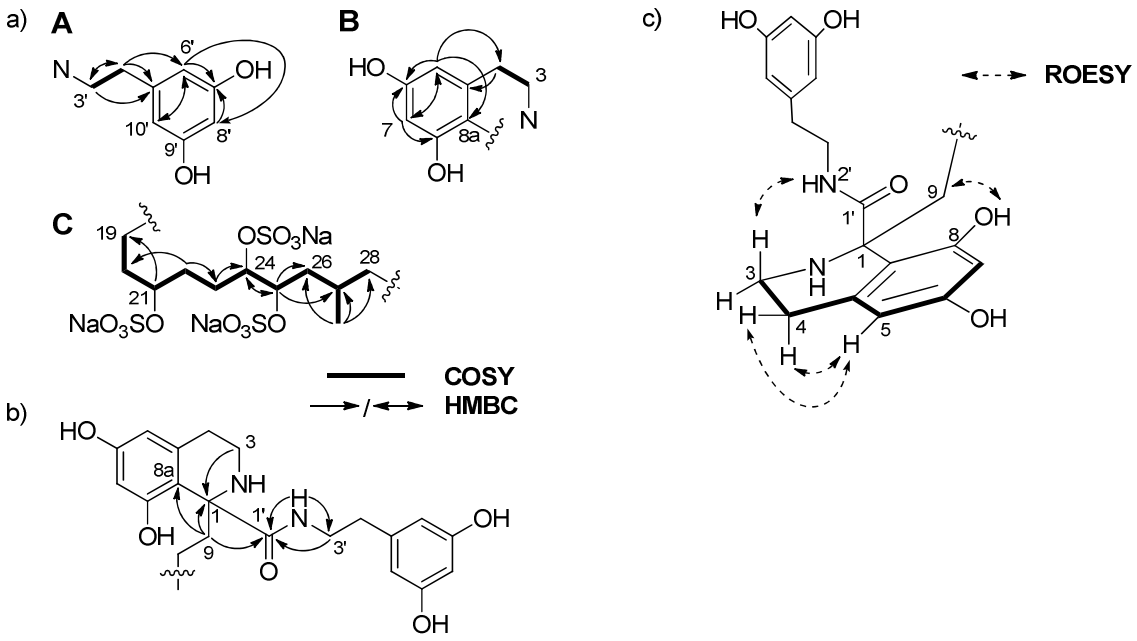

Figure 1-3. Partial structures of jasisoquinoline A (**1-1**).

There was a pair of methylene protons (H_2-9) coupled only to another pair of methylene protons (H_2-10). In the HMBC spectrum H_2-9 was correlated to a nitrogenous quaternary carbon (C-1), an aromatic carbon (C-8a), and a carbonyl carbon (C-1'). Additional HMBC correlations from H_2-3 to C-1, and NH-2' and H_2-3' to C-1' demonstrated the formation of an isoquinoline ring by incorporating C-1 to which was attached C-9 and C-1' amide carbonyl carbon (Figure 1-3b). ROESY cross-peaks between NH-2' and H-3ax, between 8-OH and H_2-9, and between H_2-4 and H-5 supported the structure of the isoquinoline moiety (Figure 1-3c).

Scheme 1-1. Chemical Degradation of Jasisoquinoline A (**1-1**)

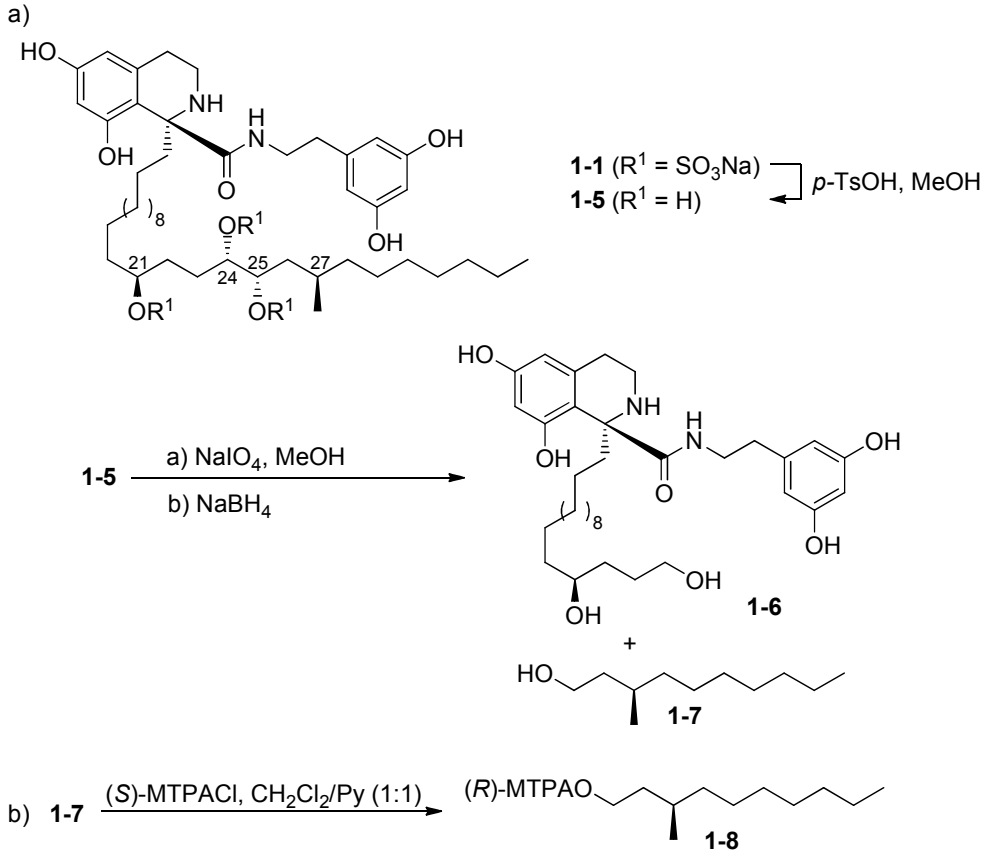

There remained one terminal methyl and 13 methylene carbons unassigned. Therefore, substructure **C** should be placed in the middle of a long alkyl chain emanating from C-9. The location and orientation of substructure **C** in the alkyl chain was determined by taking advantage of the presence of a vicinal disulfate.[39] Sulfate esters in jasisoquinoline A (**1-1**) were removed with *p*-TsOH,[42] and the resulting triol was oxidized with $NaIO_4$ (Scheme 1-1a). The product was reduced with $NaBH_4$ to furnish diol **1-6** and 3-methyldecanol (**1-7**). The FABMS data for **1-6** [*m*/*z* 601 $(M + H)^+$] were consistent with the oxidation at C-21, C-24, and C-25 in **1-5**. This assignment was supported by the tandem FABMS data for **1-5** (Figure S1-18–1-22). The absolute configuration of C-27 was determined by inspection of the ^1H NMR data for **1-7** after

converting to the (*R*)-MTPA ester **1-8** (Scheme 1-3b).[43] The ^{1}H NMR spectra for the (*S*)- and (*R*)-MTPA esters of 3-methyl-1-alkanols give characteristic patterns for the oxygenated methylene protons by reflecting the configuration of the methyl branch.[39,44] The ^{1}H NMR spectrum of **1-8** was consistent with the corresponding ester of the 3*R*-alkanols (Figure S1-16 and S1-17), indicating the 27*R* configuration. Because the relative configuration of the C-21 to C-27 portion was suggested to be identical to that of the corresponding portion of **1-3**, configurations at C-21, C-24, and C-25 were deduced to be all *S*.

We initially anticipated determining the absolute configuration of the C-1 quaternary carbon by applying the exciton chirality method because of the presence of two chromophoric resorcinol moieties.[45] However, in the CD spectrum for **1-1** (Figure 1-4), no exciton split was observed near the absorption maximum of resorcinol rings (280 nm). Instead a positive ^1L_b transition was observed at 280 nm.[46] The conformation of the tetrahydropyridine ring in schulzeine A had been assigned on the basis of the ROESY data, and its absolute configuration had been determined by the modified Mosher analysis. A positive ^1L_b band of schulzeine A (Figure S1-23) was consistent with the *P*-helicity of the tetrahydropyridine ring. On the other hand the *M*-helicity of the tetrahydropyridine ring and a negative ^1L_b band were observed for schulzeine B (Figure S1-23). It is well documented that the sign of the ^1L_b band of the fused benzene system is basically determined by the helicity of the cyclohexene, tetrahydropyridine, or dihydropyran ring (Figure 1-5), but the sign could be reversed by factors such as (1) polar substituent(s) of the benzene ring and (2) an axial substituent at the benzylic position.[46] Judging from the signs of ^1L_b bands in schulzeines, it was demonstrated that substitution of the benzene ring by two OH groups did not reverse the relationship

between the helicity and the sign of the ^1L_b band in isoquinolines: *P*- or *M*-helicity corresponds to a positive or negative ^1L_b band, respectively.[47] We were able to assign the conformation of the tetrahydropyridine ring of jasisoquinoline A (**1-1**) on the basis of the ROESY data (Figure 1-3c) and observed a positive ^1L_b band. However, the sign of the ^1L_b band is variable due to the presence of an axial substituent at the benzylic position. Because of the lack of suitable examples, it is not possible to assess the effect of quaternalization of the benzylic position toward the sign of the ^1L_b band. Therefore, we tentatively draw the structure of **1-1** by taking into account the positive ^1L_b band and by presuming that its sign was not reversed by substituents at C-1 (Figure 1-5).

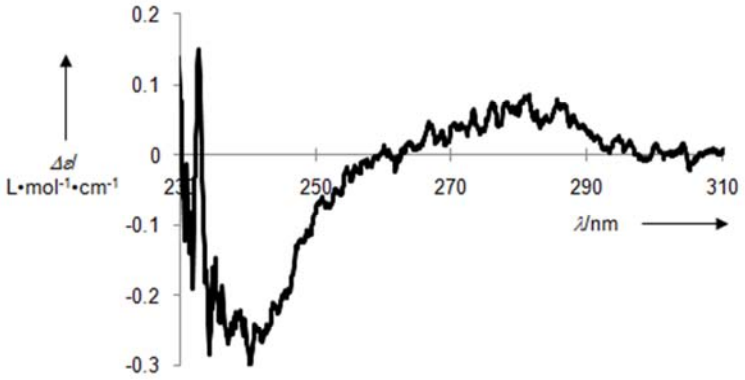

Figure 1-4. CD spectrum of jasisoquinoline A (**1-1**).

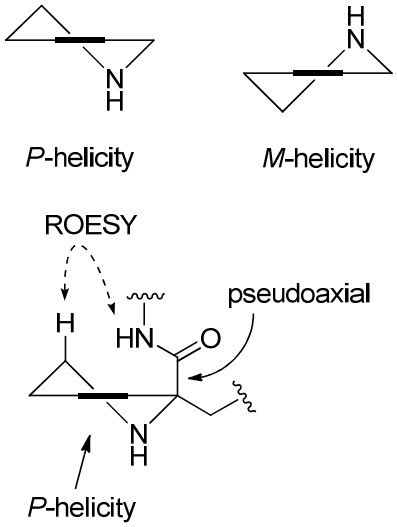

Figure 1-5. Helicity of the tetrahydropyridine ring of jasisoquinoline A (**1-1**). The bold lines represent the benzene rings.

Jasisoquinoline B (**1-2**) was smaller than **1-1** by a CH_2 unit. The ^1H NMR spectrum of **1-2** was almost identical to that of **1-1** except for the absence of the secondary methyl signal (Table 1-3). Interpretation of the COSY, HSQC, and HMBC data of **1-2** suggested that **1-2** was the 27-desmethyl analog of **1-1**. This was confirmed by the ESIMS of the $NaIO_4$ oxidation product of the desulfated **1-2**.

Table 1-1. ^{1}H and ^{13}C NMR Data for Jasisoquinoline A (**1-1**) in CD_3OD

jasisoquinoline A (**1-1**) in CD_3OD			
	^{1}H	^{13}C	HMBC
1		[b]	
3	3.39 (brs), 3.03[a]	40.9	
4	3.04[a], 2.76 (brd, 13.3)	27.7	4a
4a		137.4	
5	6.21 (brs)	109.3	4, 6, 7, 8a
6		159.4	
7	6.31 (brs)	104.0	5, 6, 8
8		156.5	
8a		110.6	
9	2.35 (m), 2.28 (m)	37.4	
10	1.16 (m)	24.1	
11-18	1.3	30.0	
19	1.41 (m)	25.6	
20	1.63 (m)	34.7	
21	4.35 (quin, 5.9)	81.0	19
22	1.72 (m)	35.2	20, 23
23	1.51 (m)	29.6	24
24	4.75 (m)	79.6	25
25	4.87[c]	77.4	24, 26, 27
26	1.56, 1.41 (m)	36.9	
27	1.76 (m)	29.6	
28	1.30, 1.18 (m)	39.0	
29-31	1.3	30.0	
32	1.28 (m)	32.9	33
33	1.30 (m)	23.6	32, 34
34	0.89 (t, 7.0)	14.2	32, 33
35	0.95 (d, 6.4)	19.6	26, 27, 28
1'		[b]	
2'			
3'	3.51, 3.43 (dt, 6.9, 13.3)	41.9	4', 5'
4'	2.64 (t, 6.8)	36.0	3', 5', 6', 10'
5'		142.1	
6'	6.10 (brd, 2.1)	108.1	7', 8', 10'
7'		159.4	
8'	6.12 (brd, 2.1)	101.6	7', 9'
9'		159.4	
10'	6.10 (brd, 2.1)	108.1	6', 8', 9'

[a] Signalls overlapped. [b] Signals were not observed in CD_3OD.

[c] This signal was overlapped with HDO signal.

Table 1-2.[a] ^{1}H and ^{13}C NMR Data for Jasisoquinoline A (**1-1**) in DMSO-d_6

jasisoquinoline A (**1-1**) in DMSO-d_6			
	^{1}H	^{13}C	HMBC
1		63.0	
3	2.42 (m), 2.93 (brd, 7.75)	39.5	1, 4a
4	2.61 (brs), 2.38 (brs)	30.2	4a
4a		138.8	
5	5.96 (d, 2.4)	107.0	4, 6, 7, 8a
6		156.2	
6-OH	9.02 (brs)		
7	6.03 (d, 2.4)	103.3	6, 8, 8a
8		164.0	
8-OH	12.0 (brs)		
8a		115.4	
9	1.94 (m), 1.8 (m)	36.8	1, 8a, 10, 1'
10	1.01 (m)	23.2	
11-18	1.2 (m)	29.2	
19	1.21 (m)	26.6	
20	1.41 (m)	33.5	
21	3.99 (quin, 5.4)	76.2	
22	1.47 (m)	34.2	21, 23
23	1.51 (m)	28.5	
24	4.36 (dt, 8.3, 4.2)	76.1	25
25	4.50 (dt, 9.5, 3.6)	73.7	24
26	1.32 (m), 1.24 (m)	35.9	35
27	1.61 (brs)	27.9	
28	1.22 (m), 1.06 (m)	37.2	26
29-31	1.2	29.2	
32	1.23 (m)	31.2	33
33	1.25 (m)	21.9	32, 34
34	0.85 (t, 7.2)	13.9	32, 33
35	0.80 (d, 6.0)	19.2	27
1'		178.1	
2'	8.78 (brd, 2.4)		1', 3'
3'	3.30[b]	40.1	1', 4', 5'
4'	2.55 (t, 7.2)	34.8	5', 6', 10'
5'		140.7	
6'	6.05 (d, 1.8)	106.6	4', 7', 8', 9', 10'
7'		158.2	
7'-OH	9.09 (brs)		
8'	6.04 (t, 1.8)	100.3	7', 9'
9'		158.2	
9'-OH	9.09 (brs)		
10'	6.05 (d, 1.8)	106.6	4', 6', 7', 8', 9'

[a] Cotaminated AcOH signals were detected: δ_H 1.88; δ_C 172.1 and 21.6.

[b] This signal was overlapped with HDO signal.

Table 1-3. ^{1}H and ^{13}C NMR Data for Jasisoquinoline B (**1-2**) in CD_3OD

jasisoquinoline B (**1-2**) in CD_3OD		
	^{1}H	^{13}C
1		[a]
3	3.25, 2.85	40.6
4	2.94, 2.69	29.0
4a		[a]
5	6.17	108.9
6		158.9
7	6.26	104.0
8		157.1
8a		109.2
9	2.24, 2.16	37.7
10	1.12	24.2
11-18	1.29	30.0
19	1.41	25.4
20	1.63	34.8
21	4.34	81.1
22	1.72	35.1
23	1.57	29.8
24	4.68	79.6
25	4.68	78.7
26	1.78	29.8
27	1.29	30.0
28	1.29	30.0
29-31	1.29	30.0
32	1.28	32.9
33	1.30	23.6
34	0.89	14.3
1'		[a]
2'		
3'	3.49, 3.45	41.5
4'	2.65	36.0
5'		142.0
6'	6.12	108.1
7'		159.5
8'	6.11	101.6
9'		159.5
10'	6.12	108.1

[a] Signals were not observed in CD_3OD.

2.3. Biological Activity

Both jasisoquinolines A (**1-1**) and B (**1-2**) inhibit cathepsin B with an IC_{50} value of 10 μg/mL. Schulzeines A (**1-3**) and C (**1-4**) also showed inhibitory activity against cathepsin B with IC_{50} values of 5.0 and 12 μg/mL, respectively. Upon desulfation the cathepsin B inhibitory activity of **1-1** was no longer detected, indicating the involvement of sulfate esters in the activity.

3. Conclusion

Jasisoquinolines are new members of isoquinolines from marine invertebrates. They are traced to a polyketide pathway, considering the substitution pattern in the benzene ring: biosynthesis of isoquinolines via a polyketide pathway is well-documented.[48] Diversification of the structures of schulzeines to jasisoquinolines, by α-oxidation of the fatty acid to be used as a substrate for a Pictet-Spengler reaction, is intriguing. It is worth noting that jasisoquinolines are, to the best of our knowledge, the first examples of natural products containing the amide form of 5-(2-aminoethyl)resorcinol.

4. Experimental Section

4.1. General Experimental Procedures

Optical rotations were measured on a JASCO DIP-1000 digital polarimeter. UV spectra were determined in MeOH using a Shimadzu BioSpec-1600 spectrophotometer. CD spectra were recorded in MeOH on a JASCO J-720 spectrapolarimeter. NMR spectra were recorded on a JEOL delta 600 NMR spectrometer at 600 MHz for ^{1}H and 150 MHz for ^{13}C. Chemical shifts were referenced to the solvent peaks: 3.31 ppm for ^{1}H and 49.15 ppm for ^{13}C in CD_3OD; 2.50 ppm for ^{1}H and 39.51 ppm for ^{13}C in DMSO-d_6. ESI mass spectra were measured on a JEOL JMS-T100LC time-of-flight mass spectrometer. FAB mass spectra were measured on a JEOL JMS-700T MStation. Fluorescence for the enzyme inhibition assay was measured on a Molecular Devices SPECTRA MAX fluorescence spectrometer.

4.2. Animal Material

The sponge sample was collected by dredging at a depth of 150 m at Oshimashinsone (28° 80’ N; 129° 30’ E) in 2004. The specimen was frozen after collection and kept at – 20 °C until extraction.

4.3. Extraction and Isolation

The sponge (400 g, wet weight) was extracted with MeOH (500 mL) and EtOH

(500 mL). The combined extracts were concentrated and partitioned between H_2O and $CHCl_3$, and the aqueous layer was further extracted with *n*-BuOH. The $CHCl_3$ layer was separated between 90% MeOH and *n*-hexane, and the 90% MeOH layer was partitioned between 60% MeOH and $CHCl_3$. The *n*-BuOH layer and the 60% MeOH layer were combined and separated by silica gel column chromatography using a stepwise gradient elution ($CHCl_3$/MeOH/H_2O 10:0:0–5:5:2). The fractions eluted with $CHCl_3$/MeOH/H_2O 6:4:1 and 5:5:2 were combined and separated by ODS flash chromatography using a stepwise gradient elution (0–70% MeOH, 70% and 80% MeCN, and 100% MeOH). The 40% MeOH eluate was chromatographed by RP-HPLC (Cosmosil AR-II; 10 × 250 mm) with 50% MeCN containing 1.0 M $NaClO_4$. Active fractions were further purified by RP-HPLC (Develosil C_{30}-UG-5; 20 × 250 mm) with 50% MeCN containing 0.7 M $NaClO_4$ to afford jasisoquinolines A (**1-1**, 2.0 mg), B (**1-2**, 0.7 mg), schulzeines A (**1-3**, 4.0 mg), and C (**1-4**, 1.5 mg).

*Jasisoquinoline A (**1-1**)*: white amorphous powder; $[\alpha]_D^{24}$ – 1.1 (*c* 0.05, MeOH); UV (MeOH) λ_{max} 211 nm (ε 17,000), 278 nm (ε 1760); CD (MeOH) λ 284 nm (Δε + 0.1), 242 nm (Δε – 0.3); ^{1}H and ^{13}C NMR data, see Table 1-1 and 1-2; HRFABMS *m*/*z* 1053.3705 $[M - Na]^-$ [$C_{45}H_{71}O_{17}N_2S_3Na_2$ (Δ – 0.4 mmu)].

*Jasisoquinoline B (**1-2**)*: white amorphous powder; $[\alpha]_D^{24}$ + 7.6 (*c* 0.03, MeOH); UV (MeOH) λ_{max} 215 nm (ε 16,200), 282 nm (2720); ^{1}H and ^{13}C NMR data, see Table 1-3; HRFABMS *m*/*z* 1039.3582 $[M - Na]^-$ [$C_{44}H_{69}O_{17}N_2S_3Na_2$ (Δ + 2.8 mmu)].

4.4. Chemical Degradation of Jasisoquinoline A (**1-1**)

1-1 (1 mg) was diluted with MeOH (1 mL) and desulfated with *p*-TsOH (catalytic amount) at room temperature for 2 h. The reaction mixture was neutralized with 10% $NaHCO_3$ followed by desalting with Inertsep RP-1. The resulting triol **1-5** was cleaved by the treatment with 2 eq. of $NaIO_4$ in 75% MeOH at room temperature followed by reduction with 50 mg of $NaBH_4$. The reaction mixture was quenched with AcOH and extracted with CH_2Cl_2 to give diol **1-6** and primary alcohol **1-7**. The presence of **1-6** was verified by FABMS analysis (*m*/*z* 601 $[M + H]^+$).

4.5. Preparation of (*R*)-MTPA Ester of 3-Methyl-1-decanol **1-7**

0.1 mg portion of **1-7** was treated with (*S*)-MTPACl in CH_2Cl_2/pyridine (1:1, 100 μL). The reaction mixture was partitioned between H_2O and $CHCl_3$, and the organic layer was purified by RP-HPLC (Develosil C_{30}-UG-5; 10 × 250 mm) with a linear gradient of 80–100% aqueous MeOH to give (*R*)-MTPA ester **1-8**.

*(R)-MTPA ester **1-8***: NMR (CD_3OD) δ 7.72, 7.63, 4.22 (H1), 3.64 (OMe), 1.69 (H3), 1.44 (H2), 1.3-0.87 (H4 – H11).

4.6. Cathepsin B Inhibition Assay

The Cathepsin B inhibition assay was carried out according to a modified method of Hiwasa *et al*.[49] A stock solution of bovine cathepsin B (Sigma; 1 unit/mL in

0.05 M MES pH 6.0 and 0.1% Brij-35) was diluted 100 times with the buffer. A 50 μL portion of 25 μM substrate solution (Z-Arg-Arg-AMC; Peptide Institute, Inc.) in DMSO was added to a mixture of 100 μL cathepsin B solution and a test solution (4 μL), and the mixture was incubated at 37 °C for 30 min. The fluorescence of the reaction mixtures was measured with an excitation at 345 nm and an emission at 440 nm.

5. Supporting Information

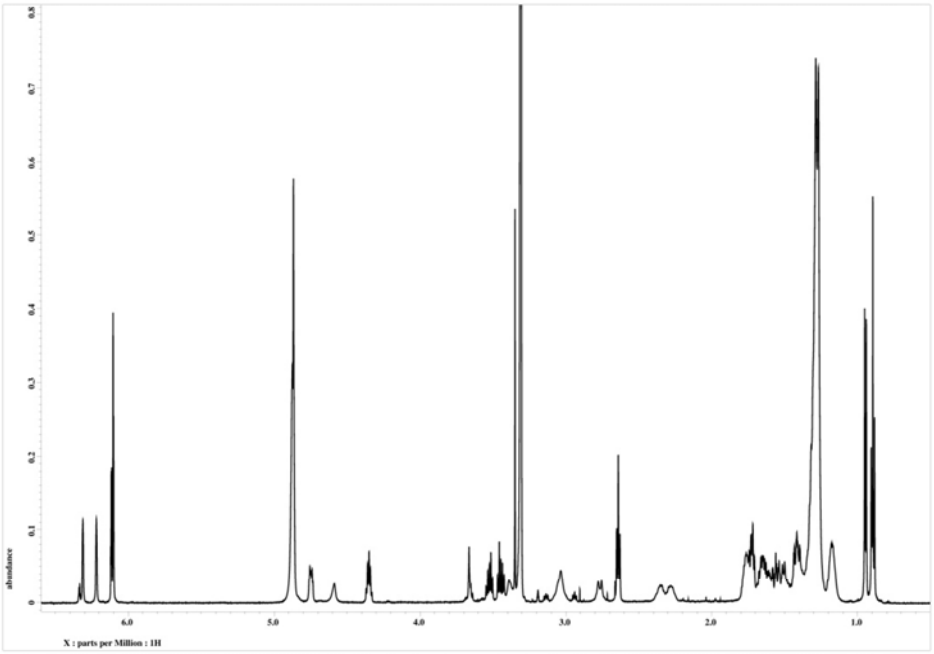

Figure S1-1. ^{1}H NMR spectrum of jasisoquinoline A (**1-1**) in CD_3OD.

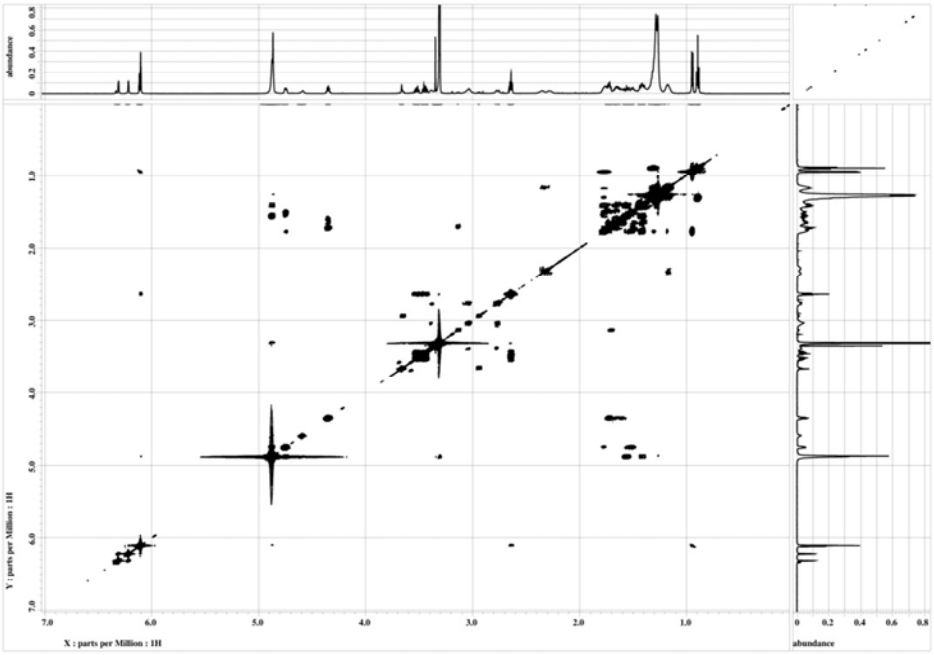

Figure S1-2. COSY spectrum of jasisoquinoline A (**1-1**) in CD_3OD.

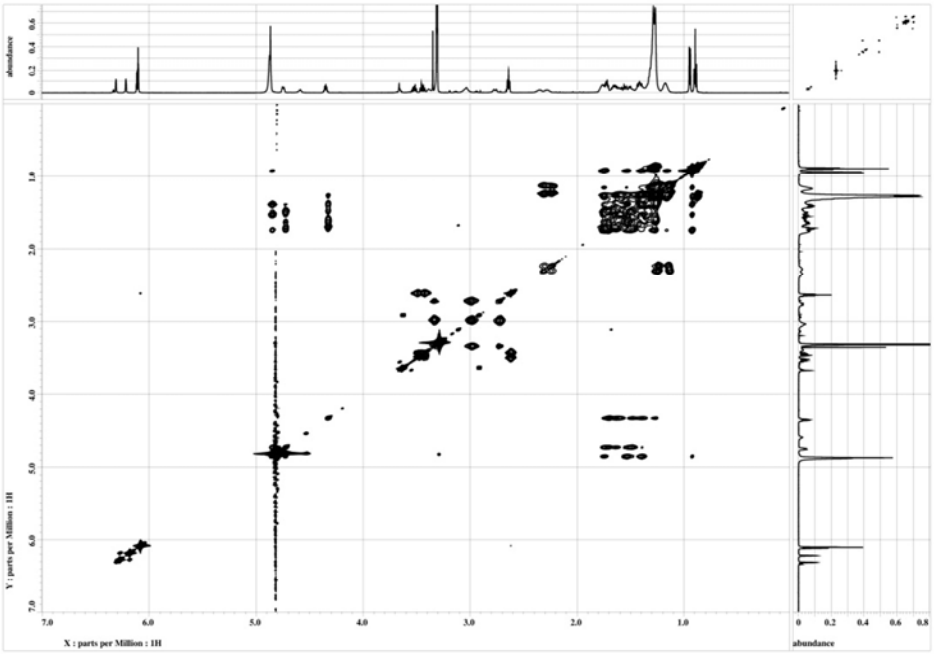

Figure S1-3. TOCSY spectrum of jasisoquinoline A (**1-1**) in CD_3OD.

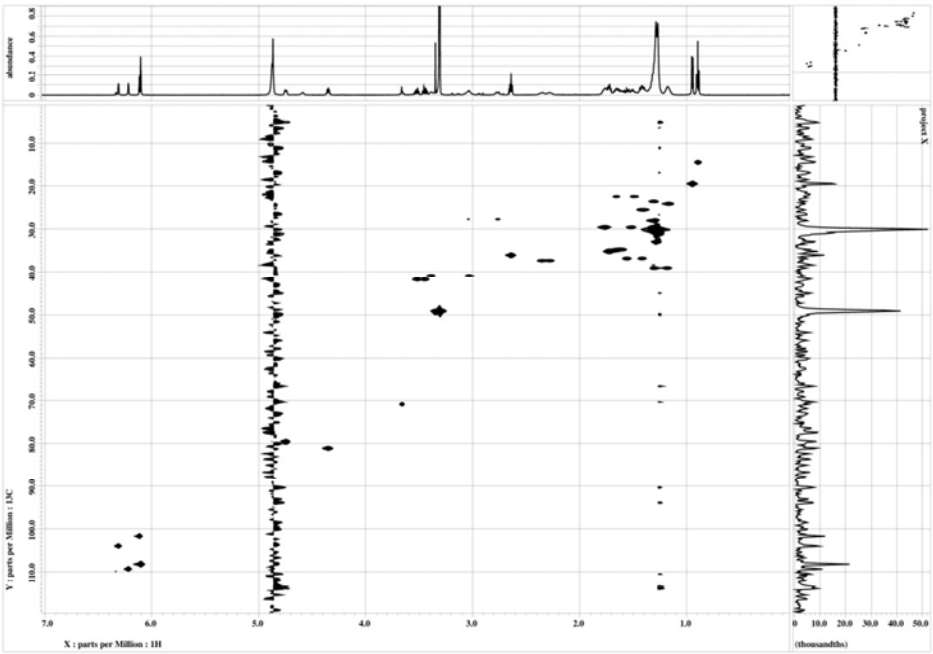

Figure S1-4. HSQC spectrum of jasisoquinoline A (**1-1**) in CD_3OD.

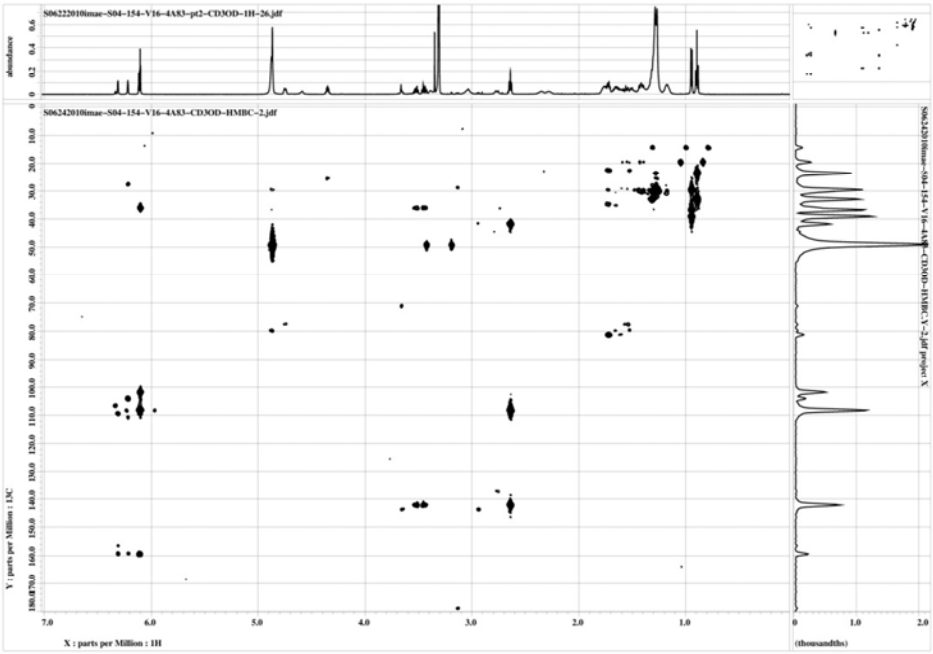

Figure S1-5. HMBC spectrum of jasisoquinoline A (**1-1**) in CD_3OD.

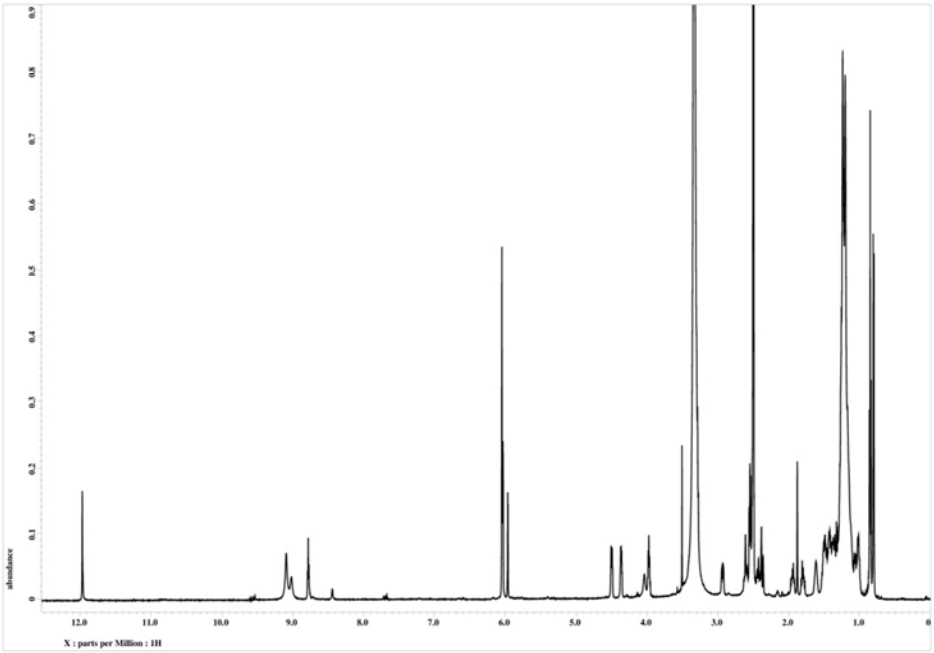

Figure S1-6. ^{1}H NMR spectrum of jasisoquinoline A (**1-1**) in DMSO-d_6.

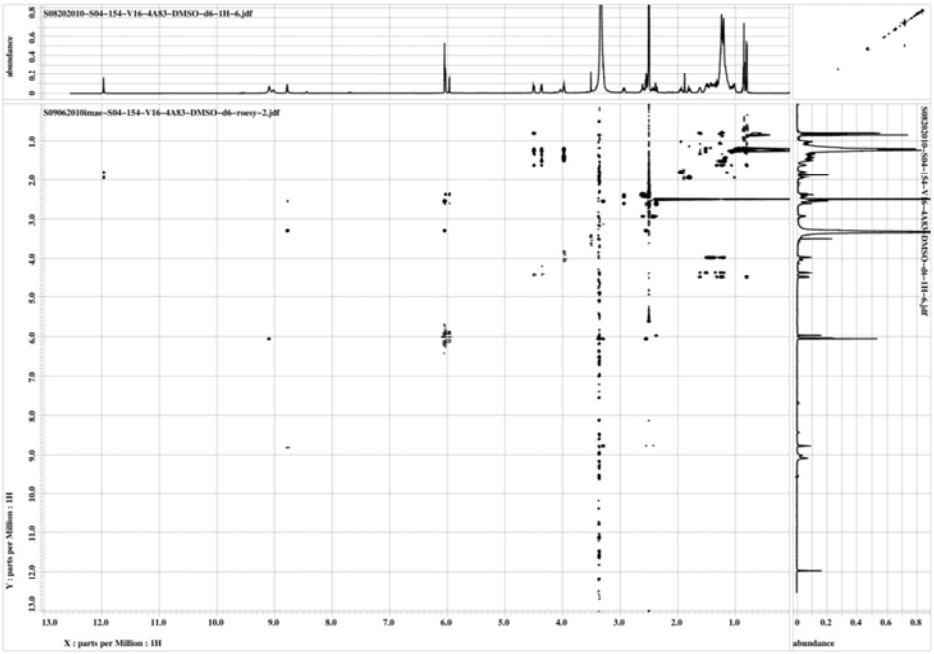

Figure S1-7. ROESY spectrum of jasisoquinoline A (**1-1**) in DMSO-d_6.

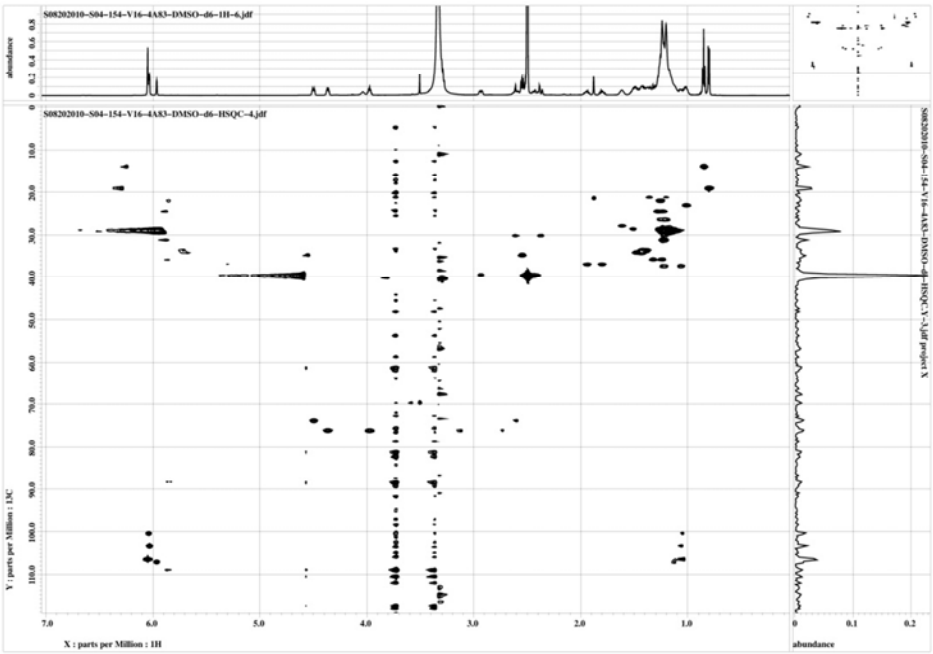

Figure S1-8. HSQC spectrum of jasisoquinoline A (**1-1**) in DMSO-d_6.

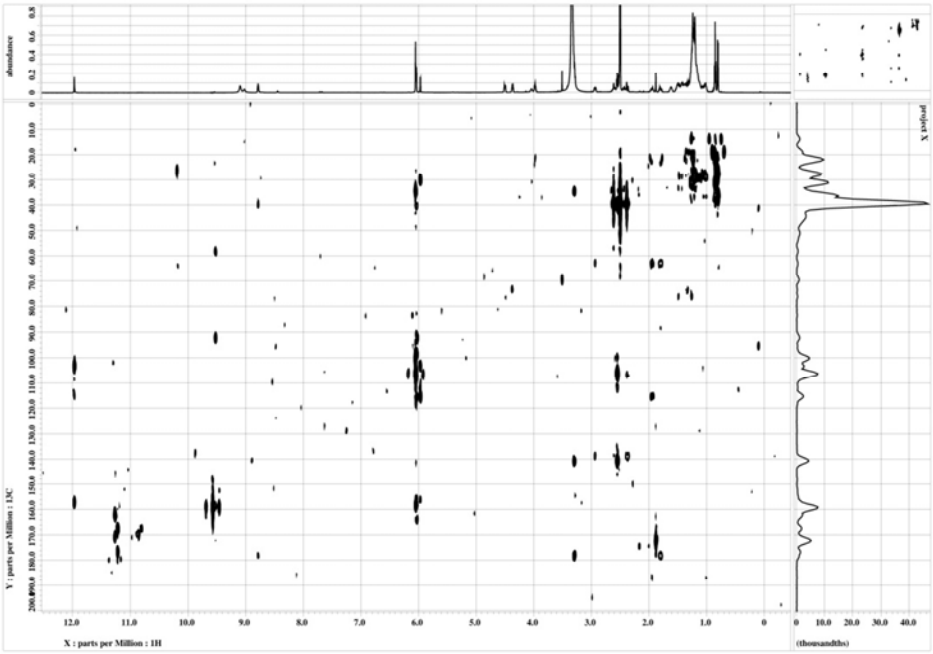

Figure S1-9. HMBC spectrum of jasisoquinoline A (**1-1**) in DMSO-d_6.

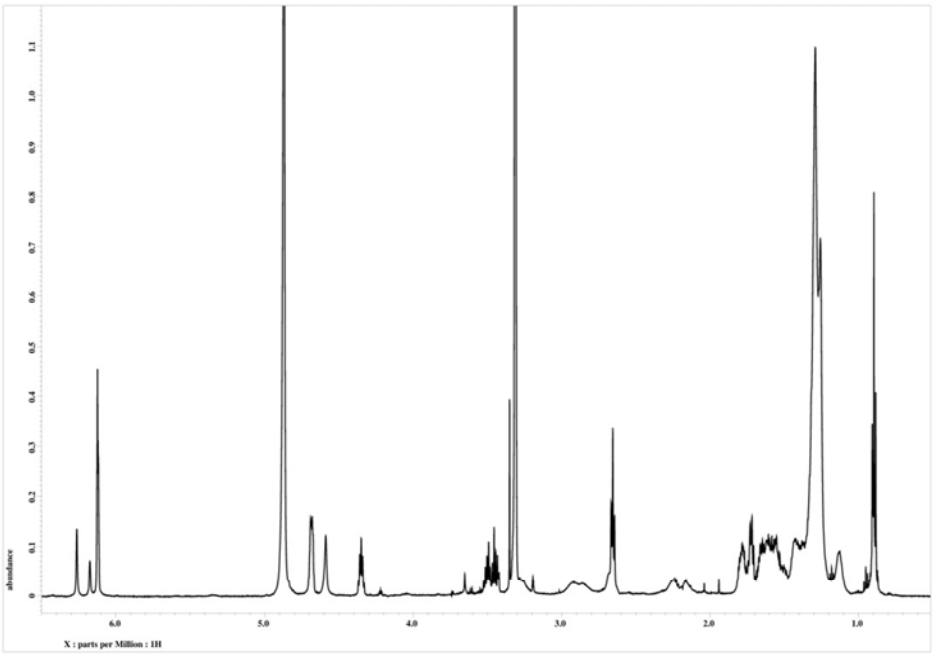

Figure S1-10. ^{1}H NMR spectrum of jasisoquinoline B (**1-2**) in CD_3OD.

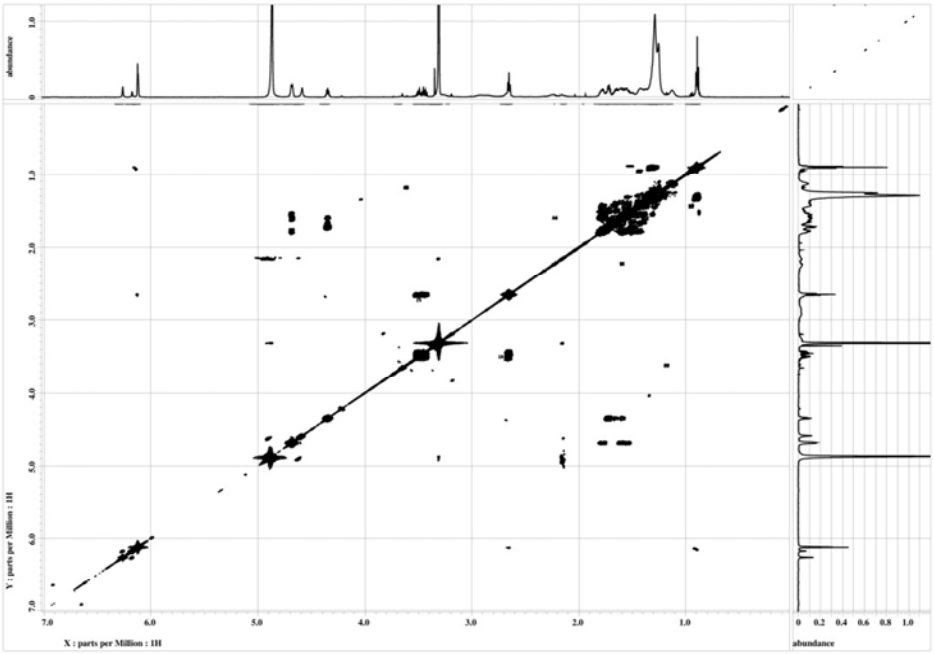

Figure S1-11. COSY spectrum of jasisoquinoline B (**1-2**) in CD_3OD.

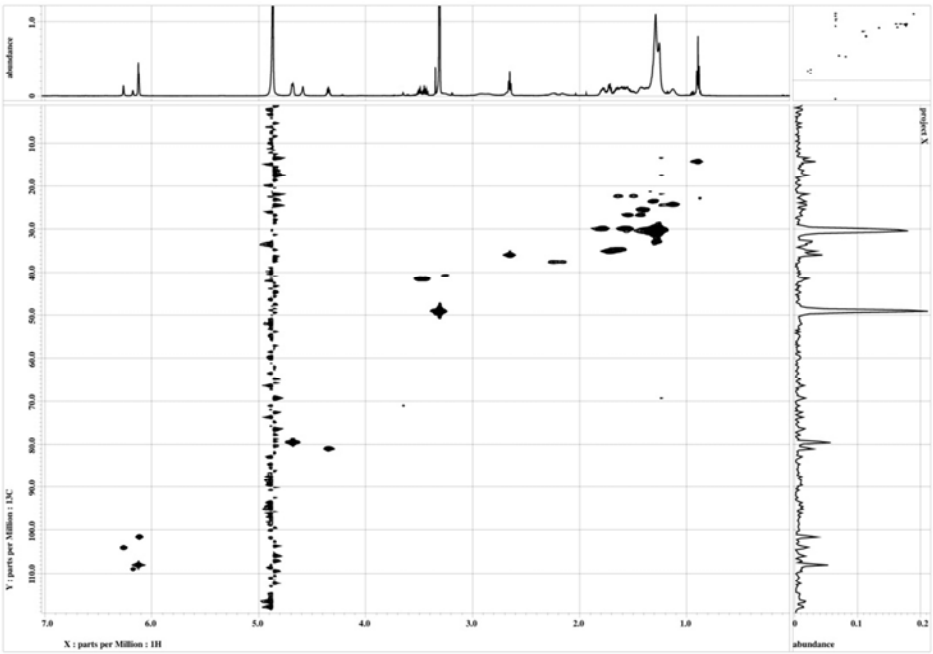

Figure S1-12. HSQC spectrum of jasisoquinoline B (**1-2**) in CD_3OD.

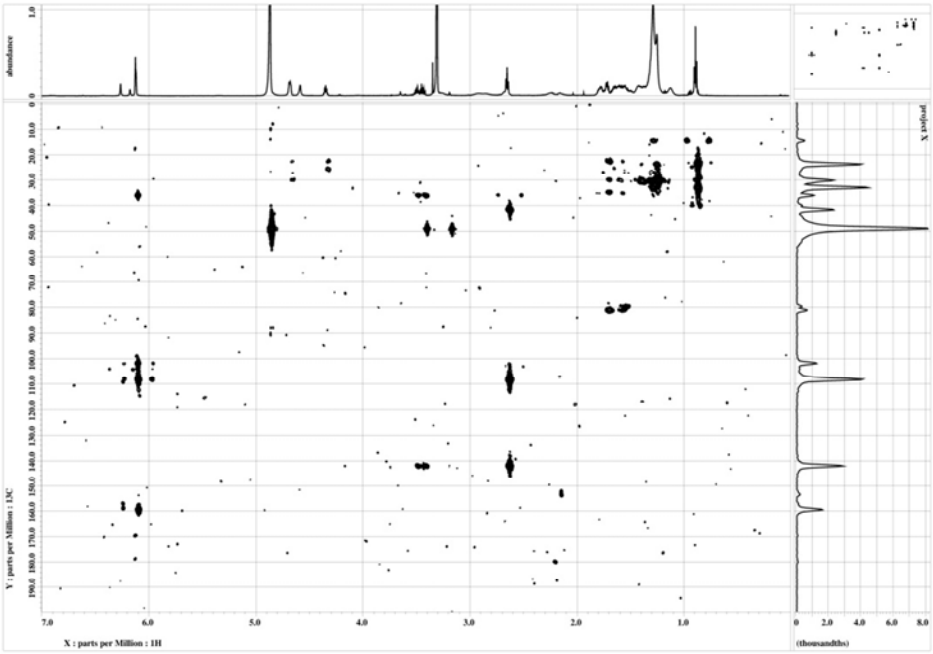

Figure S1-13. HMBC spectrum of jasisoquinoline B (**1-2**) in CD_3OD.

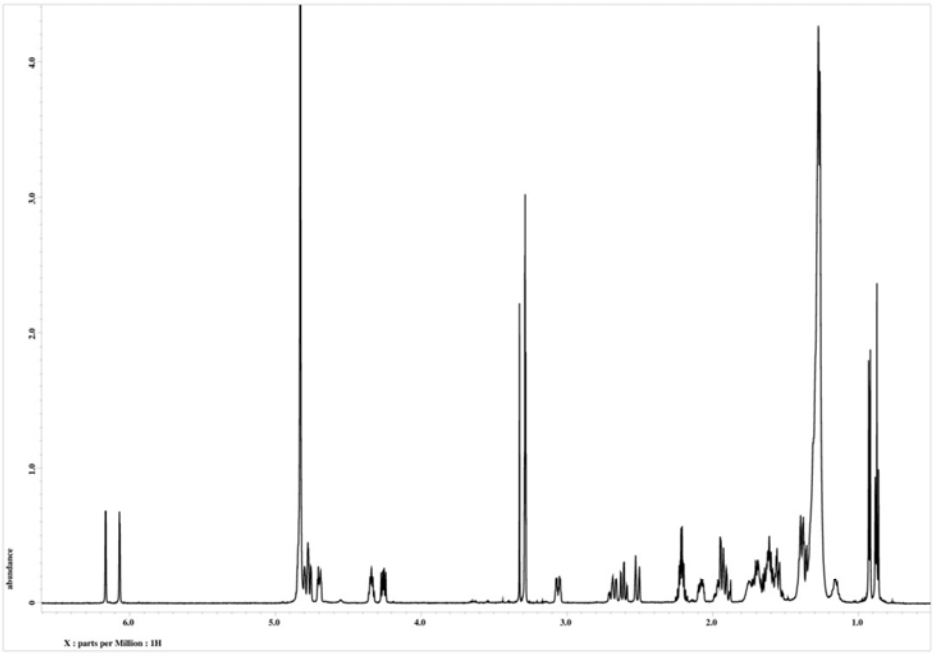

Figure S1-14. ^1H NMR spectrum of schulzeine A (**1-3**) in CD_3OD.

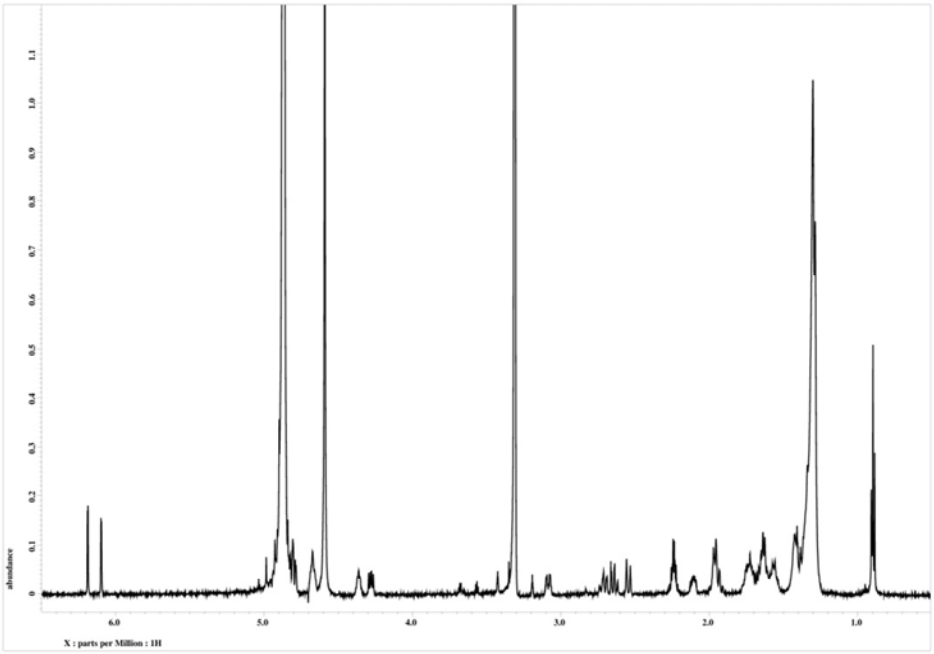

Figure S1-15. ^{1}H NMR spectrum of schulzeine C (**1-4**) in CD_3OD.

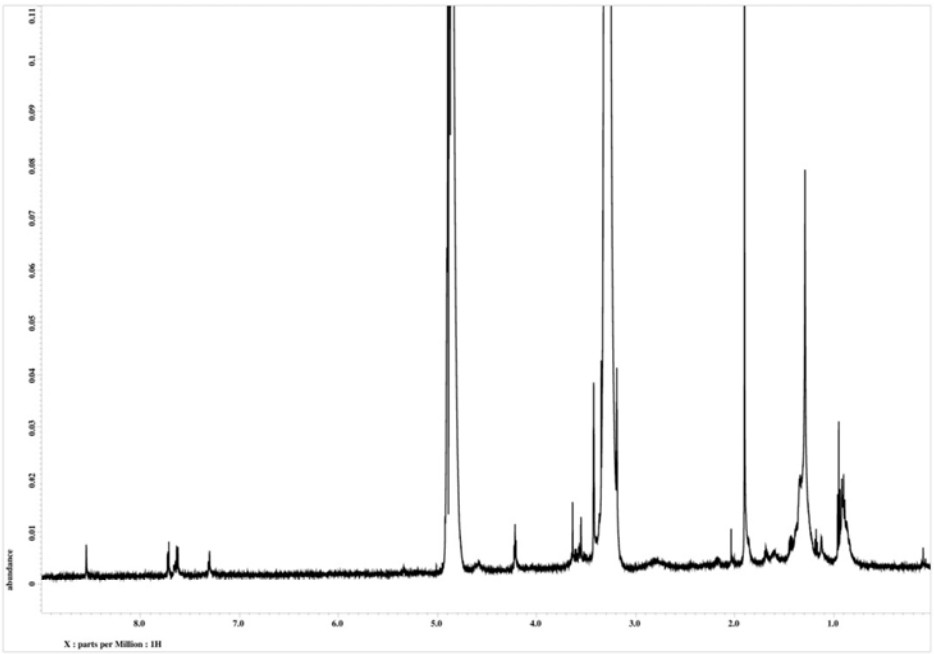

Figure S1-16. ^{1}H NMR spectrum of (*R*)-MTPA ester (**1-8**) in CD_3OD.

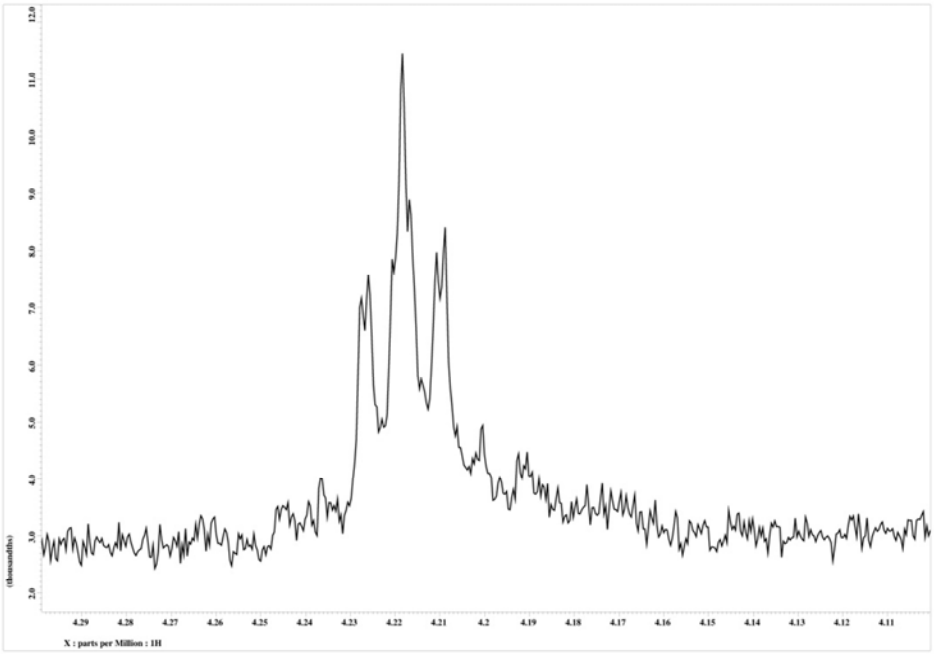

Figure S1-17. Partial ^{1}H NMR spectrum of (*R*)-MTPA ester (**1-8**) in CD_3OD.

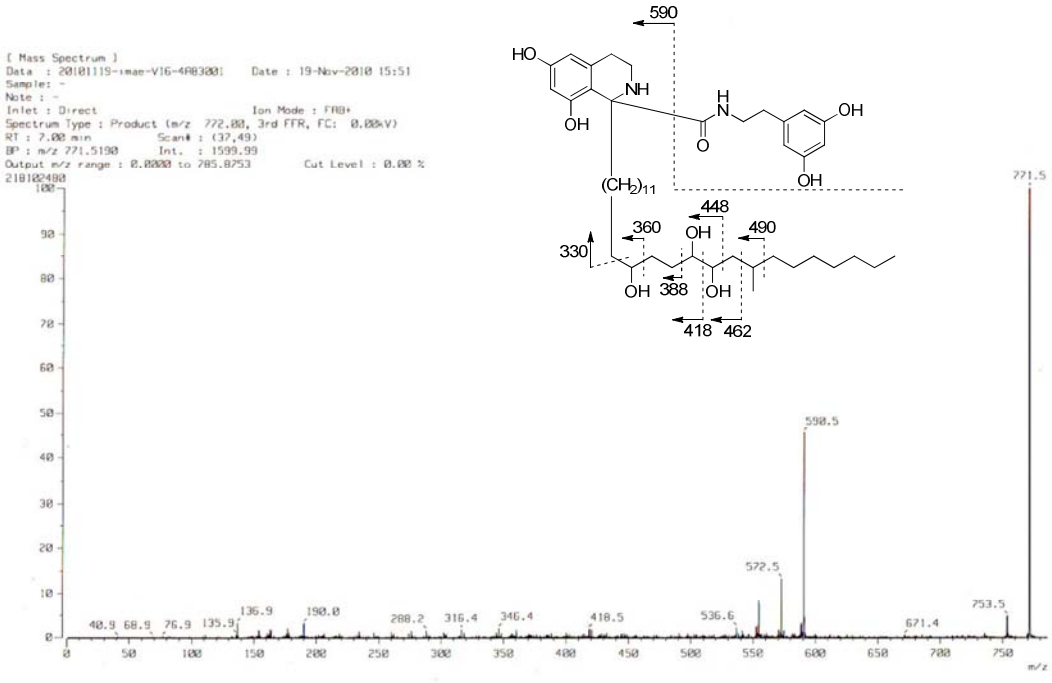

Figure S1-18. FAB-MS/MS data for **1-5** (*m*/*z* 0–772).

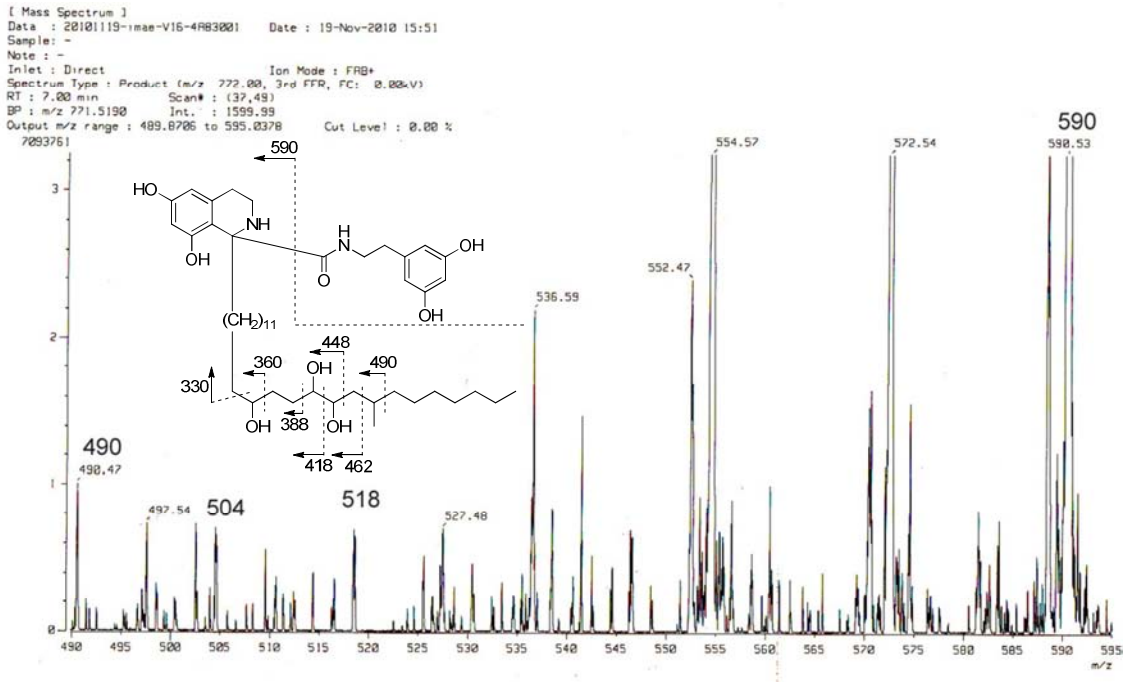

Figure S1-19. FAB-MS/MS data for **1-5** (*m*/*z* 490–595).

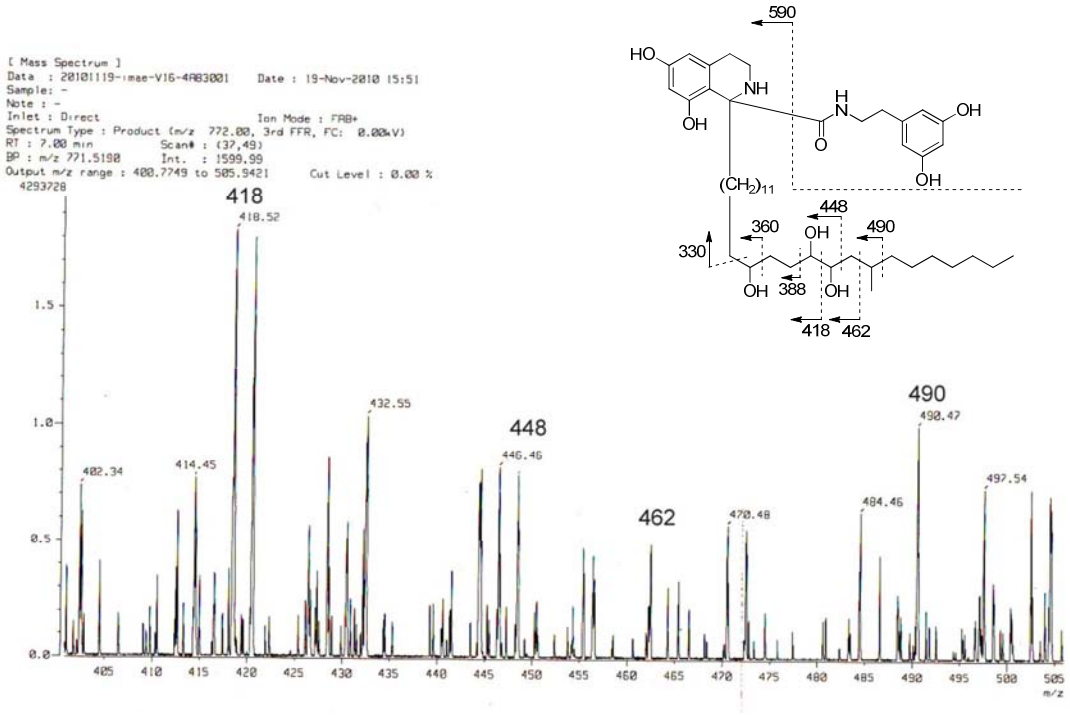

Figure S1-20. FAB-MS/MS data for **1-5** (*m*/*z* 400–505).

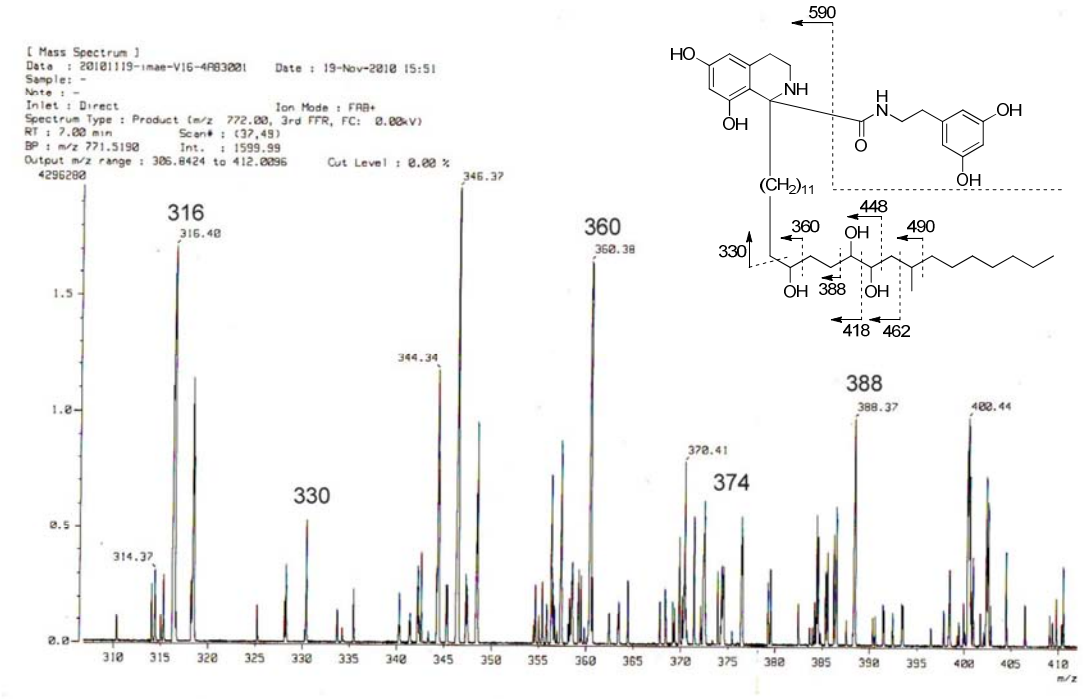

Figure S1-21. FAB-MS/MS data for **1-5** (*m*/*z* 310–410).

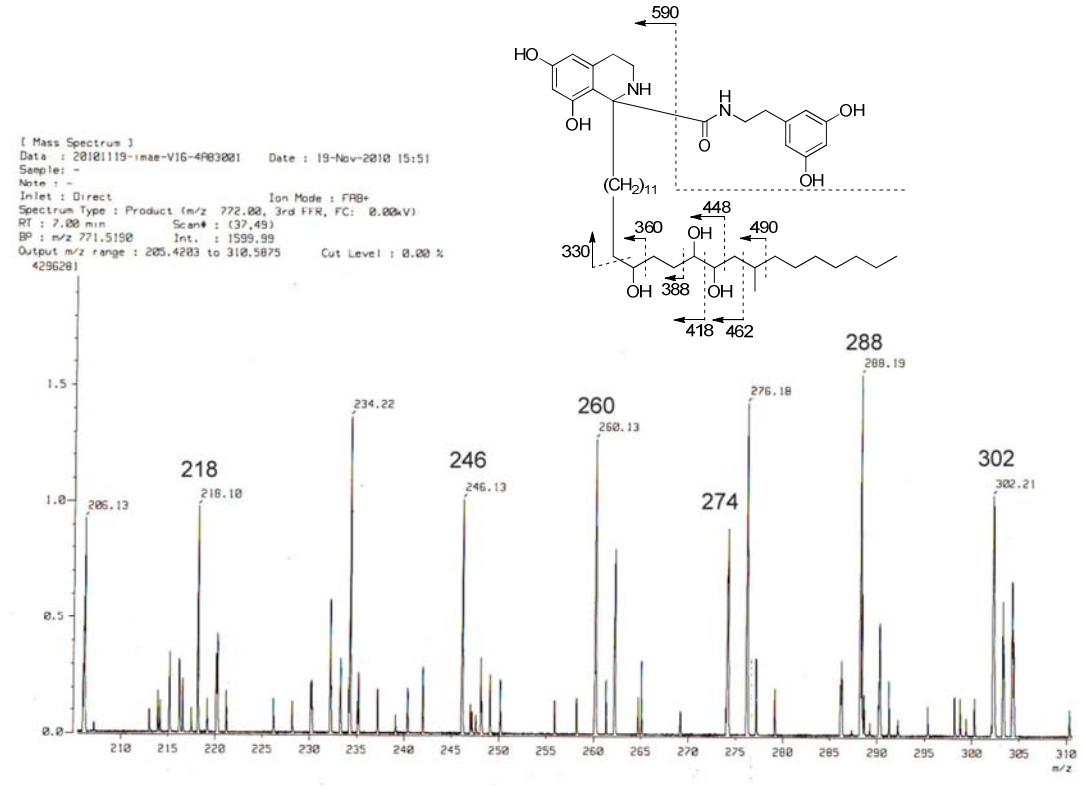

Figure S1-22. FAB-MS/MS data for **1-5** (*m*/*z* 205–310).

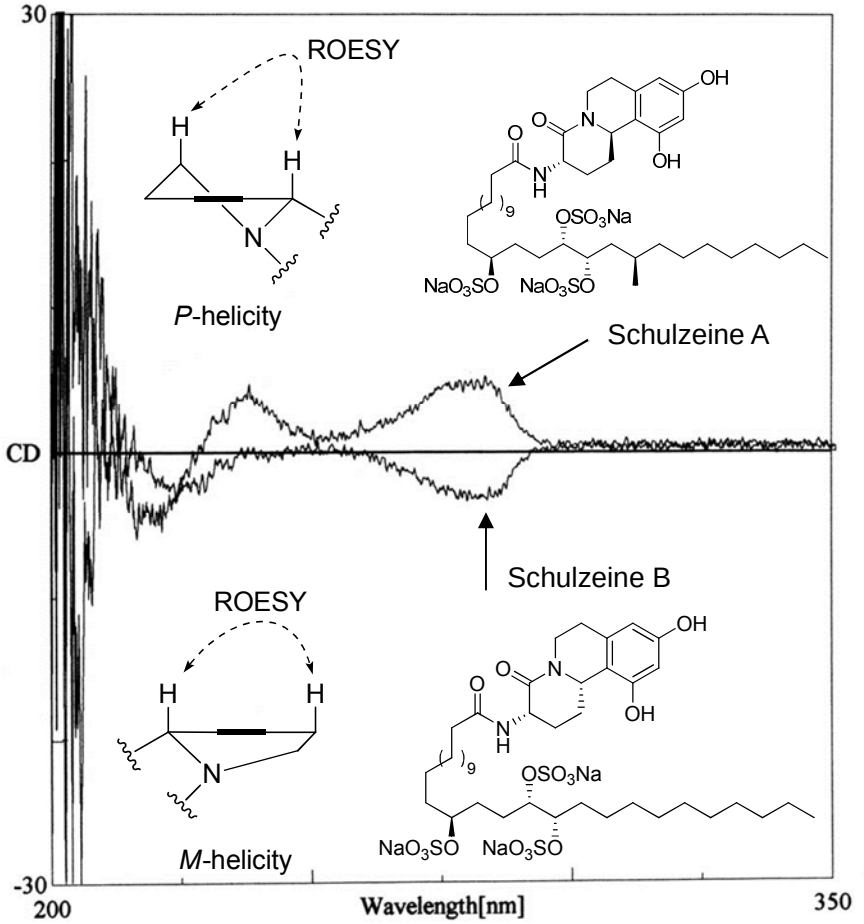

Figure S1-23. CD spectra and the structures of schulzeines A and B.[39]

Chapter II

Isolation of Ciliatamide D from a Marine Sponge *Stelletta* sp. and a Reinvestigation of the Configuration of Ciliatamide A

1. Introduction

In the course of our exploration of bioactive secondary metabolites from sponges, we fractionated the extract of a marine sponge *Stelletta* sp. collected at Oshimashinsone (Figure 2-1) on the basis of cathepsin B inhibitory activity. After HPLC separation of an active fraction, we isolated a new lipopeptide named ciliatamide D (**2-1**), which was not associated with the activity. Ciliatamide D (**2-1**) is a congener of ciliatamides A (**2-2**), B, and C, previously isolated from a marine sponge *Aaptos ciliata*.[50] We have determined the structure of **2-1** to be a lipopeptide consisting of two L-amino acid residues. This raised a question regarding the validity of the structural revision of **2-2** by chemical synthesis.[51] Therefore, from the current extract of *Stelletta* sp. we have isolated **2-2** which exhibited identical properties as those previously reported for ciliatamide A. A thorough investigation on the configuration of **2-2** allowed us to conclude that the initial assignment was correct.[50] This chapter presents the isolation, structure elucidation, and the biological activity of ciliatamide D (**2-1**) and the detailed investigation of the configuration of ciliatamide A (**2-2**).

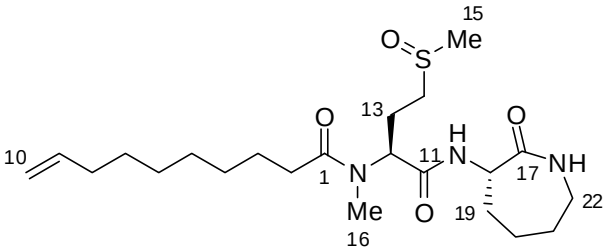

2-1

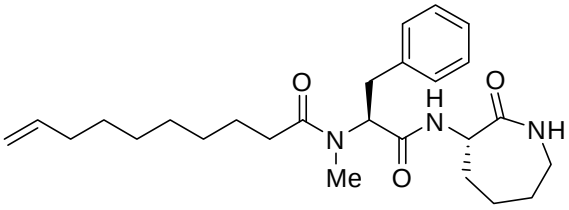

2-2

2. Results and Discussion

2.1. Extraction and Isolation of Ciliatamide D (**2-1**)

The EtOH extracts of *Stelletta* sp. (800 g, wet weight) were combined and fractionated by solvent partitioning, ODS flash chromatography, and RP-HPLC to furnish 0.8 mg of ciliatamide D (**2-1**, Figure 2-2).

Figure 2-1. *Stelletta* sp. collected at Oshimashinsone.

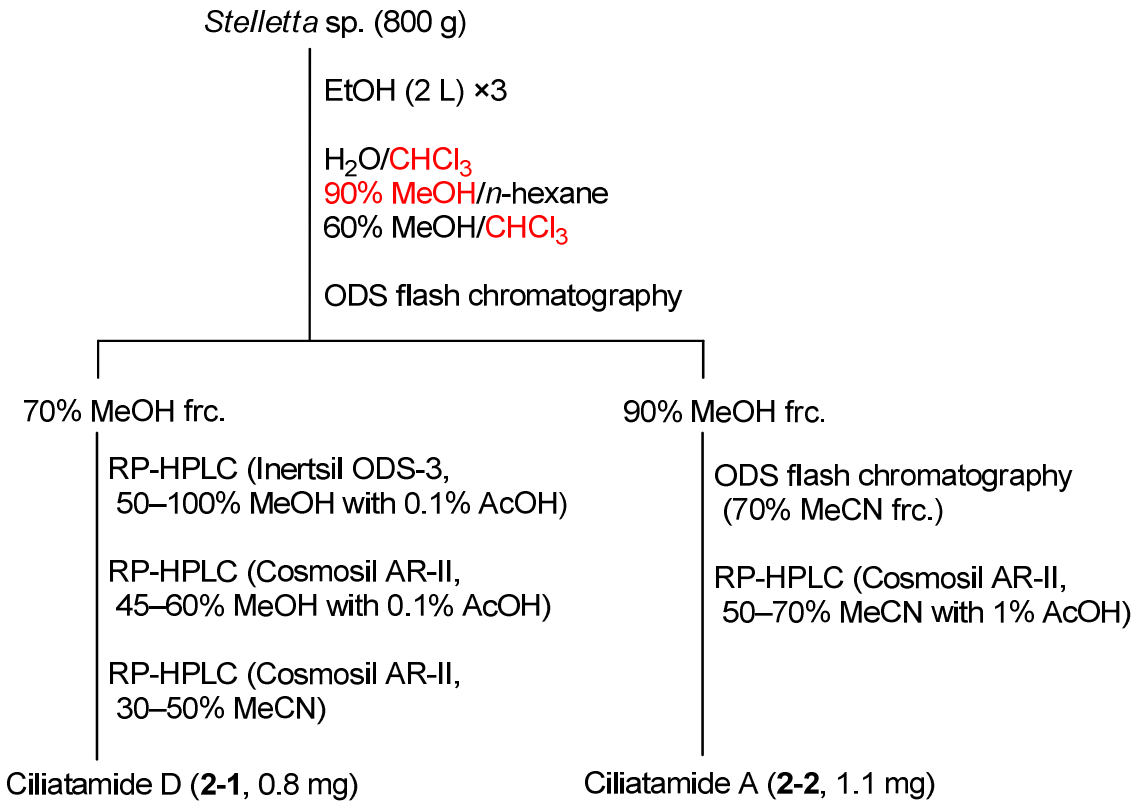

Figure 2-2. Isolation procedure of ciliatamides D (**2-1**) and A (**2-2**).

2.2. Structure Elucidation of Ciliatamide D

Ciliatamide D (**2-1**) had a molecular formula of $C_{22}H_{39}O_4N_3S$ as determined by HRESIMS. An analysis of the ^{1}H NMR data in combination with the HSQC spectrum showed the presence of two amide protons, one of which appeared in a 3:1 ratio, two α-protons and an *N*-methyl signal both emerging in a 3:1 ratio, one finely split *S*-methyl, one terminal vinyl group, three low-field methylenes, and 10 other methylenes (Table 2-1 and Figure 2-3). The duplication of some signals implied the presence of a chemical equilibrium or an inseparable mixture, or both.

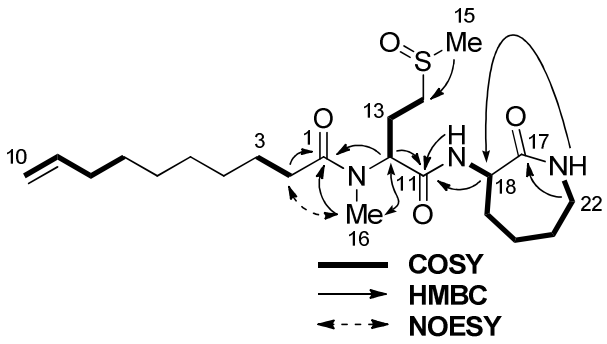

Figure 2-3. Selected COSY, HMBC, and NOESY correlations for **2-1**.

Interpretation of the COSY and TOCSY data demonstrated a spin system from duplicated signals for NH-18 (δ_H 7.57, 7.58) to another amide NH-22 (δ_H 7.86) via an α-methine and four contiguous methylenes, indicating the presence of a lysine residue or derivative. HMBC correlations from a methylene proton H-22 (δ_H 3.05) to the amide carbonyl carbon (C-17, δ_C 173.8) and from NH-22 to the α-carbon (C-18, δ_C 51.3) suggested that the lysine residue forms an ε-caprolactam. The COSY data showed another spin system from H-12 (δ_H 5.12, 5.13) to H_2-14 (δ_H 2.54 and 2.63). An HMBC correlation from a duplicated singlet peak for H_3-15 (δ_H 2.516, 2.517) to C-14 (δ_C 49.8) as well as ^{13}C chemical shift values of C-14 and C-15 (δ_C 37.6) indicated that C-14 and C-15 could be linked via a sulfur atom of a sulfoxide group, suggesting the presence of a methionine sulfoxide residue, which was in agreement with a 1:1 duplication of ^{1}H NMR signals due to the asymmetry of the sulfur atom.[52,*] An HMBC correlation from the *N*-methyl protons [H_3-16 (δ_H 2.85, 2.86)] to C-12 (δ_C 54.4) and a correlation from H-12 to C-16 (δ_C 30.5) indicated that the methionine sulfoxide residue was

[*] The 1:1 NMR signal doubling was abolished after converting **2-1** to the corresponding sulfone by the treatment with OXONE.

N-methylated. The remaining signals consisted of one carbonyl carbon (δ_C 173.4), seven methylenes, and a terminal mono-substituted olefin, indicating the presence of 9-decenoyl group. The linkage between the cyclized lysine and *N*-methyl methionine sulfoxide was established by the HMBC correlations from lysine NH-18 and H-18 (δ_H 4.33, 4.35) to C-11 (δ_C 168.5). HMBC cross-peaks from H-12, H_3-16, and H_2-2 to C-1 suggested the connection between *N*-methyl methionine sulfoxide and 9-decenoyl group, completing the planar structure of **2-1**.

The differences of ^{13}C chemical shifts between the major and the minor conformer were mainly observed around C-1, C-12, and C-16, which implied geometrical isomerism of the amide bond between C-1 and N-12. In the NOESY data for the major conformer a cross-peak between H_3-16 and methylene protons H_2-2 was observed, suggesting that the amide bond was *Z*, while the amide bond in the minor conformer was *E* as deduced from the NOESY cross-peak between H_2-12 (δ_H 4.63, 4.64) and H-2 (δ_H 2.34).

The absolute configurations of the amino acid residues in **2-1** were determined by Marfey's method.[53] Standard *N*-methyl-D- and *N*-methyl-L-methionine sulfone (**2-3d**) were prepared from commercially available *N*-Boc-D- and *N*-Boc-L-methionine (**2-3a**), respectively (Scheme 2-1a). Ciliatamide D (**2-1**) was converted to the sulfone, which was more stable toward acid hydrolysis condition, and hydrolyzed with 6 N HCl to provide lysine and *N*-methyl-methionine sulfone. The standard amino acids and the hydrolysates of **2-1** were derivatized with L-FDAA followed by LC-MS analysis, which showed that the two amino acids had the L-configuration.

Scheme 2-1. Preparation of Standard *N*-Methyl-D- and *N*-Methyl-L-Methionine Sulfone (**2-3d**) and *N*-Methyl-D- and *N*-Methyl-L-Phenylalanine (**2-4c**)

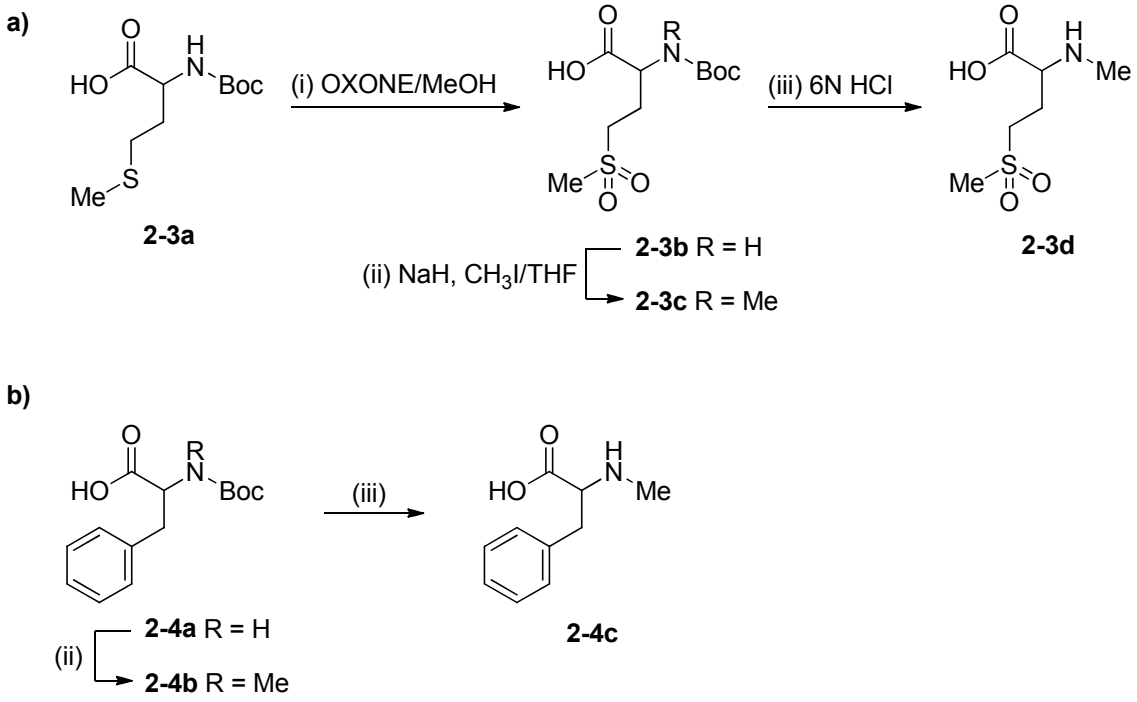

Table 2-1. ^{1}H and ^{13}C NMR Data for Ciliatamide D (**2-1**) in DMSO-d_6

	2-1 (major conformer)					**2-1** (minor conformer)	
Position	δ_H (J in Hz)	δ_C	HMBC	NOESY		δ_H (J in Hz)	δ_C
1		173.3					172.5
2	2.34 (dt, 7.6, 4.1)	32.4	1, 3	3, 16		2.34 (dt, 7.6, 4.1)	32.4
3	1.50 (m)	24.2	1, 2	2, 16		1.50 (m)	24.2
4-6	1.2[b]	28.5				1.2[b]	28.5
7	1.34 (m)	28.0	8, 9	8		1.34 (m)	28.0
8	2.0 (dt, 7.4, 7.0)	32.9	7, 9, 10	7, 10b		2.0 (dt, 7.4, 7.0)	32.9
9	5.79 (ddt, 10.1, 17.1, 6.6)	138.5	7, 8	10a		5.79 (ddt, 10.1, 17.1, 6.6)	138.5
10a	4.93 (dd, 1.8, 10.1)	114.5	8	9		4.93 (dd, 1.8, 10.1)	114.5
10b	4.99 (ddt, 1.8, 17.1, 3.7)		8, 9	8		4.99 (ddt, 1.8, 17.1, 3.7)	
11		168.5					168.3
12	5.12, 5.13 (t, 5.0)[a]	54.4	1, 11, 13, 14, 16	13ab, 14ab,16, NH-18		4.63, 4.64 (t, 5.6)[a]	57.9
13a	1.88 (m)	20.5		12,13b, 14ab		1.91 (m)	20.6
13b	2.18 (m)			12, 13a, 14ab		2.14 (m)	
14a	2.54 (m)	49.8		12, 13ab		2.54 (m)	49.8
14b	2.63 (m)		15	12, 13ab		2.63 (m)	
15	2.516, 2.517 (s)[a]	37.6	14			2.546, 2.547 (s)[a]	37.6
16	2.85, 2.86 (s)[a]	30.5	1, 12	2, 3, 12, NH-18		2.736, 2.737 (s)[a]	28.0
17		173.9					173.9
18	4.33, 4.35 (dd, 6.4, 1.2)[a]	51.3	11, 17, 19, 20	NH-18, 19ab, 20ab, NH-22		4.39, 4.41 (brd, 6.8)[a]	51.3
NH-18	7.57, 7.58 (d, 6.4)[a]		11, 17, 18	12, 16, 18, 19ab		7.97 (d, 6.8)	
19a	1.35 (m)	30.5	17, 21	18		1.35 (m)	30.5
19b	1.79 (m)		17, 21	18		1.79 (m)	
20a	1.62 (m)	27.4		18, 20b		1.62 (m)	27.4
20b	1.86 (m)			18, 20a		1.86 (m)	
21a	1.27 (m)	28.5				1.27 (m)	28.5
21b	1.73 (m)		20	22ab		1.73 (m)	
22a	3.05 (m)	40.3	17, 20	21b, NH-22		3.05 (m)	40.3
22b	3.15 (m)		20	21b, NH-22		3.15 (m)	
NH-22	7.86 (t, 5.9)		18, 22	18, 22ab		7.86 (t, 5.9)	

[a] Indicates *R*/*S* diastereomers at stereogenic S atom. [b] Signals were overlapped.

2.3. Investigation of the Configuration of Ciliatamide A

With the configurations of the amino acid residues in ciliatamide D (**2-1**) securely determined, a question arose as to the absolute configurations of the two constituent amino acid residues in ciliatamide A (**2-2**), both of which had been revised from the L- to D-form by chemical synthesis.[51] Fortunately ciliatamide A (**2-2**) that showed identical physicochemical properties with those reported[50] was isolated from the current sponge extract (Figure 2-2).[†] Because racemization during configurational analysis had been pointed out as the source of misassignments,[51] we conducted acid hydrolysis of **2-2** for 2, 5, and 16 hours to examine whether racemization of the amino acids took place during acid hydrolysis. The hydrolysates, DL-lysine, and *N*-methyl-D- and *N*-methyl-L-phenylalanine (**2-4c**) prepared from *N*-Boc-D- and *N*-Boc-L-phenylalanine (**2-4a**; Scheme 2-1b) were subjected to the Marfey's analyses.[53] The LC-MS data unambiguously demonstrated that the two amino acids in the acid hydrolysates had the L-configuration and that racemization did not occur during the hydrolysis nor derivatization for the Marfey's analysis (Figure S2-8 and S2-9). We have therefore concluded that our previous configurational assignment of ciliatamide A (**2-2**) was correct.[‡]

[†] See Experimental Section and Figure S2-7.

[‡] Even if racemization did occur under the hydrolysis or derivatization conditions, a 50:50 mixture of D- and L-forms would be expected, not inversion to the opposite configuration. We asked the authors of the synthesis paper to share a sample of the synthetic ciliatamide A, but the request was unsuccessful because the sample was no longer available.

2.4. Biological Activity

Ciliatamide D (**2-1**) did not show inhibitory activity against cathepsin B at 50 μg/mL nor cytotoxicity against HeLa cells at 50 μg/mL.

3. Conclusion

In this study, a new lipopeptide ciliatamide D (**2-1**) was isolated from a marine sponge *Stelletta* sp., together with the known compound ciliatamide A (**2-2**). Marfey's analyses demonstrated that all the amino acid residues in **2-1** and **2-2** were in L-form. This observation and spectral data for **2-2** including the optical rotation established that **2-2** had the initially reported configuration.[50]

4. Experimental Section

4.1. General Experimental Procedures

Optical rotations were measured on a JASCO DIP-1000 digital polarimeter. UV spectra were determined in MeOH using a Shimadzu BioSpec-1600 spectrophotometer. NMR spectra were recorded on a JEOL delta 600 NMR spectrometer at 600 MHz for ^{1}H and 150 MHz for ^{13}C. Chemical shifts were referenced to the solvent peaks of DMSO-d_6: 2.50 ppm for ^{1}H and 39.51 ppm for ^{13}C. ESI mass spectra were measured on a JEOL JMS-T100LC time-of-flight mass spectrometer. FAB mass spectra were measured on a JEOL JMS-700T MStation. Fluorescence for the enzyme inhibition assay was measured on a Molecular Devices SPECTRA MAX fluorescence spectrometer. Marfey's analyses were conducted with a Shimadzu Prominence UFLC equipped with Bruker amaZon SL.

4.2. Animal Material

The sponge *Stelletta* sp. was collected by dredging at a depth of 170 m at a seamount Oshimashinsone (between 28° 52.19′ N, 129° 32.96′ E and 28° 52.25′ N, 129° 32.94′ E), southern Japan, during a cruise of T/S Nagasaki-Maru, on June 5, 2008. Sponge description: subspherical with an optimally smooth surface; no visible oscule; surface dark brown, choanosome brown; consistency hard. Cortex 4.0–5.0 mm thick, made of perpendicularly arranged megascleres. Megascleres orthotrianes in two size classes, anatrianes, plagiotrianes, and oxeas in two size classes, with few protrianes.

Microscleres tylasters. The specimen used for identification (NSMT-Po-1977) was deposited at National Museum of Nature and Science, Tokyo.

4.3. Extraction and Isolation

The sponge (800 g, wet weight) was homogenized and extracted with EtOH (2 L) three times. The combined extracts were concentrated and partitioned between H_2O and $CHCl_3$. The organic layer was partitioned between 90% MeOH and *n*-hexane, and the 90% MeOH layer was partitioned between $CHCl_3$ and 60% MeOH. The latter $CHCl_3$ layer was separated by ODS flash column chromatography using a stepwise gradient elution (0–100% MeOH). The 70% MeOH eluate was chromatographed by RP-HPLC (Inertsil ODS-3; 20 × 250 mm) with a linear gradient elution of 50–100% MeOH containing 0.1% AcOH (60 min). The fraction eluted between 23 and 25 min was further separated by RP-HPLC (Cosmosil AR-II; 20 × 250 mm) with a linear gradient elution of 45–60% MeOH containing 0.1% AcOH (75 min). The fraction eluted between 68 and 72 min was purified by RP-HPLC (Cosmosil AR-II; 10 × 250 mm) with a linear gradient elution of 30–50% MeCN (50 min) to afford ciliatamide D (**2-1**, 0.8 mg). The 90% MeOH fraction of the ODS flash column chromatography was further separated by ODS flash column chromatography using a stepwise gradient elution (50%, 70% MeOH, 70%, 90% MeCN, and MeOH). The 70% MeCN fraction was purified by RP-HPLC (Cosmosil AR-II; 10 × 250 mm) with a linear gradient elution of 50–70% MeCN containing 1% AcOH (50 min) to afford ciliatamide A (**2-2**, 1.1 mg).

*Ciliatamide D (**2-1**)*: white amorphous powder; $[\alpha]_D^{24}$ + 58 (*c* 0.035, MeOH);

UV (MeOH) λ_{max} 212 nm (ε 4,800); ^{1}H and ^{13}C NMR data, see Table 2-1; HRESIMS *m*/*z* 464.2570 $[M + Na]^+$ (calcd for $C_{22}H_{39}O_4N_3SNa$, 464.2559).

*Ciliatamide A (**2-2**)*: yellow oil; $[\alpha]_D^{22}$ + 52 (*c* 0.05, MeOH); UV (MeOH) λ_{max} 209 nm (ε 8,800); ^{1}H NMR spectrum, see Figure S2-7; HRESIMS *m*/*z* 464.2890 $[M + Na]^+$ (calcd for $C_{22}H_{39}O_4N_3SNa$, 464.2889).

4.4. Preparation of *N*-Methyl-D- and *N*-Methyl-L-Methionine Sulfone (**2-3d**) and *N*-Methyl-D- and *N*-Methyl-L-Phenylalanine (**2-4c**).

To a solution of *N*-Boc-L-methionine (L-**2-3a**, 100 mg) in MeOH (2.5 mL) was added OXONE (500 mg) and the solution was stirred at room temperature for 2 h. The mixture was diluted with H_2O and extracted with CH_2Cl_2 to give *N*-Boc-L-methionine sulfone (L-**2-3b**, *m*/*z* 282 $[M + H]^+$). To a solution of the above L-**2-3b** in THF (2 mL) was added NaH (50 mg) and MeI (330 μL) and the mixture was stirred at room temperature for 24 h. The reaction mixture was diluted with H_2O and extracted with EtOAc. The aqueous layer was acidified with 20% aqueous citric acid and extracted with EtOAc. The combined organic layer was concentrated to afford *N*-Boc-*N*-methyl-L-methionine sulfone (L-**2-3c**, *m*/*z* 296 $[M + H]^+$), which was dissolved in 6 N HCl (1 mL) and heated at 110 °C for 2 h. The solution was concentrated to provide *N*-methyl-L-methionine sulfone (L-**2-3d**, *m*/*z* 196 $[M + H]^+$). This material was used for the Marfey's analysis. *N*-methyl-D-methionine sulfone (D-**2-3d**) was synthesized from *N*-Boc-D-methionine (D-**2-3a**) in the same manner.

N-Methyl-D- and *N*-Methyl-L-phenylalanine (**2-4c**) were prepared from

commercially available *N*-Boc-D- and *N*-Boc-L-phenylalanine (**2-4a**), respectively, by *N*-methylation and deprotection as described above.

4.5. Oxidation of Ciliatamide D (**2-1**)

To a solution of ciliatamide D (**2-1**, 0.1 mg) in MeOH (0.5 mL) was added OXONE (5 mg in 100 μL of H_2O), and the mixture was stirred at room temperature for 2 h. The solution was diluted with H_2O, applied on InertSep RP-1 (GL Science), washed with 10% MeOH, and eluted with MeOH to afford ciliatamide D sulfone (*m*/*z* 458 $[M + H]^+$).

4.6. Marfey's Analysis[53]

Ciliatamide D sulfone was dissolved in 6 N HCl (150 μL) and heated at 110 °C for 2 h. The solution was concentrated and redissolved in 50 μL of H_2O. 1% L-FDAA in acetone (100 μL) and 1 M $NaHCO_3$ (20 μL) were added to the solution. The mixture was heated at 40 °C for 1 h. After cooling to room temperature, the reaction mixtures were quenched with 5 N HCl (4 μL), concentrated, and redissolved in DMSO. D- and L-amino acid standards were treated with L-FDAA in the same manner. The L-FDAA derivatives were analyzed by LC-MS [Cosomosil 2.5C_{18}-MS-II (2.0 × 100 mm); flow rate, 0.5 mL/min; solvent, 10–50% MeCN containing 0.5% AcOH (22 min)]. Retention time (Rt) of each amino acid was as follows: L-lysine (17.2 min), D-lysine (18.4), *N*-methyl-L-methionine sulfone (9.5), and *N*-methyl-D-methionine sulfone (10.2). The absolute configurations of the amino acids in **2-1** were determined as L-lysine (Rt 17.2

min) and *N*-methyl-L-methionine sulfone (Rt 9.5 min). Ciliatamide A (**2-2**, 0.05 mg) was analyzed in the same manner. The absolute configurations of the amino acids in **2-2** were determined as L-lysine (Rt 17.2 min) and *N*-methyl-L-phenylalanine (Rt 16.2 min): retention times of standard *N*-methyl-L-phenylalanine and *N*-methyl-D-phenylalanine were 16.2 and 18.3 min, respectively.

4.7. Cathepsin B Inhibition Assay

The cathepsin B inhibitory activity was determined according to the method described in Chapter I.

4.8. MTT Assay against HeLa Cells

HeLa human cervical cancer cells (Cell Resource Center for Biomedical Research, Tohoku University) were cultured in Dulbecco's modified Eagle's medium containing 10% fetal bovine serum and 2 μg/mL of antibiotic-antimycotic (Gibco) at 37 °C under an atmosphere of 5% CO_2. To each well of the 96-well microplate containing 200 μL tumor cell suspension (1×10^4 cells/mL), the test solution was added and the plate was incubated at 37 °C for 72 h. After addition of 50 μL of 3-(4,5-dimethylthiazol-2-yl)-2,5-diphenyltetrazolium bromide (MTT) saline solution (1 mg/mL) to each well, the plate was incubated for 3 h under the same condition. After the incubation, the supernatant was removed and the cells dissolved in 150 μL of DMSO to determine the IC_{50} values.

5. Supporting Information

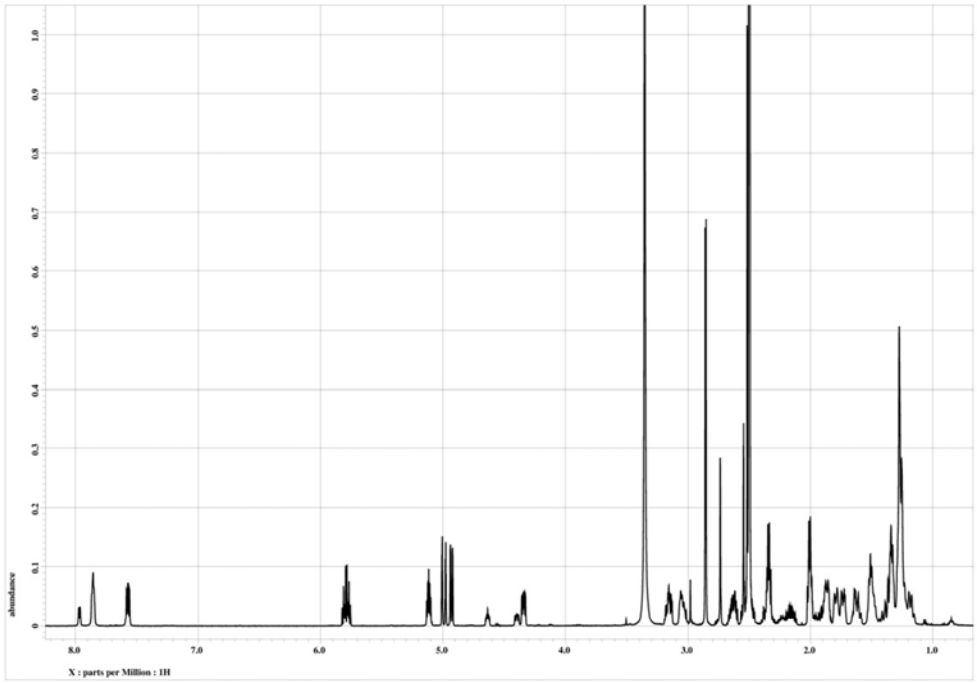

Figure S2-1. ^{1}H NMR spectrum of ciliatamide D (**2-1**) in DMSO-d_6.

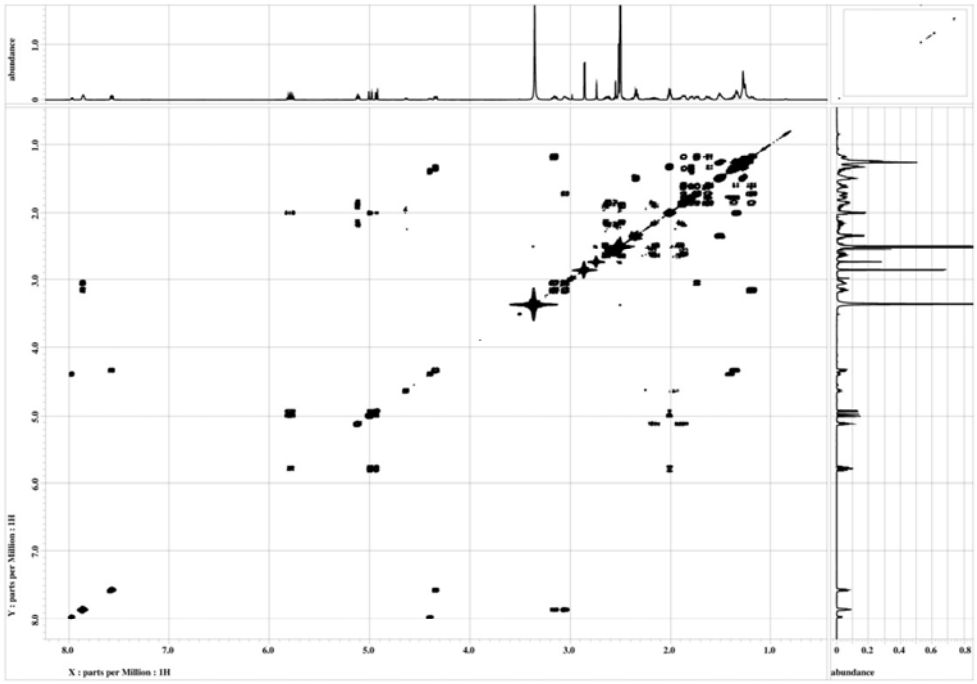

Figure S2-2. COSY spectrum of ciliatamide D (**2-1**) in DMSO-d_6.

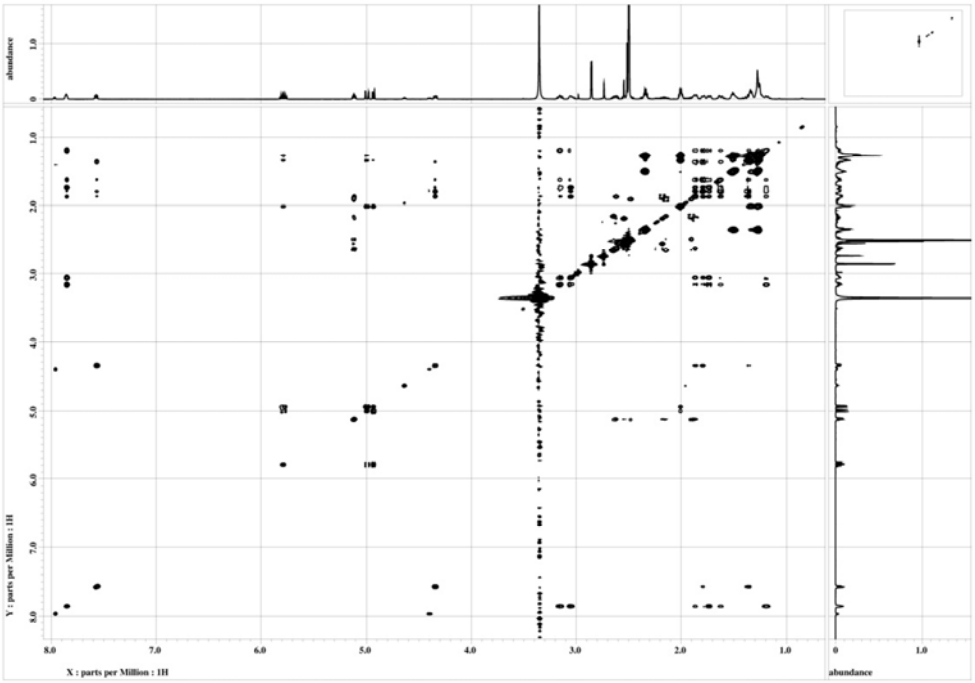

Figure S2-3. TOCSY spectrum of ciliatamide D (**2-1**) in DMSO-d_6.

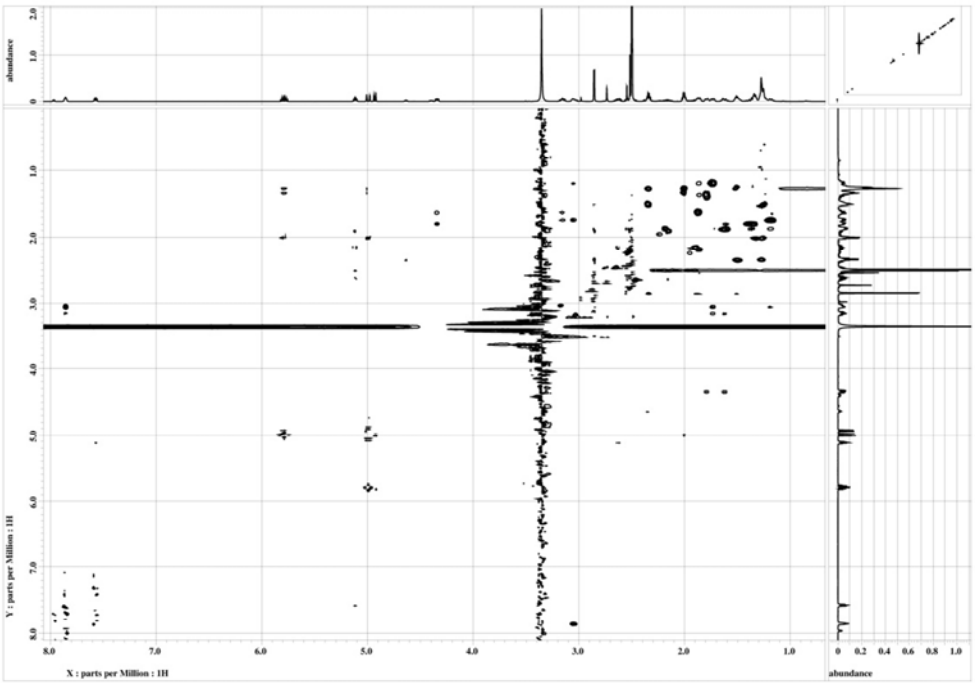

Figure S2-4. NOESY spectrum of ciliatamide D (**2-1**) in DMSO-d_6.

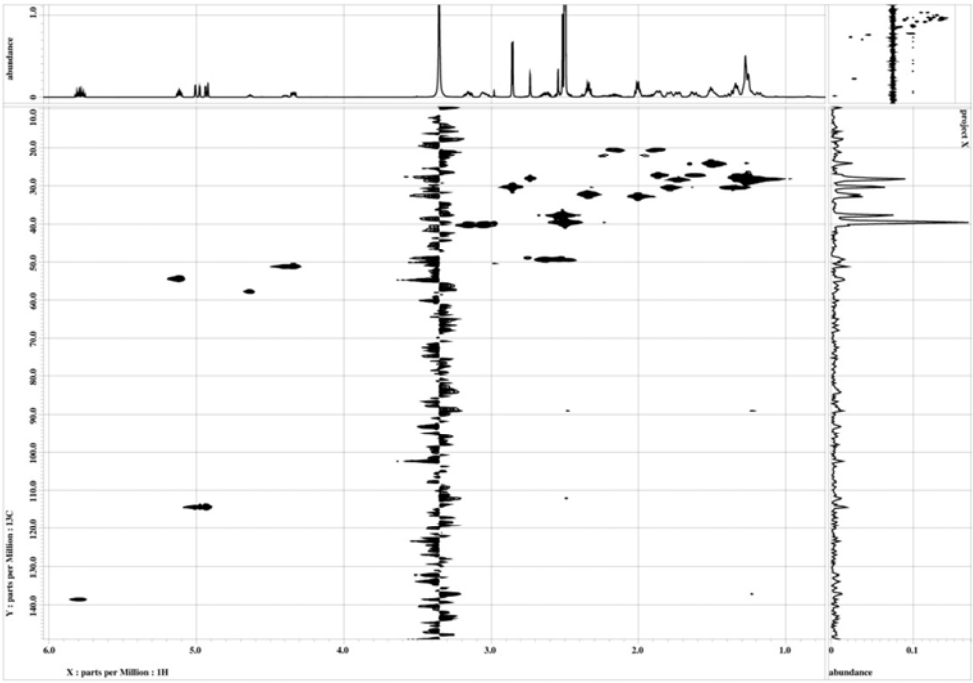

Figure S2-5. HSQC spectrum of ciliatamide D (**2-1**) in DMSO-d_6.

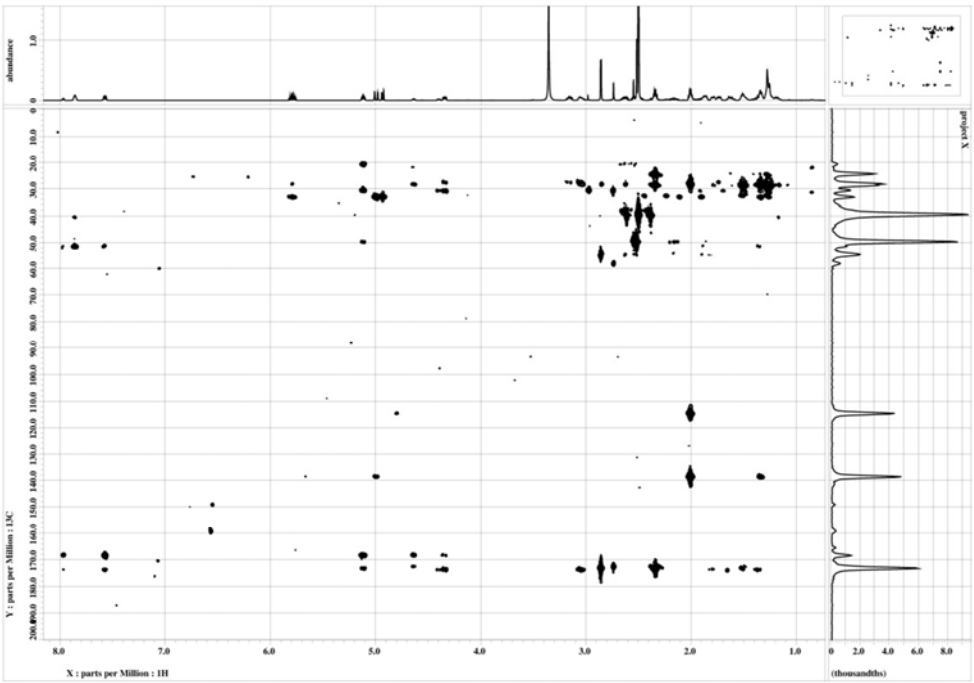

Figure S2-6. HMBC spectrum of ciliatamide D (**2-1**) in DMSO-d_6.

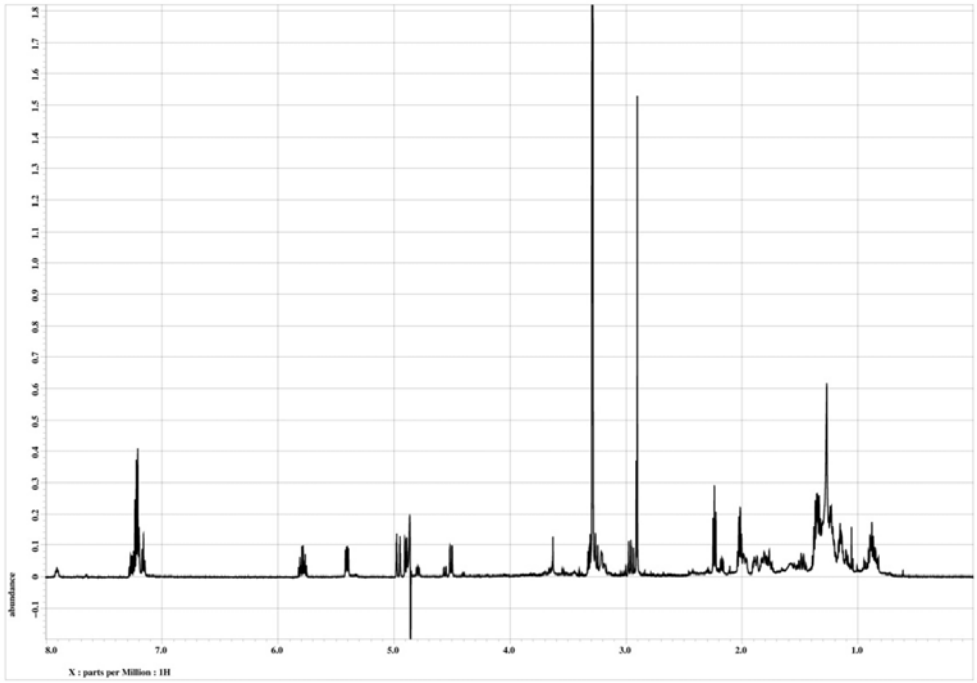

Figure S2-7. ^{1}H NMR spectrum of ciliatamide A (**2-2**) in CD_3OD.

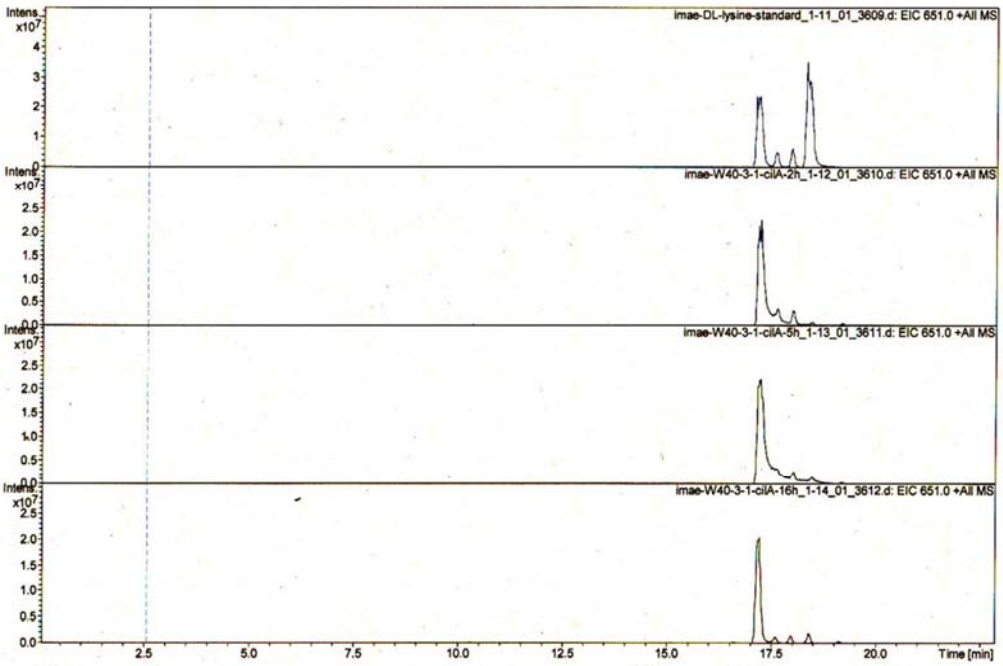

Figure S2-8. LC-MS chromatogram charts of L-FDAA derivatives of Lys.
(a) L-Lys (left) and D-Lys (right); (b) Lys in 2 h hydrolysates;
(c) Lys in 5 h hydrolysates; (d) Lys in 16 h hydrolysates (top to bottom).

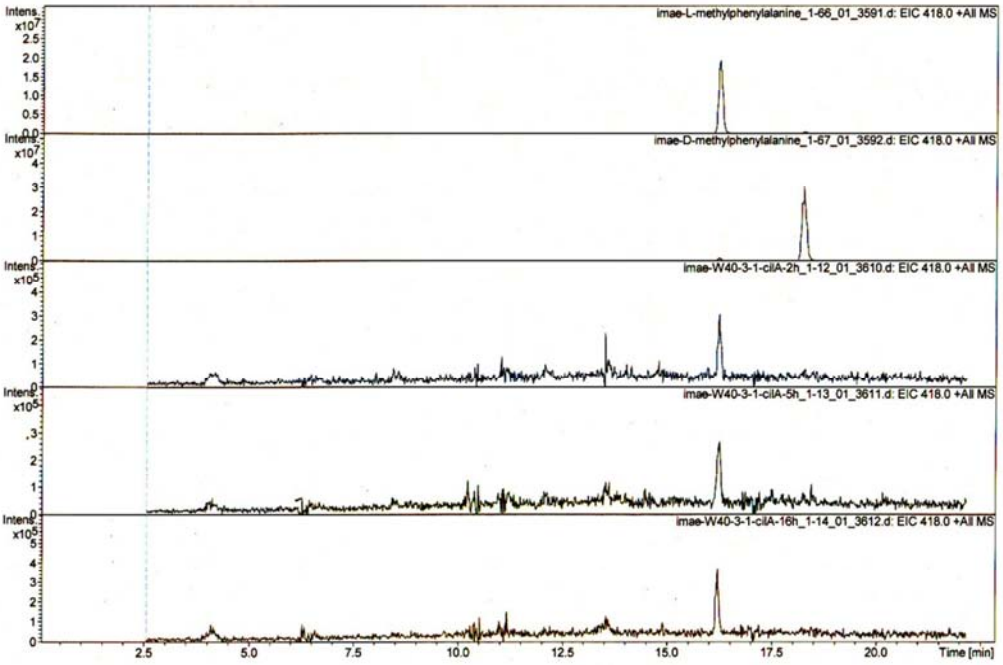

Figure S2-9. LC-MS chromatogram charts of L-FDAA derivatives of *N*-Me-Phe.
(a) *N*-Me-L-Phe; (b) *N*-Me-D-Phe; (c) *N*-Me-Phe in 2 h hydrolysates;
(d) *N*-Me-Phe in 5 h hydrolysates; (e) *N*-Me-Phe in 16 h hydrolysates (top to bottom).

Chapter III

Isolation of New HDAC1 Inhibitors from an Unidentified Japanese Marine Sponge

1. Introduction

The extract of an unidentified marine sponge collected at Yakushinsone (Figure 3-1) exhibited significant inhibitory activity against HDAC1. Bioassay-guided fractionation of the extract afforded four active compounds, tentatively named compounds A–D (**3-1**–**3-4**). The planar structures of **3-1**–**3-3** were determined by spectroscopic methods including FAB-MS/MS analysis to be composed of an *O*-methyl proline and a penta-oxygenated fatty acid. The relative configuration of the 1,2,3-trioxygenated moiety in the fatty acid was determined by comparing the chemical shift values of the degradation products with those in the literature. The absolute configuration of the proline residue was elucidated by chemical methods. This chapter deals with the isolation, planar structures, stereochemical study, and the biological activity of compounds A–D.

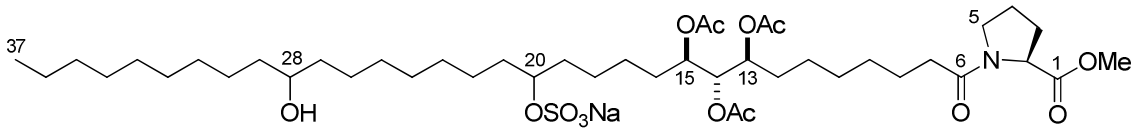

Compound A (**3-1**)

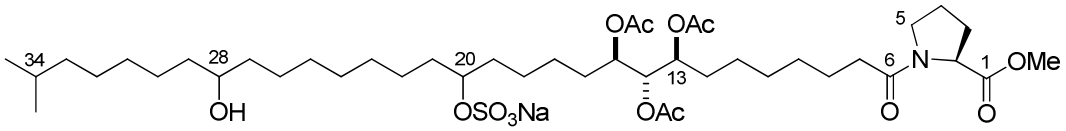

Compound B (**3-2**)

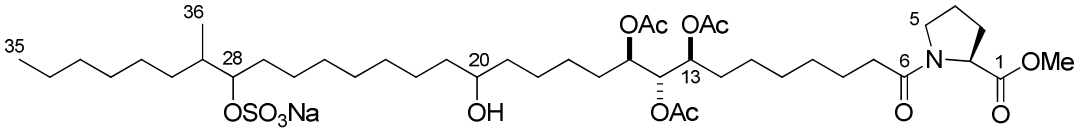

Compound C (**3-3**)

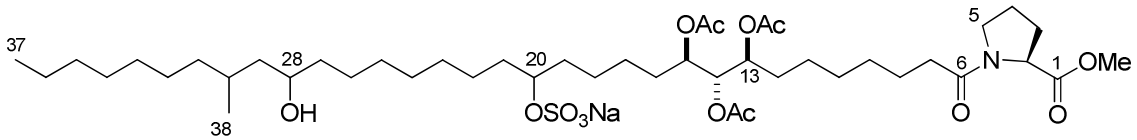

Compound D (**3-4**)

2. Results and Discussion

2.1. Extraction and Isolation

The MeOH and EtOH extracts of the marine sponge (340 g, wet weight) were combined and subjected to solvent partitioning, ODS flash chromatography, gel filtration, SiO_2 column chromatography, and RP-HPLC (Figure 3-2) to provide compound A (**3-1**, 8.4 mg), compound B (**3-2**, 5.6 mg), compound C (**3-3**, 5.7 mg), and compound D (**3-4**, 5.8 mg).

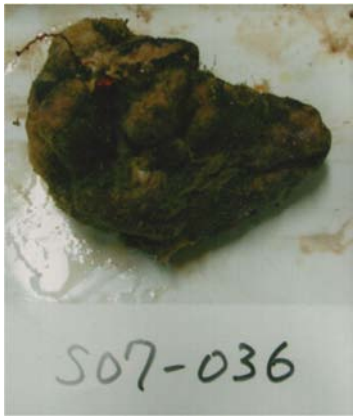

Figure 3-1. An unidentified marine sponge collected at Yakushinsone.

Sponge (340 g)

MeOH (900 mL) ×2
EtOH (900 mL) ×1

H_2O/$CHCl_3$
90% MeOH/*n*-hexane
60% MeOH/$CHCl_3$

ODS flash chromatography (70% MeCN frc.)

Gel filtration

SiO_2 column chromatography

RP-HPLC
(Cosmosil AR-II ×2,
MeOH with phosphate buffer)

RP-HPLC
(Cosmosil AR-II,
MeCN with phosphate buffer)

Compound A (**4-1**, 8.4 mg)
Compound B (**4-2**, 5.6 mg)
Compound C (**4-3**, 5.7 mg)
Compound D (**4-4**, 5.8 mg)

Figure 3-2. Isolation procedure of compound A–D (**3-1**–**4**).

2.2. Structure Elucidation

Compound A (**3-1**) had a molecular formula of $C_{44}H_{78}O_{14}NSNa$ as determined by HRESIMS. A fragment ion peak due to a loss of SO_3Na (*m*/*z* 102) was observed in the positive FABMS, indicating the presence of a sulfate group.[41] An analysis of the ^1H NMR data in combination with the HSQC spectrum exhibited the presence of five oxygenated methines, one methoxy, one nitrogenous methine, one nitrogenous methylene, three singlet methyls, one terminal methyl, and a large methylene envelope (Table 3-1, Figure S3-1 and S3-6). Some signals were split in a 6:1 ratio, which implied the presence of a conformational equilibrium.

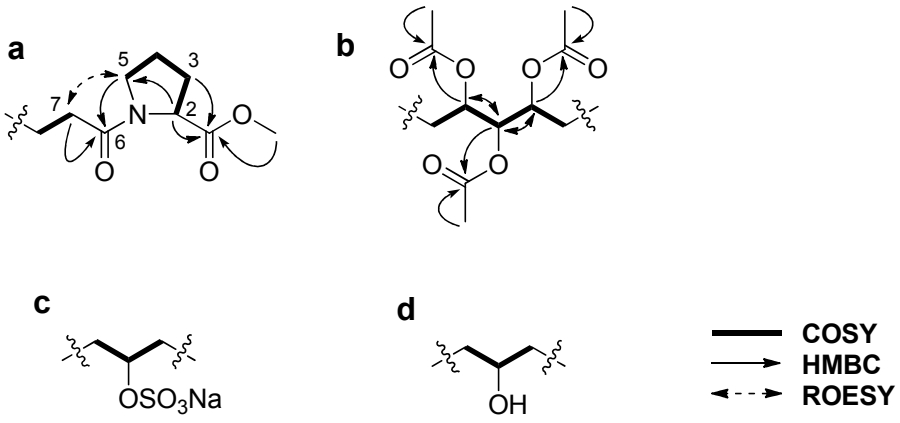

Figure 3-3. Partial structures of compound A (**3-1**).

Interpretation of the COSY and HMBC data established the presence of a proline residue (Figure 3-3, substructure **a**). HMBC correlations from H-2 (δ_H 4.41), H_2-3 (δ_H 2.24 and 1.95), and 1-OMe protons (δ_H 3.70) to C-1 (δ_C 174.3) suggested the proline residue was *O*-methylated. HMBC correlations from H_2-5 (δ_H 3.65 and 3.31)

and methylene protons H_2-7 (δ_H 2.39 and 2.34) to C-6 (δ_C 174.3) demonstrated the connection between the proline residue and a fatty acid via an amide bond. Analysis of the HSQC and HMBC spectra revealed the presence of three acetyl groups, two of which had identical ^{1}H and ^{13}C chemical shifts. The three acetyl groups were vicinally placed to form a 1,2,3-trioxygenated system, which was established by interpretation of the COSY and HMBC data (substructure **b**). The ^{1}H and ^{13}C chemical shift values (δ_H 4.31, H-20; δ_C 80.5, C-20) indicated that C-20, one of the two remaining oxygenated methines, was sulfated (substructure **c**). There remained one oxygenated methine, one terminal methyl, and unfunctionalized methylenes, suggesting that the oxygenated methine was substituted by a hydroxyl group (substructure **d**). Therefore, **3-1** should be an *O*-methyl proline derivative connected to a long-chain fatty acid through an amide bond. To determine the location of the substituents in the alkyl chain, we conducted FAB-MS/MS analysis of compound **3-5**, one of the acid hydrolysates of **3-1**. The FAB-MS/MS data for **3-5** indicated that C-13, C-14, C-15, C-20, and C-28 were oxygenated (Figure 3-4 and S3-39), establishing that C-13, C-14, and C-15 were all substituted by an acetoxy group.

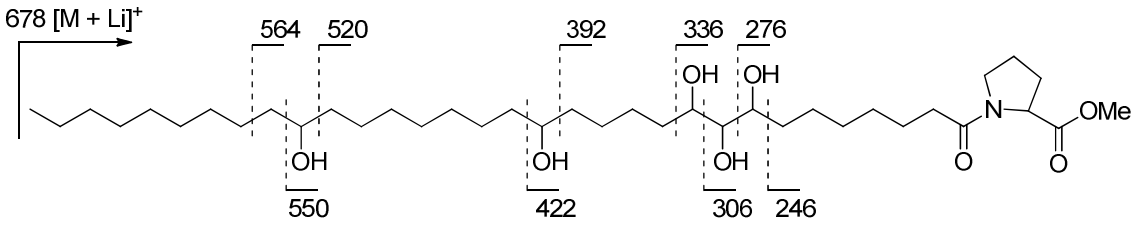

Figure 3-4. FAB-MS/MS analysis of **3-5**.

Interpretation of the HSQC-TOCSY data for **1** permitted us to determine the position of sulfation. In the HSQC-TOCSY data, a correlation from an acetoxylated

methine proton H-15 (δ_H 5.02) to C-19 (δ_C 35.0), the neighboring carbon of the sulfated methine, was observed (Figure S3-9). This evidence suggested that the sulfate was located at C-20, completing the planar structure of compound A.

The signal splitting in a 6:1 ration due to a conformational equilibrium was observed at signals for ^{1}H and ^{13}C composing the proline residue, implying geometrical isomerism of the amide bond. It is well documented that *cis*/*trans* conformational differences of proline bonds can be distinguished by the chemical shift differential values between proline β- and γ-carbons ($\Delta\delta_{\beta\gamma}$).[54] In the major conformer of **3-1** the differential value $\Delta\delta_{\beta\gamma}$ was 4.5 ppm, indicating that the amide bond was *trans*, while the amide bond in the minor conformer was *cis* ($\Delta\delta_{\beta\gamma}$ = 8.6 ppm). The *trans* conformation in the major conformer was also supported by a ROESY cross-peak between H_2-5 and H_2-7 (Figure 3-3).

The relative configuration of the triacetoxy moiety was determined by comparing ^{1}H and ^{13}C chemical shifts of **3-5** and those of 1,5,6,7-decanetetraol (**3-9a**–**3-9d**).[55] The ^{1}H and ^{13}C chemical shift values of **3-5** were consistent with (α,β,α)-1,5,6,7-decanetetraol (**3-9b**, *anti-anti* configuration), indicating that the triacetoxy moiety of **3-1** and **3-5** had *anti-anti* configuration (Figure 3-5, Table S3-1, and S3-2).

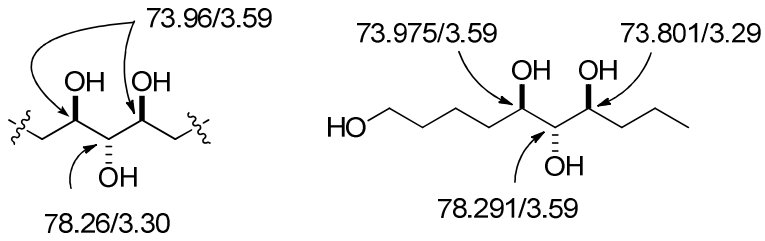

Figure 3-5. ^{13}C and ^{1}H NMR chemical shift values (δ_C/δ_H) of **3-5** (left) and **3-9b** (right) in CD_3OD.[55]

The absolute configuration of the proline residue in **3-1** was elucidated by Marfey's method.[53] The standard D- and L-proline and the hydrolysates of **3-1** were derivatized with L-FDAA followed by LC-MS analysis, which demonstrated that the proline residue in **3-1** had L-configuration.

Compound B (**3-2**) had a molecular formula of $C_{43}H_{76}O_{14}NSNa$, which is smaller than **3-1** by a CH_2 unit. The ^{1}H and ^{13}C NMR spectra for **3-2** were almost identical to those for **3-1** except for the presence of an isopropyl moiety instead of a terminal methyl. FAB-MS/MS analysis of **3-6**, a hydrolysate of **3-2**, revealed that the oxygenation pattern of **3-2** was same as that of **3-1** (Figure 3-6 and S3-40). The location of the sulfate was determined by interpretation of the HSQC-TOCSY data for **3-2** (Figure S3-18), which completed the planar structure of **3-2**.

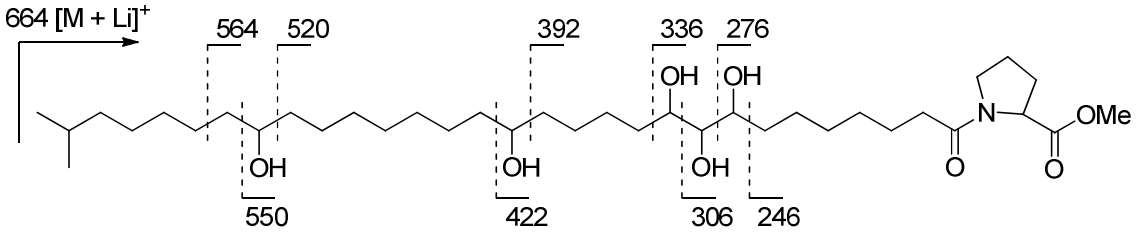

Figure 3-6. FAB-MS/MS analysis of **3-6**.

The molecular formula of compound C (**3-3**) was identical to that of **3-2** ($C_{43}H_{76}O_{14}NSNa$). The COSY and HMBC data for **3-3** demonstrated the presence of a methyl branch adjacent to the sulfated carbon. The locations of the other substituents were established by FAB-MS/MS analysis of an acid hydrolysate **3-8**, revealing that the oxygenation sites of **3-7** were identical to those of **3-1** and C-29 was methylated (Figure 3-7 and S3-41). This indicated that the sulfate was attached to C-28. The sulfation of C-28 and the hydroxylation of C-20 were supported by the HSQC-TOCSY spectrum (Figure S3-27), in which correlations from acetoxylated methine proton H-15 (δ_H 5.03) to C-19 (δ_C 38.3) and from hydroxylated methine proton H-20 (δ_H 3.49) to C-16 (δ_C 30.5) were observed.

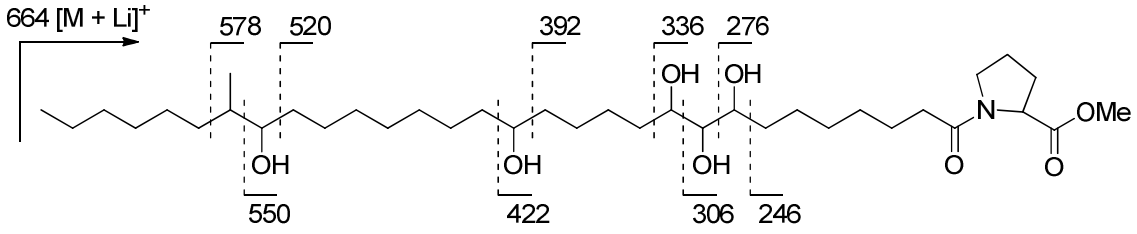

Figure 3-7. FAB-MS/MS analysis of **3-7**. The peak for *m*/*z* 564 was not observed.

Compound D (**3-4**) had a molecular formula of $C_{45}H_{80}O_{14}NSNa$, which is

larger than **3-1** by a CH_2 unit. Interpretation of the COSY, HSQC, and HMBC data revealed that **3-4** had the same substructures as **3-1** except for the presence of an additional secondary methyl. FAB-MS/MS analysis of **3-8**, an acid hydrolysate of **3-4**, demonstrated that the secondary methyl was attached to C-30 (Figure 3-8 and S3-42). In the HSQC-TOCSY spectrum of **3-4**, correlations from an acetoxylated methine proton H-15 (δ_H 5.02) to C-19 (δ_C 35.1) and from the hydroxyl methine proton H-28 (δ_H 3.61) to the secondary methyl carbon C-38 (δ_C 21.0) were observed (Figure S3-36), which suggested the sulfation of C-20 and the hydroxylation of C-28.

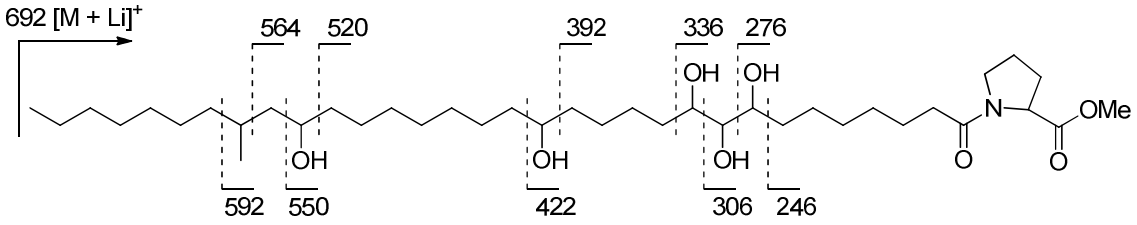

Figure 3-8. FAB-MS/MS analysis of **3-8**. The peak for *m*/*z* 578 was not observed.

Table 3-1. ^{1}H and ^{13}C NMR Data for Compounds A (**3-1**) and B (**3-2**) in CD_3OD

	Compound A (**3-1**)			Compound B (**3-2**)	
Position	δ_H (J in Hz)	δ_C	Position	δ_H (J in Hz)	δ_C
1		174.3 [174.1][a]	1		174.4 [174.0][a]
2	4.41 (dd, 8.7, 4.3) [4.62 (dd, 8.7, 2.5)][a]	60.1 [60.8][a]	2	4.41 (dd, 8.7, 4.4) [4.63 (dd, 8.7, 2.5)][a]	60.1 [60.8][a]
3	2.24, 1.95 (m) [2.31, 2.17 (m)][a]	30.1 [32.0][a]	3	2.24, 1.95 (m) [2.32, 2.17 (m)][a]	30.0 [32.0][a]
4	2.01 (m) [1.93, 1.87 (m)][a]	25.6 [23.4][a]	4	2.02 (m) [1.93, 1.87 (m)][a]	25.6 [23.4][a]
5	3.65, 3.61 (m) [3.55, 3.50 (m)][a]	48.4 [47.4][a]	5	3.65, 3.61 (m) [3.55, 3.50 (m)][a]	48.3 [47.3][a]
1-OMe	3.70 (s) [3.76 (s)][a]	52.6 [53.1][a]	1-OMe	3.70 (s) [3.76 (s)][a]	52.5 [53.0][a]
6		174.3 [174.6][a]	6		174.4 [174.6][a]
7	2.39, 2.34 (dt, 7.6, 7.7) [2.12, 2.26 (m)][a]	34.9	7	2.39, 2.34 (dt, 7.5, 7.7) [2.12, 2.26 (m)][a]	34.9
8	1.62 (m)	25.6	8	1.60 (m)	25.6
9	1.35 (m)	29.9	9	1.35 (m)	29.9
10	1.3[b]	30[b]	10	1.3[b]	30[b]
11	1.38 (m)	26.0	11	1.40 (m)	25.9
12	1.65 (m), 1.61 (m)	30.5	12	1.65, 1.61 (m)	30.4
13	5.02 (m)	73.0	13	5.02 (m)	73.1
14	5.11 (t, 5.0)	74.6	14	5.11 (t, 5.0)	74.6
15	5.02 (m)	73.0	15	5.02 (m)	73.1
16	1.65, 1.61 (m)	30.5	16	1.65, 1.61 (m)	30.4
17	1.3[b]	30.6	17	1.3[b]	30[b]
18	1.40 (m)	25.6	18	1.40 (m)	25.8
19	1.62 (m)	35.0	19	1.62 (m)	35.0
20	4.31 (dt, 5.9, 5.9)	80.5	20	4.31 (dt, 5.9, 5.9)	80.5
21	1.64 (m)	35.3	21	1.63 (m)	35.2
22	1.40 (m)	25.6	22	1.40 (m)	25.8
23	1.3[b]	30[b]	23	1.3[b]	30[b]
24	1.3[b]	30[b]	24	1.3[b]	30[b]
25	1.3[b]	30.5	25	1.3[b]	30[b]
26	1.43, 1.32 (m)	26.7	26	1.44, 1.32 (m)	26.7
27	1.42 (m)	38.3	27	1.43 (m)	38.4
28	3.50 (m)	72.3	28	3.50 (m)	72.2
29	1.42 (m)	38.3	29	1.43 (m)	38.4
30	1.43, 1.32 (m)	26.7	30	1.44, 1.32 (m)	26.7
31	1.3[b]	30.5	31	1.3[b]	30[b]
32	1.3[b]	30[b]	32	1.3[b]	30[b]
33	1.3[b]	30[b]	33	1.19 (m)	40.0
34	1.3[b]	30.3	34	1.53 (dq, 6.6, 6.6)	29.1
35	1.29 (m)	32.9	35	0.88 (d, 6.6)	22.9
36	1.31 (m)	23.6	36	0.88 (d, 6.6)	22.9
37	0.90 (t, 7.1)	14.4			
13-OAc C=O		172.0	13-OAc C=O		172.1
CH_3	2.04 (s)	20.8	CH_3	2.04 (s)	20.7
14-OAc C=O		171.5	14-OAc C=O		171.6
CH_3	2.07 (s)	20.6	CH_3	2.07 (s)	20.6
15-OAc C=O		172.0	15-OAc C=O		172.1
CH_3	2.04 (s)	20.8	CH_3	2.04 (s)	20.7

[a] Signals for the minor conformer. [b] Signals were overlapped.

Table 3-2. ^{1}H and ^{13}C NMR Data for Compounds C (**3-3**) and D (**3-4**) in CD_3OD

	Compound C (**3-3**)				Compound D (**3-4**)	
Position	δ_H (J in Hz)	δ_C		Position	δ_H (J in Hz)	δ_C
1		174.6 [174.3][a]		1		174.5 [174.2][a]
2	4.41 (dd, 8.7, 4.3) [4.63 (dd, 8.7, 2.5)][a]	60.1 [60.8][a]		2	4.42 (dd, 8.7, 4.3) [4.63 (dd, 8.7, 2.5)][a]	60.2 [60.9][a]
3	2.24, 1.95 (m) [2.32, 2.17 (m)][a]	30.2 [32.2][a]		3	2.25, 1.96 (m) [2.32, 2.18 (m)][a]	30.3 [32.1][a]
4	2.02 (m) [1.93, 1.87 (m)][a]	25.9 [23.6][a]		4	2.02 (m) [1.93, 1.87 (m)][a]	25.8 [23.5][a]
5	3.65, 3.61 (m) [3.55, 3.50 (m)][a]	48.5 [47.5][a]		5	3.66, 3.62 (m) [3.56, 3.50 (m)][a]	48.4 [47.6][a]
1-OMe	3.70 (s) [3.76 (s)][a]	52.8 [53.1][a]		1-OMe	3.71 (s) [3.77 (s)][a]	52.6 [53.3][a]
6		174.6 [174.8][a]		6		174.5 [174.7][a]
7	2.39, 2.34 (dt, 7.6, 7.7) [2.12, 2.26 (m)][a]	35.2		7	2.39, 2.34 (dt, 7.6, 7.7) [2.12, 2.26 (m)][a]	35.1
8	1.60 (m)	25.6		8	1.61 (m)	25.7
9	1.35 (m)	29.9		9	1.35 (m)	30.1
10	1.3[b]	30[b]		10	1.3[b]	30[b]
11	1.36 (m)	26.5		11	1.40 (m)	26.0
12	1.66, 1.61 (m)	30.5		12	1.67, 1.61 (m)	30.7
13	5.03 (m)	73.1		13	5.02 (m)	73.1
14	5.11 (t, 5.0)	74.7		14	5.12 (t, 5.0)	74.8
15	5.03 (m)	73.1		15	5.02 (m)	73.1
16	1.66, 1.61 (m)	30.5		16	1.67, 1.61 (m)	30.7
17	1.3[b]	30[b]		17	1.3[b]	30[b]
18	1.3[b]	30[b]		18	1.40	26.0
19	1.44, 1.38 (m)	38.3		19	1.62 (m)	35.1
20	3.49 (m)	72.4		20	4.32 (dt, 5.9, 5.9)	80.7
21	1.43 (m)	38.6		21	1.62 (m)	35.3
22	1.3[b]	30[b]		22	1.40 (m)	26.0
23	1.3[b]	30[b]		23	1.3[b]	30[b]
24	1.3[b]	30[b]		24	1.3[b]	30[b]
25	1.3[b]	30[b]		25	1.3[b]	30[b]
26	1.44, 1.33 (m)	26.5		26	1.43, 1.33 (m)	26.6
27	1.69, 1.59 (m)	32.0		27	1.43, 1.36 (m)	38.7
28	4.24 (ddd, 6.5, 6.3, 3.7)	84.4		28	3.61 (m)	70.4
29	1.85 (m)	37.1		29	1.35, 1.28 (m)	46.1
30	1.58, 1.14 (m)	33.4		30	1.60 (m)	30.4
31	1.33 (m)	28.6		31	1.38, 1.10 (m)	37.9
32	1.3[b]	30[b]		32	1.3[b]	30[b]
33	1.30 (m)	33.2		33	1.3[b]	30[b]
34	1.31 (m)	23.9		34	1.3[b]	30[b]
35	0.90 (t, 6.3)	14.6		35	1.30 (m)	33.1
36	0.90 (d, 6.7)	15.3		36	1.32 (m)	23.7
				37	0.91 (t, 7.0)	14.4
				38	0.90 (d, 6.9)	21.0
13-OAc C=O		172.0		13-OAc C=O		172.1
CH_3	2.04 (s)	20.9		CH_3	2.05 (s)	21.0
14-OAc C=O		171.6		14-OAc C=O		171.7
CH_3	2.07 (s)	20.6		CH_3	2.07 (s)	20.8
15-OAc C=O		172.0		15-OAc C=O		172.1
CH_3	2.04 (s)	20.9		CH_3	2.05 (s)	21.0

[a] Signals for the minor conformer. [b] Signals were overlapped.

2.3. Biological Activity

Compound A (**3-1**), B (**3-2**), C (**3-3**), and D (**3-4**) inhibited HDAC1 with IC_{50} values of 6.5, 21, 10, and 5.7 μg/mL, respectively.

3. Conclusion

In this study, four new compounds (**3-1**–**3-4**) were isolated from an unidentified marine sponge collected at Yakushinsone. Compounds A–D (**3-1**–**3-4**) encompass a proline residue and a sulfated fatty acid, analogous to penarolide sulfates A_1 (**3-10**), A_2 (**3-11**),[56] and penasulfate A (**3-12**).[57] The most significant structural difference of compounds A–D from the known natural products is the presence of the contiguous triacetoxy substituents. The regioselectivity of sulfation in their biosynthesis is intriguing, which results in the diversification of sulfated position in the fatty acid of compounds A–D.

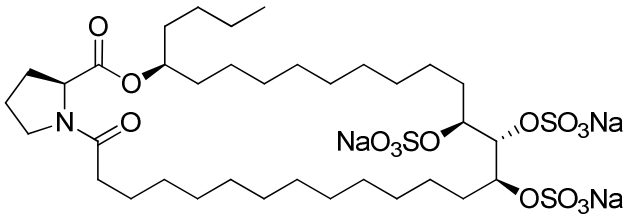

3-10

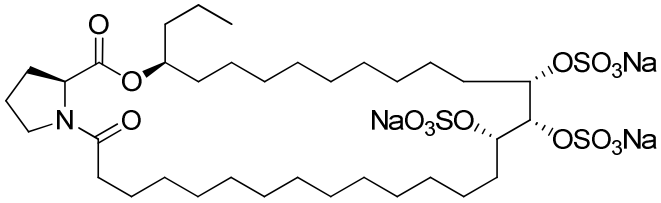

3-11

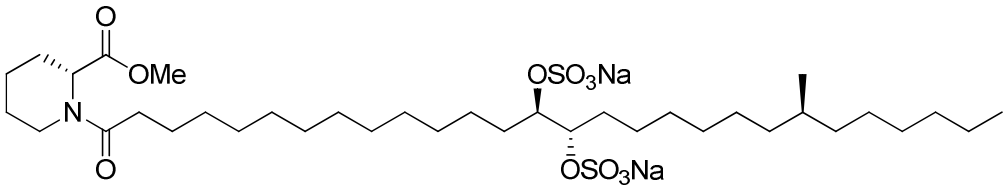

3-12

Figure 3-9. Structures of the related compounds.

4. Experimental Section

4.1. General Experimental Procedures

Optical rotations were measured on a JASCO DIP-1000 digital polarimeter. UV spectra were determined in MeOH using a Shimadzu BioSpec-1600 spectrophotometer. NMR spectra were recorded on a JEOL delta 600 NMR spectrometer at 600 MHz for ^{1}H and 150 MHz for ^{13}C. Chemical shifts were referenced to the solvent peaks of CD_3OD: 3.31 ppm for ^{1}H and 49.15 ppm for ^{13}C. ESI mass spectra were measured on a JEOL JMS-T100LC time-of-flight mass spectrometer. FAB mass spectra were measured on a JEOL JMS-700T MStation. Fluorescence for the enzyme inhibition assay was detected on a Molecular Devices SPECTRA MAX fluorescence spectrometer. Marfey's analyses were conducted with a Shimadzu Prominence UFLC equipped with Bruker amaZon SL.

4.2. Animal Material

The sponge sample was collected by dredging at a depth of 130 m at Yakushinsone (29° 47' N; 130° 20' E) in 2007. The specimen was frozen after collection and kept at – 20 °C until extraction.

4.3. Extraction and Isolation

The sponge (340 g, wet weight) was homogenized and extracted with MeOH

(900 mL) twice and EtOH (900 mL) once. The extracts were combined and partitioned between H_2O and $CHCl_3$. The $CHCl_3$ layer was concentrated and partitioned between 90% MeOH and *n*-hexane. The 90% MeOH layer was diluted with H_2O to give a 60% MeOH solution, which was extracted with $CHCl_3$. The latter $CHCl_3$ layer was separated with ODS flash chromatography using a stepwise gradient elution (20–70% MeOH, 70–90% MeCN, and MeOH). The 70% MeCN fraction was separated by gel filtration on Sephadex LH-20 column with $CHCl_3$/MeOH (1:1). The active fractions were combined and chromatographed on silica gel using a stepwise gradient elution ($CHCl_3$/MeOH/H_2O: 98:2:0, 9:1:0, 8:2:0.1, 7:3:0.5, 6:4:1, and 5:5:1). The fractions eluted with 9:1:0 and 8:2:0.1 of $CHCl_3$/MeOH/H_2O were combined and separated by RP-HPLC using two columns connected in tandem (Cosmosil AR-II; 20 × 250 mm, 8.0 mL/min) with eluent consisting of 8:2 of MeOH/phosphate buffer I (28 mM Na_2HPO_4 and 12 mM KH_2PO_4) to provide four active fractions; fraction C eluted retention times between 40 and 44 min; fraction B eluted between 46 and 49 min; fraction A eluted between 66 and 72 min; and fraction D eluted between 79 and 86 min. Fraction A was purified by RP-HPLC (Cosmosil AR-II; 20 × 250 mm) with eluent consisting of 6:4 of MeCN/phosphate buffer II (14 mM Na_2HPO_4 and 8 mM KH_2PO_4) to afford compound A (**3-1**, 8.4 mg). Fraction B was purified by RP-HPLC (Cosmosil AR-II; 20 × 250 mm) with eluent consisting of 55:45 of MeCN/phosphate buffer II to furnish compound B (**3-2**, 5.6 mg). Fraction C was purified by RP-HPLC (Cosmosil AR-II; 20 × 250 mm) with eluent consisting of 5:5 of MeCN/phosphate buffer II to give compound C (**3-3**, 5.7 mg). Fraction D was purified by RP-HPLC (Cosmosil AR-II; 20 × 250 mm) with eluent consisting of 65:35 of MeCN/phosphate buffer II to provide compound D (**3-4**, 5.8 mg).

*Compound A (**3-1**)*: clear oil; $[\alpha]_D^{25}$ – 20 (*c* 0.4, MeOH); UV (MeOH) λ_{max} 216 nm (ε 4,700); ^{1}H and ^{13}C NMR data, see Table 3-1; HRESIMS *m*/*z* 922.4983 $[M + Na]^+$ (calcd for $C_{44}H_{78}O_{14}NSNa_2$, 922.4938).

*Compound B (**3-2**)*: clear oil; $[\alpha]_D^{24}$ – 15 (*c* 0.2, MeOH); UV (MeOH) λ_{max} 208 nm (ε 4,100); ^{1}H and ^{13}C NMR data, see Table 3-1; HRESIMS *m*/*z* 908.4768 $[M + Na]^+$ (calcd for $C_{43}H_{76}O_{14}NSNa_2$, 908.4782).

*Compound C (**3-3**)*: clear oil; $[\alpha]_D^{23}$ – 26 (*c* 0.25, MeOH); UV (MeOH) λ_{max} 209 nm (ε 4,900); ^{1}H and ^{13}C NMR data, see Table 3-2; HRESIMS *m*/*z* 908.4767 $[M + Na]^+$ (calcd for $C_{43}H_{76}O_{14}NSNa_2$, 908.4782).

*Compound D (**3-4**)*: clear oil; $[\alpha]_D^{24}$ – 26 (*c* 0.25, MeOH); UV (MeOH) λ_{max} 206 nm (ε 6,700); ^{1}H and ^{13}C NMR data, see Table 3-2; HRESIMS *m*/*z* 936.5058 $[M + Na]^+$ (calcd for $C_{45}H_{80}O_{14}NSNa_2$, 936.5095).

4.4. Acid Hydrolysis of **3-1**, **3-2**, **3-3**, and **3-4**.

A 0.5 mg portion of **3-1** was dissolved in 5 N HCl/MeOH (1:4) and heated at 100 °C for 1 h. The solution was neutralized with 1 N $NaHCO_3$ and desalted with InertSep RP-1 to give compound **3-5**. In the same manner **3-6**, **3-7**, and **3-8** were prepared from **3-2**, **3-3**, and **3-4**, respectively.

3-5: ^{1}H NMR (CD_3OD) δ 4.4 (H-2), 3.70 (1-OMe), 3.65 and 3.61 (H_2-5), 3.59

(H-14), 3.51 (H-20 and H-28), 3.30 (H-13 and H-15), 2.37 (H_2-7), 2.24 and 1.96 (H_2-3), 2.02 (H_2-4), 1.43 (H_2-19, H_2-21, H_2-27, and H_2-29), 1.42 (H_2-12 and H_2-16), 1.31 (H_2-36), 0.90 (H_3-37); ^{13}C chemical shifts (HSQC) δ 78.3 (C-13 and C-15), 60.1 (C-2), 52.7 (1-OMe), 48.4 (C-5), 38.4 (C-19, C-21, C-27, and C-29), 35.1 (C-7), 33.5 (C-12 and C-16), 30.2 (C-3), 25.7 (C-4), 23.7 (C-36), 14.4 (C-37); FABMS *m*/*z* 694 $[M + Na]^+$.

4.5. Marfey's Analysis[53]

Compound A (**3-1**) was dissolved in 6 N HCl (150 μL) and heated at 110 °C for 2 h. The solution was concentrated and redissolved in 50 μL of H_2O. 1% L-FDAA in acetone (100 μL) and 1 M $NaHCO_3$ (20 μL) were added to the solution. The mixture was heated at 40 °C for 1 h. After cooling to room temperature, the reaction mixtures were quenched with 5 N HCl (4 μL), concentrated, and redissolved in DMSO. DL- and L-proline standards were treated with L-FDAA in the same manner. The L-FDAA derivatives were analyzed by LC-MS [Cosomosil 2.5C_{18}-MS-II (2.0 × 100 mm); flow rate, 0.5 mL/min; solvent, 10–50% MeCN containing 0.5% AcOH (22 min)]. Retention time (Rt) of each amino acid was as follows: L-proline (10.5 min), DL-proline (10.4 and 11.3 min). The absolute configuration of the proline residue in **3-1** was determined as L (Rt 10.5 min)

4.6. Cell Culture

HeLa cells overexpressing Flag-tagged HDAC1 were cultured in D-MEM

medium (High Glucose; Wako) supplemented with 10% fetal bovine serum and 1% penicillin-streptomycin (GIBCO) at 37 °C under an atmosphere of 5% CO_2 in a 10 cm dish.

4.7. Extraction of HDAC1

HeLa cells overexpressing Flag-tagged HDAC1 cultured in a 10 cm dish were washed with 5 mL of PBS, scraped, suspended in 1 mL of PBS, and centrifuged at 2,000 rpm for 1 min. The pellet was suspended in 400 μL of lysis buffer (50 mM Tris-HCl, 120 mM NaCl, 5 mM EDTA, 0.5% Nonidet P-40, adjusted to pH 7.5), which was sonicated at 0 °C and centrifuged at 15,000 rpm for 15 min at 4 °C. To the cooled supernatant was added 40 μL of Protein A/G PLUS-Agarose (Santa Cruz), and the mixture was stirred overnight at 4 °C. The mixture was centrifuged at 3,000 rpm for 5 min. The pellet was removed and 20 μg of α Flag M2 Antibody (Sigma) was added to the supernatant. The mixture was stirred for 2 hours at 4 °C. After the stir, 40 μL of Protein A/G PLUS-Agarose was added to the mixture, which was stirred overnight at 4 °C. The stirred mixture was centrifuged at 3,000 rpm for 5 min to remove the supernatant, and the precipitated agarose beads were washed with 1 mL of lysis buffer three times. The washed beads were suspended in 1 mL of HD buffer (20 mM Tris-HCl, 150 mM NaCl, 10% glycerol, adjusted to pH 8.0) and centrifuged at 2,000 rpm for 1 min. The pellet was resuspended in 200 μL of HD buffer. To the mixture was added 40 μg of Flag peptide (Sigma), and stirred at 4 °C for over 2 hours. The mixture was centrifuged at 3,000 rpm for 5 min to obtain HDAC1 solution as the supernatant.

4.8. HDAC1 Inhibition Assay

Substrate solution (Boc-Lys(Ac)-AMC, 2mM in DMSO) was diluted with eight volumes of HD buffer. A 9 μL portion of the diluted substrate solution was added to each well of 96 well microtiter plates. To each substrate solution, a test solution (1 μL) and HDAC1 solution (10 μL) were added. After 30 min incubation at 37 °C, 30 μL of trypsin solution (20 mg/mL in H_2O) was added to each mixture. The mixture was incubated for 15 min at 37 °C. The fluorescence of the reaction mixture was measured with an excitation at 390 nm and an emission at 460 nm.

5. Supporting Information

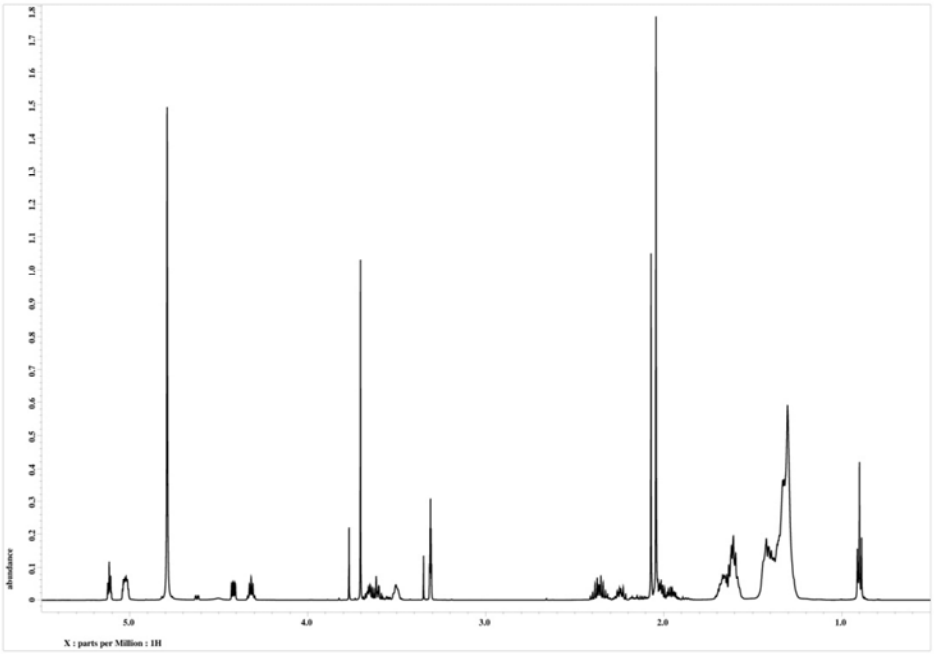

Figure S3-1. ^{1}H NMR spectrum of compound A (**3-1**) in CD_3OD.

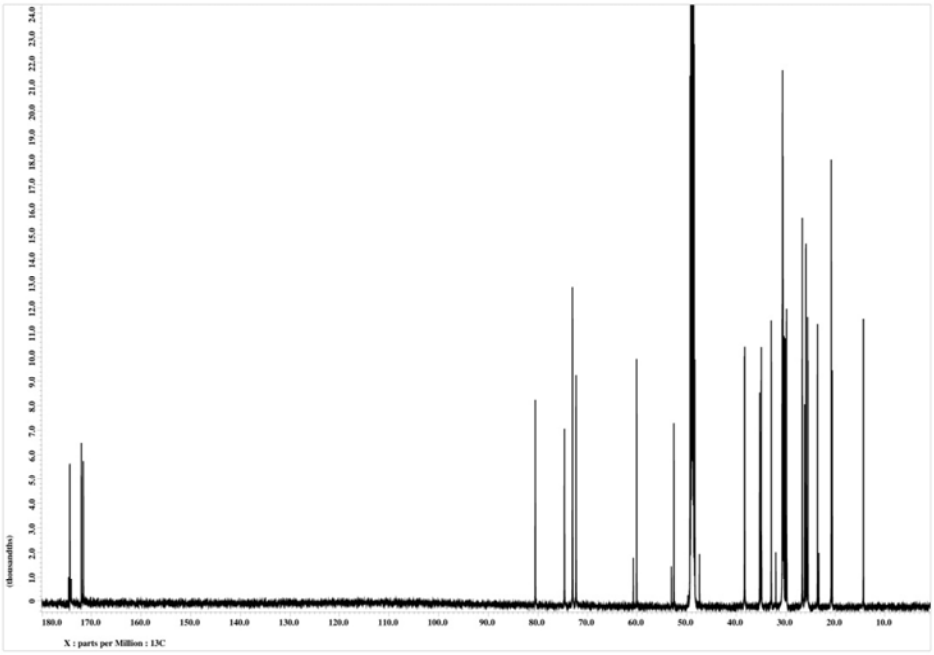

Figure S3-2. ^{13}C NMR spectrum of compound A (**3-1**) in CD_3OD.

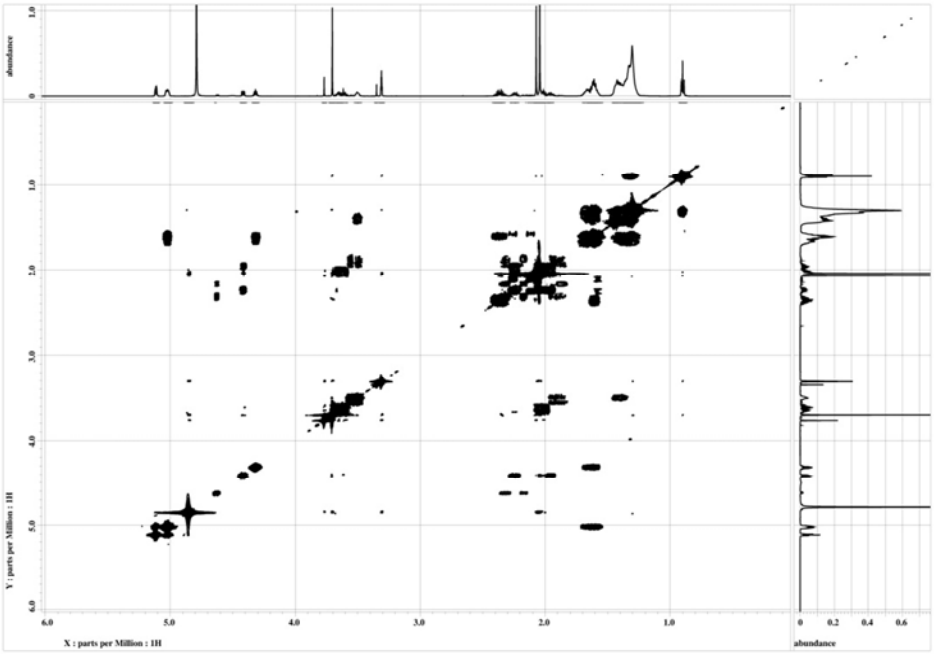

Figure S3-3. COSY spectrum of compound A (**3-1**) in CD_3OD.

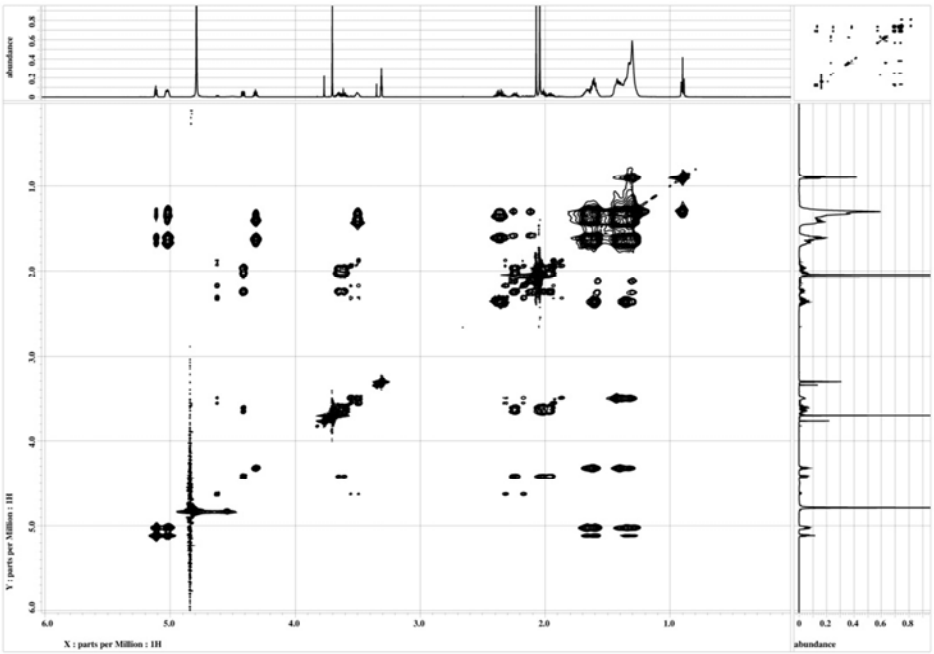

Figure S3-4. TOCSY spectrum of compound A (**3-1**) in CD_3OD.

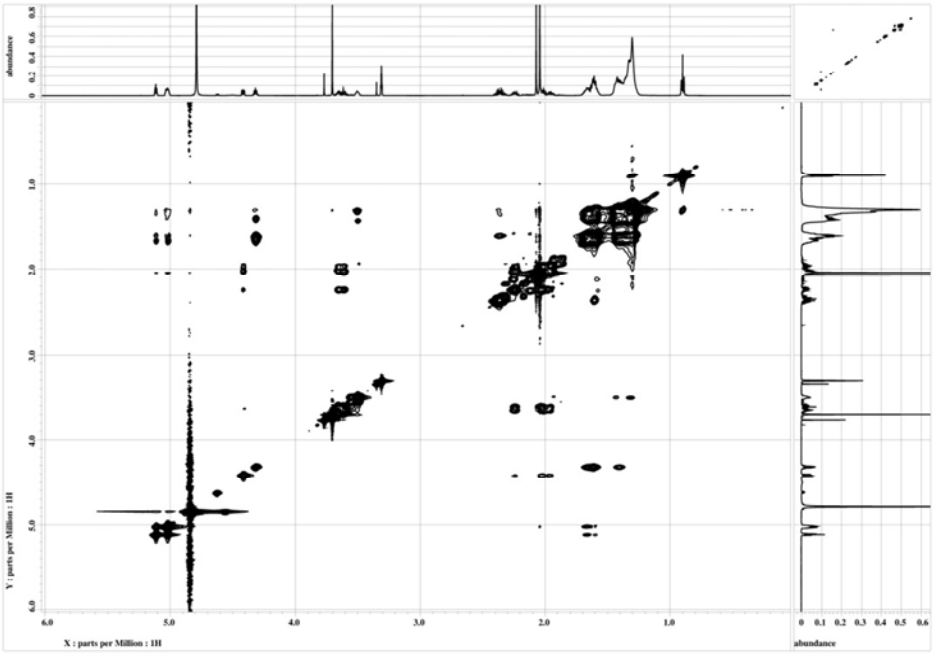

Figure S3-5. ROESY spectrum of compound A (**3-1**) in CD_3OD.

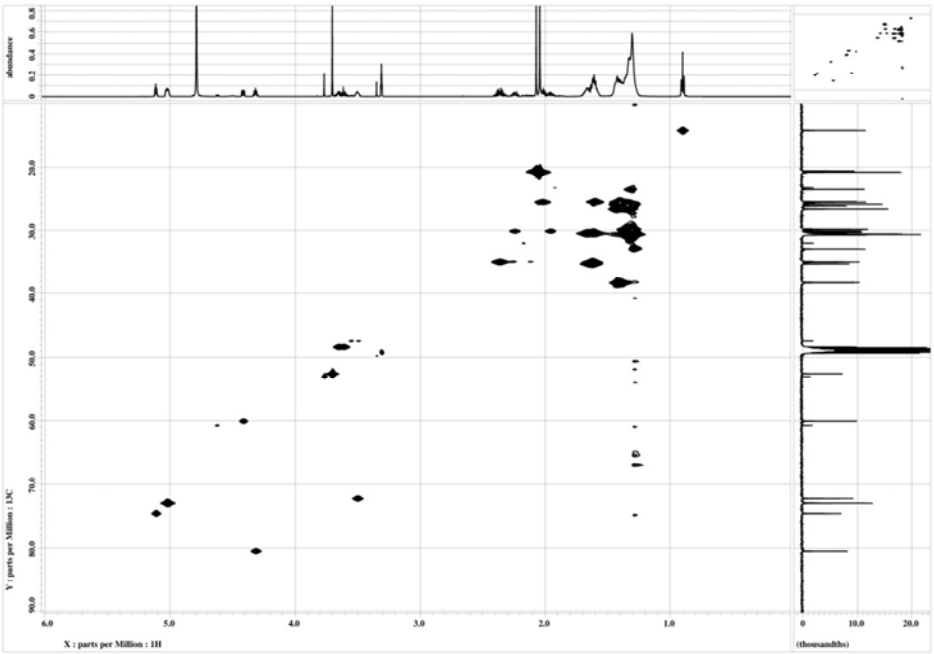

Figure S3-6. HSQC spectrum of compound A (**3-1**) in CD_3OD.

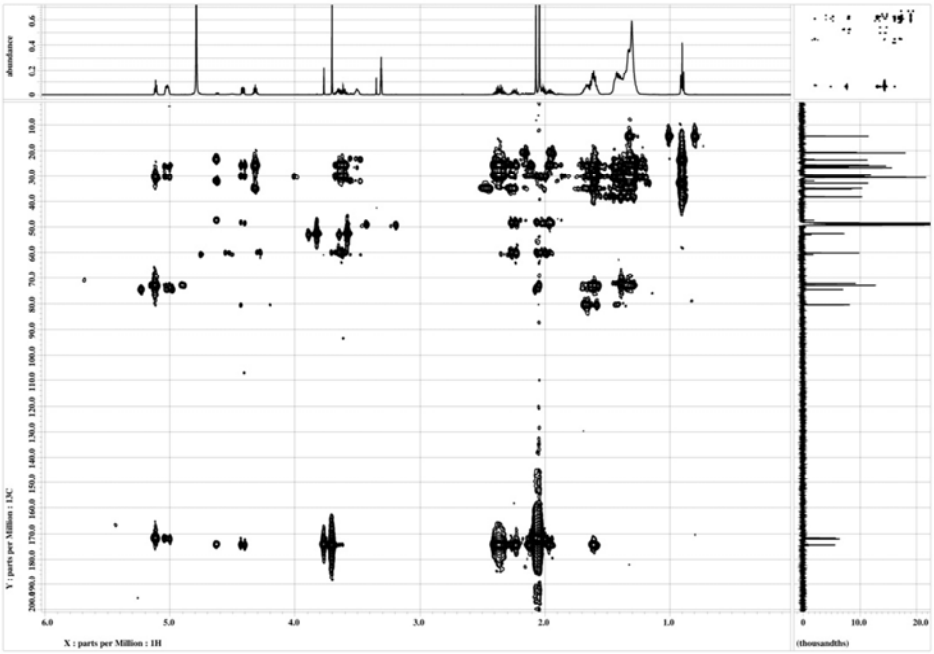

Figure S3-7. HMBC spectrum of compound A (**3-1**) in CD_3OD.

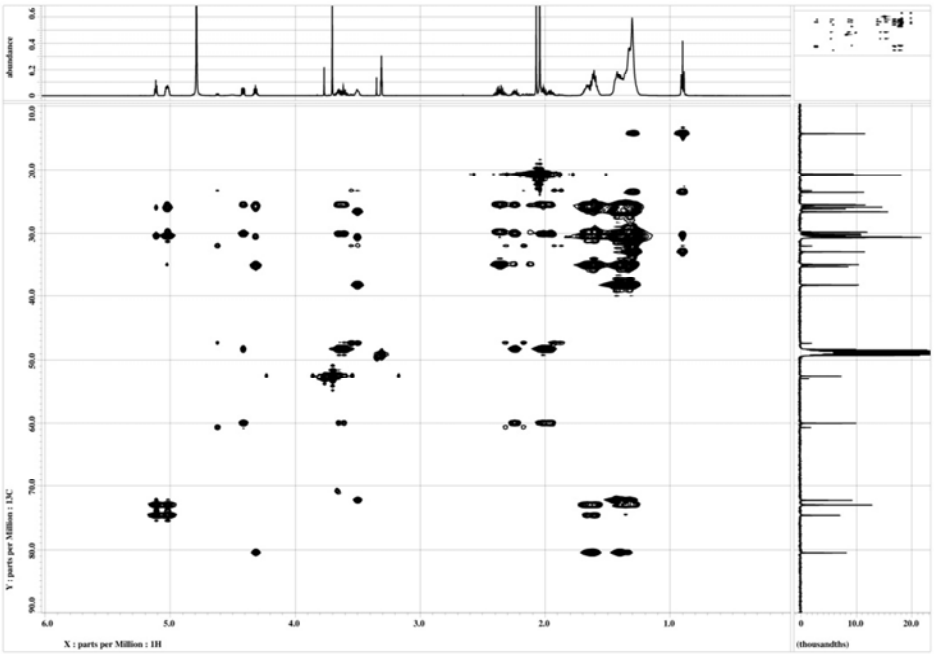

Figure S3-8. HSQC-TOCSY spectrum of compound A (**3-1**) in CD_3OD.

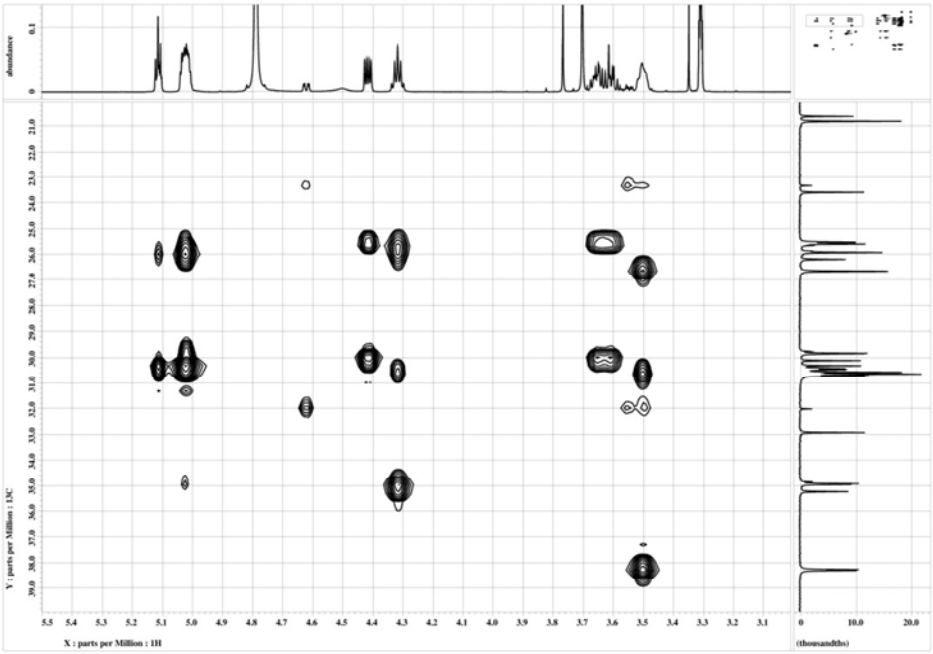

Figure S3-9. Partial HSQC-TOCSY spectrum of compound A (**3-1**) in CD_3OD.

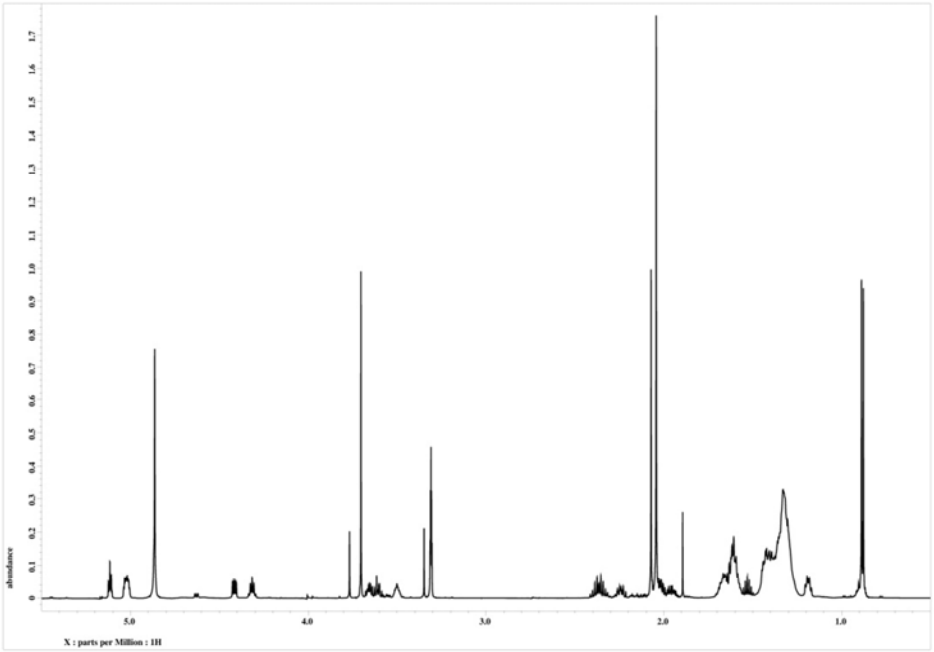

Figure S3-10. ^1H NMR spectrum of compound B (**3-2**) in CD_3OD.

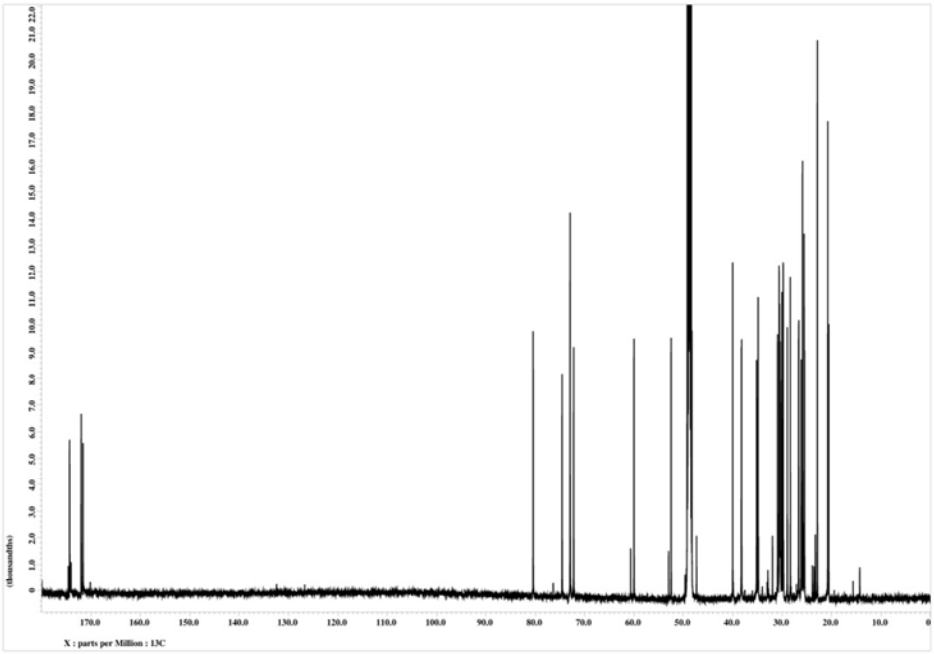

Figure S3-11. ^{13}C NMR spectrum of compound B (**3-2**) in CD_3OD.

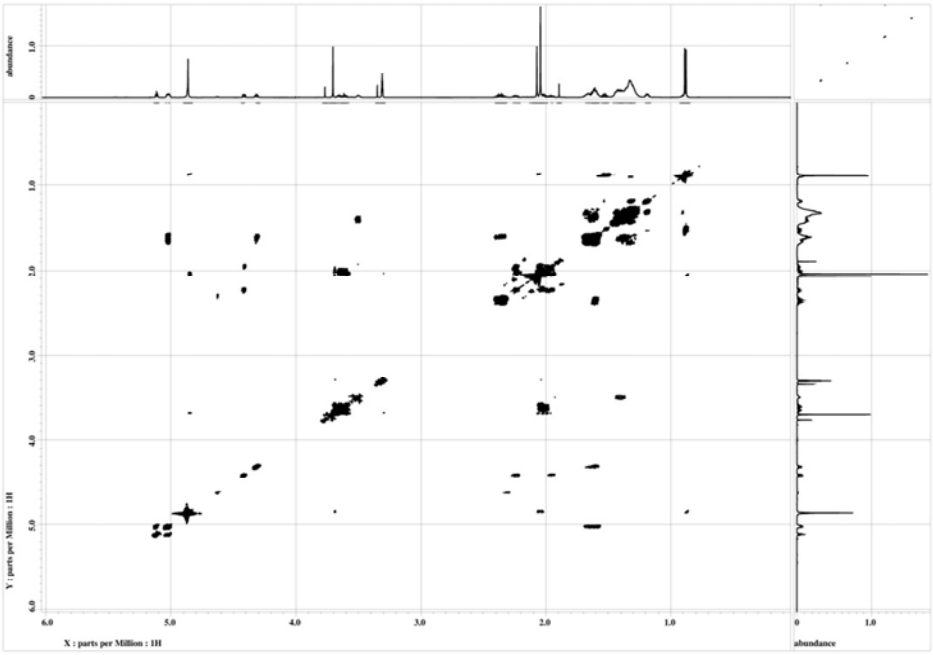

Figure S3-12. COSY spectrum of compound B (**3-2**) in CD_3OD.

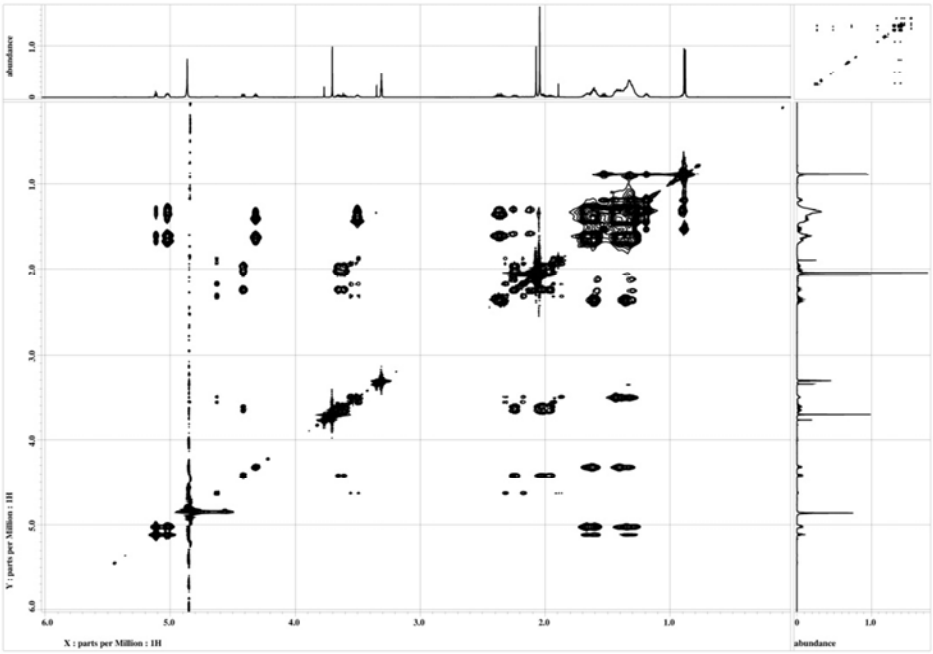

Figure S3-13. TOCSY spectrum of compound B (**3-2**) in CD_3OD.

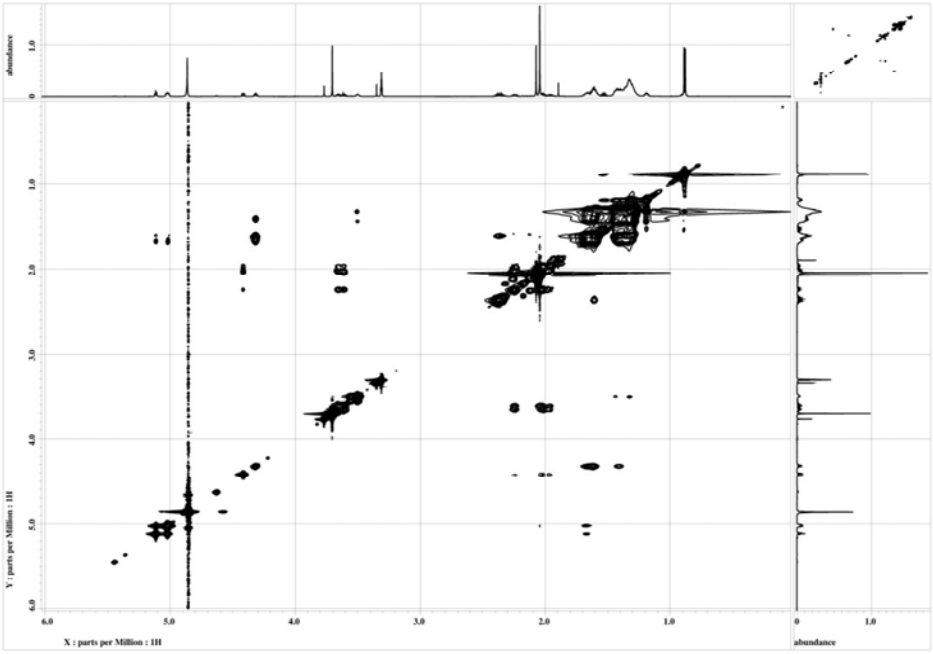

Figure S3-14. ROESY spectrum of compound B (**3-2**) in CD_3OD.

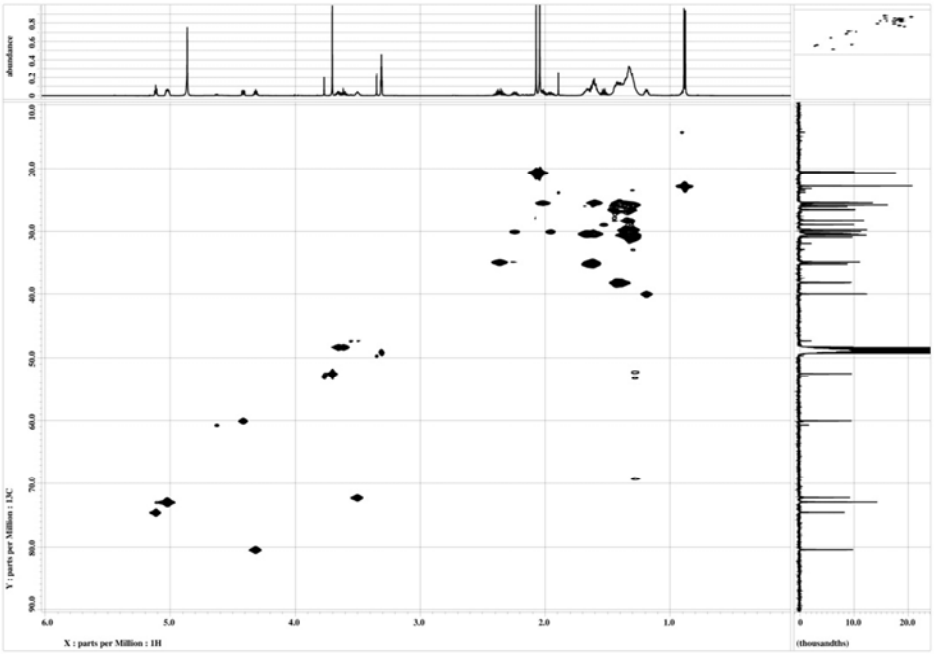

Figure S3-15. HSQC spectrum of compound B (**3-2**) in CD_3OD.

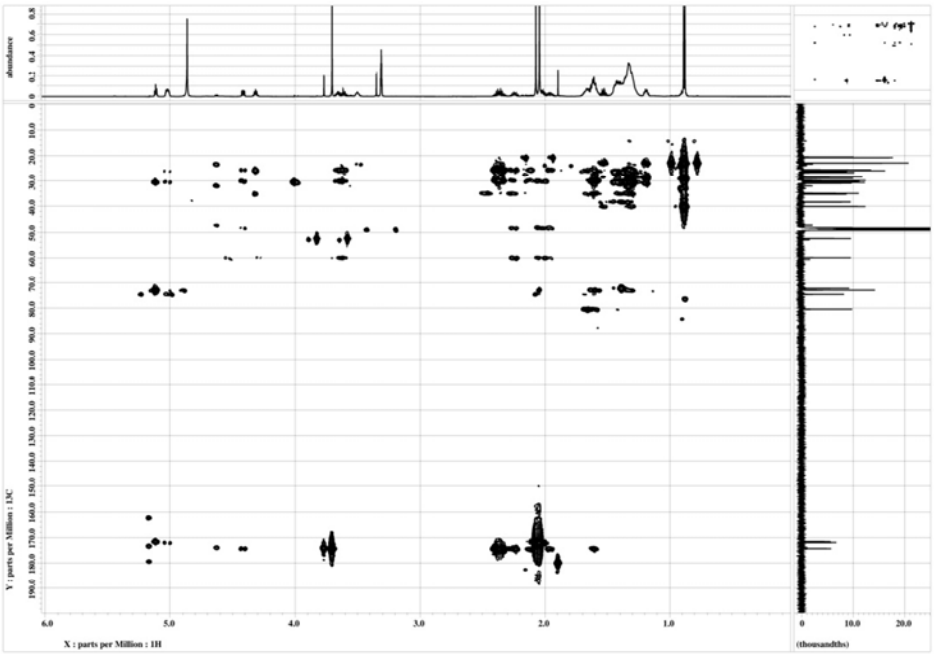

Figure S3-16. HMBC spectrum of compound B (**3-2**) in CD_3OD.

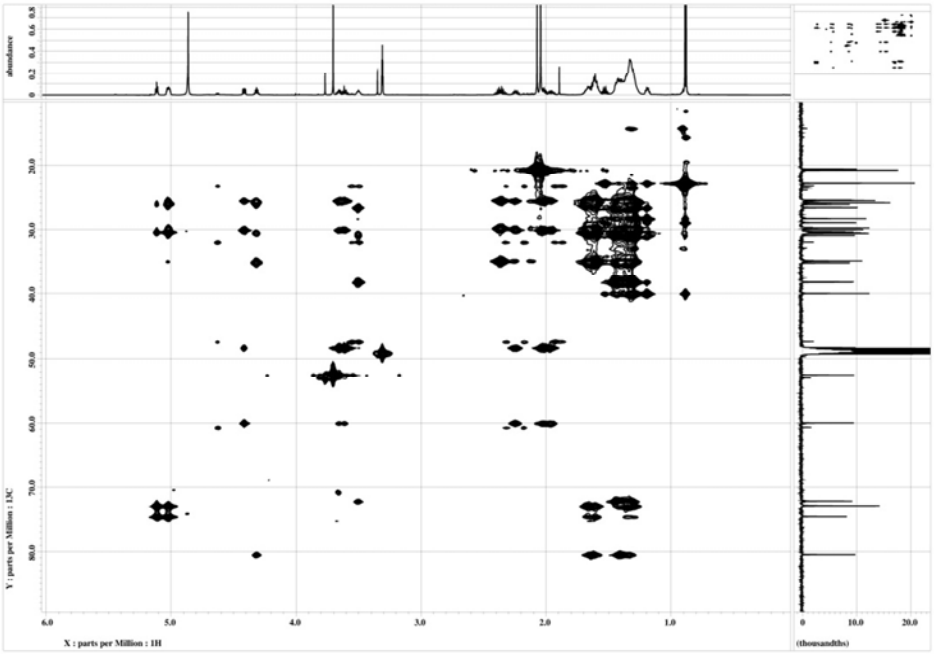

Figure S3-17. HSQC-TOCSY spectrum of compound B (**3-2**) in CD_3OD.

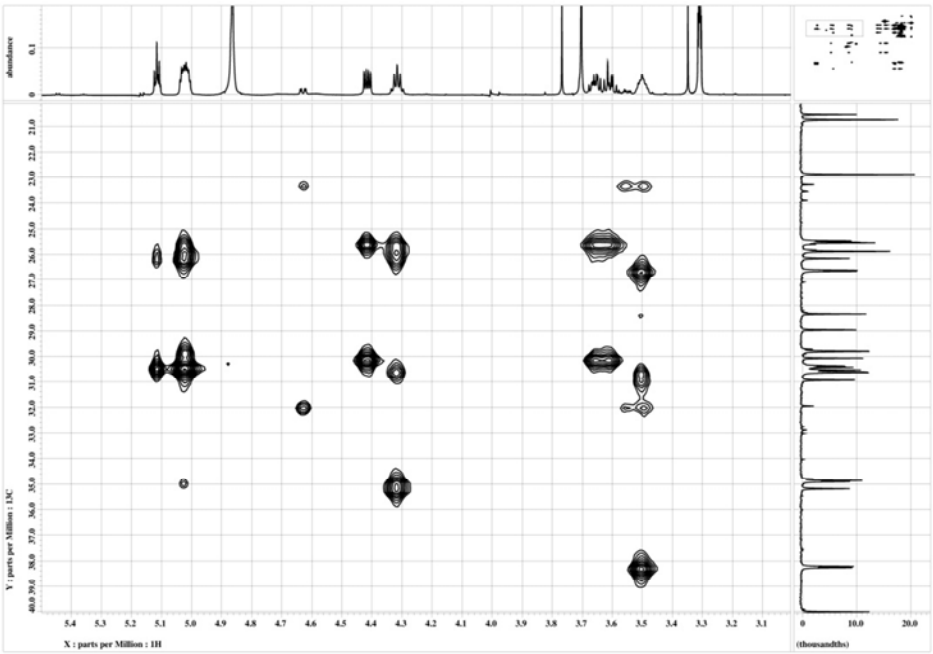

Figure S3-18. Partial HSQC-TOCSY spectrum of compound B (**3-2**) in CD_3OD.

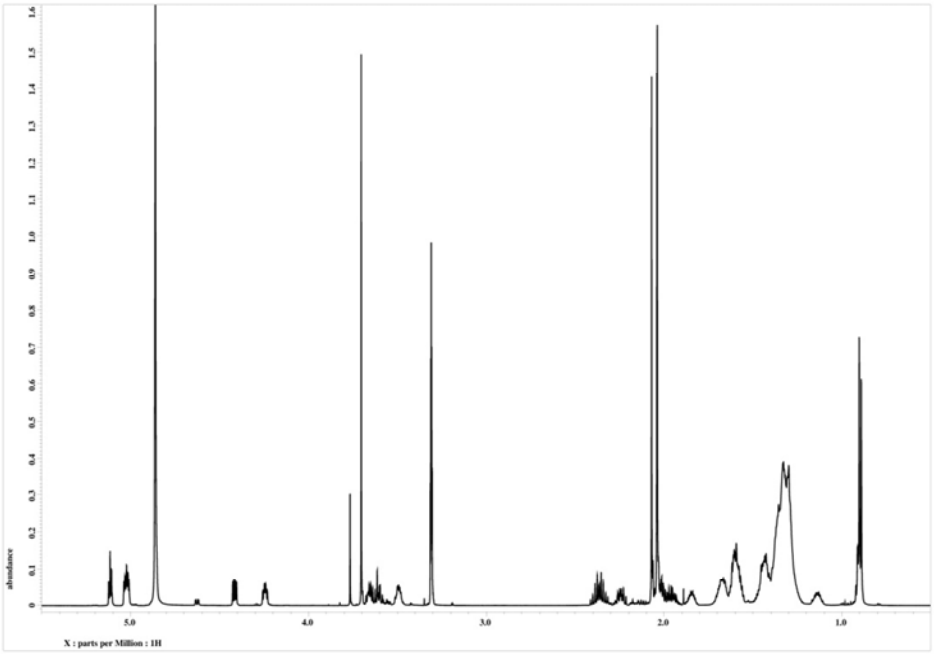

Figure S3-19. ^{1}H NMR spectrum of compound C (**3-3**) in CD_3OD.

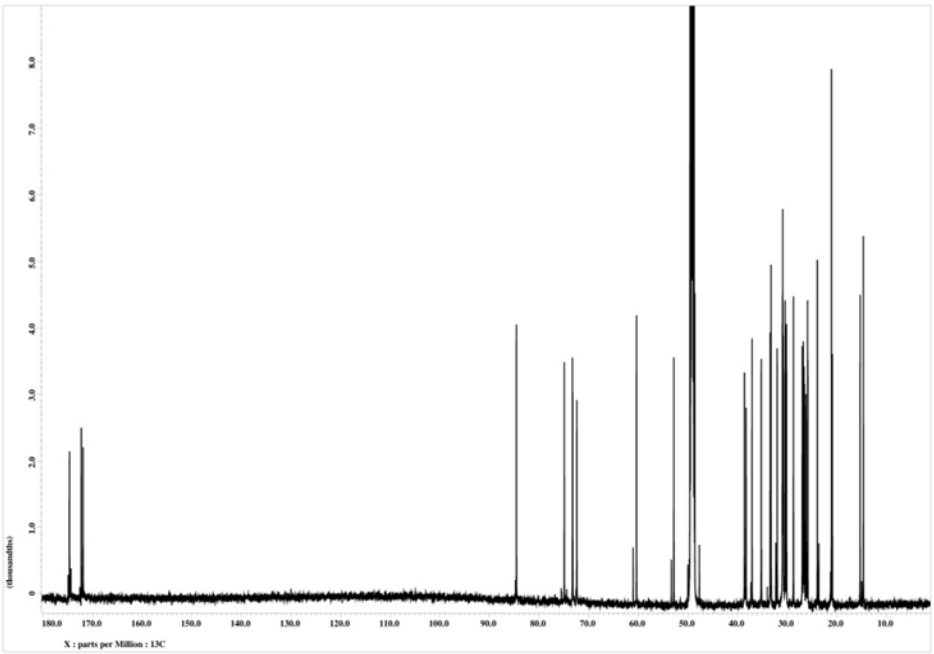

Figure S3-20. ^{13}C NMR spectrum of compound C (**3-3**) in CD_3OD.

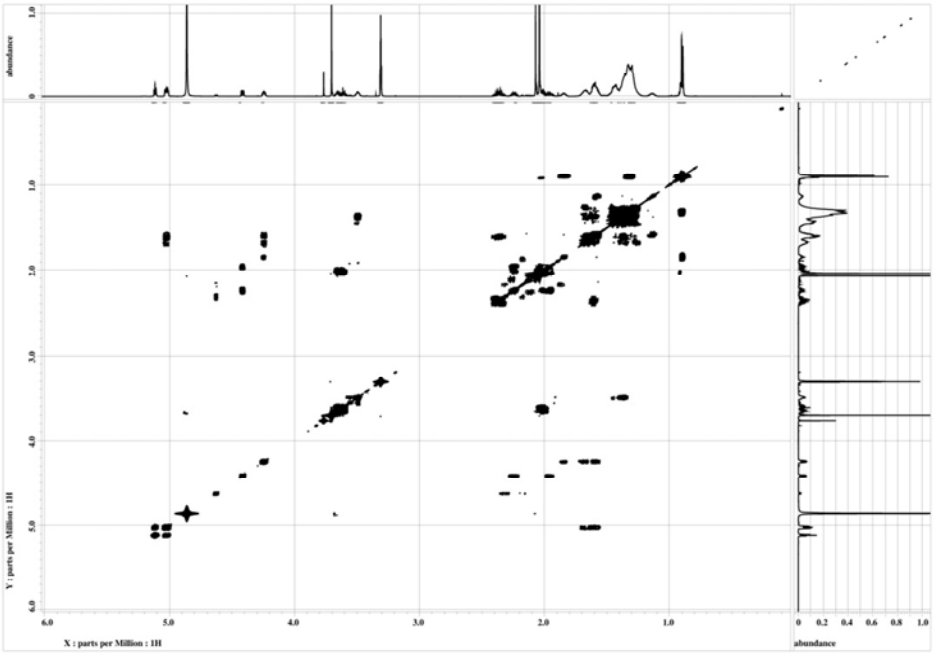

Figure S3-21. COSY spectrum of compound C (**3-3**) in CD_3OD.

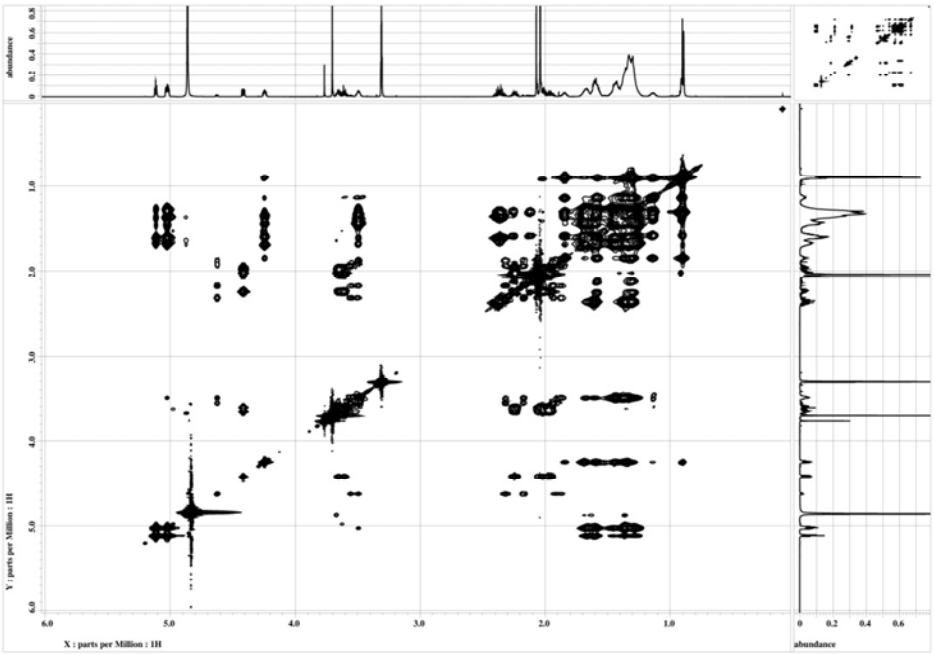

Figure S3-22. TOCSY spectrum of compound C (**3-3**) in CD_3OD.

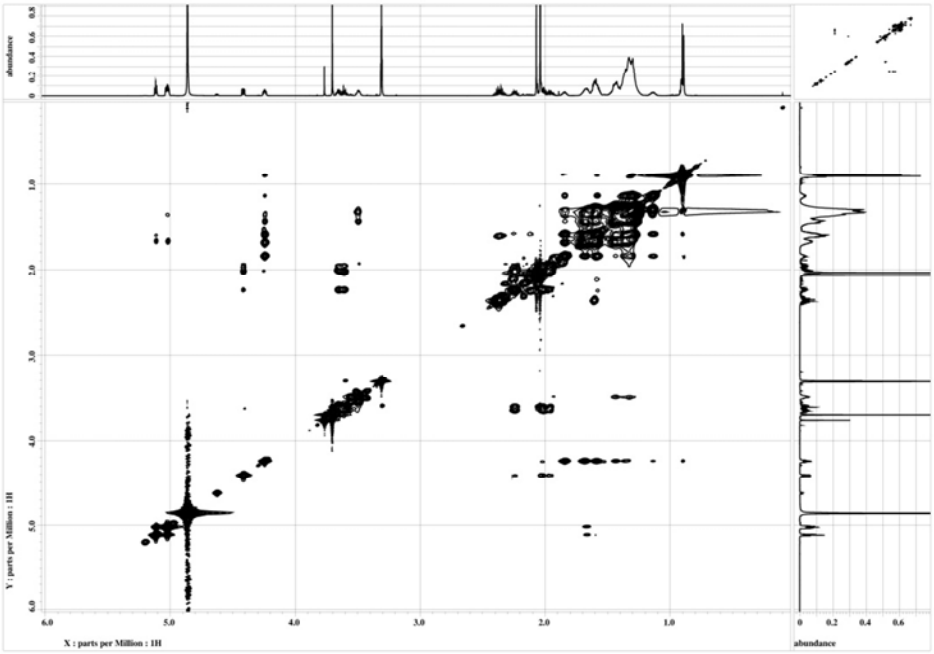

Figure S3-23. ROESY spectrum of compound C (**3-3**) in CD_3OD.

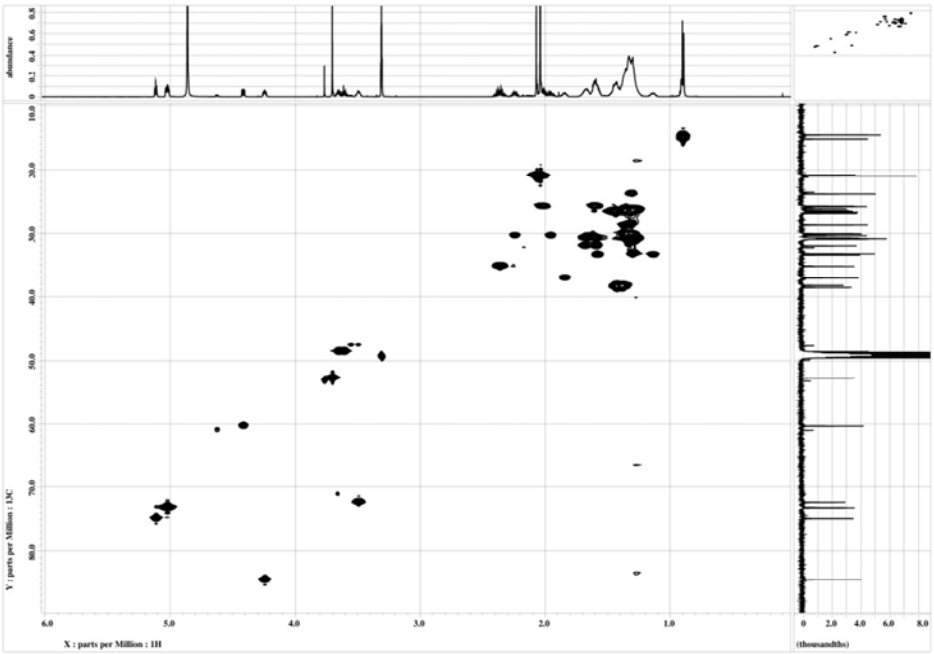

Figure S3-24. HSQC spectrum of compound C (**3-3**) in CD_3OD.

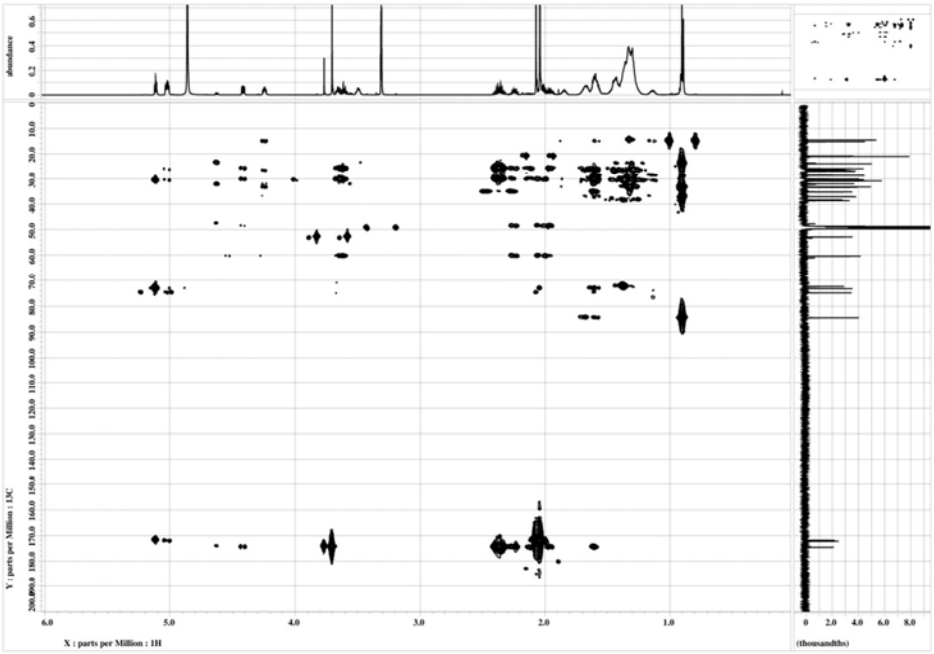

Figure S3-25. HMBC spectrum of compound C (**3-3**) in CD_3OD.

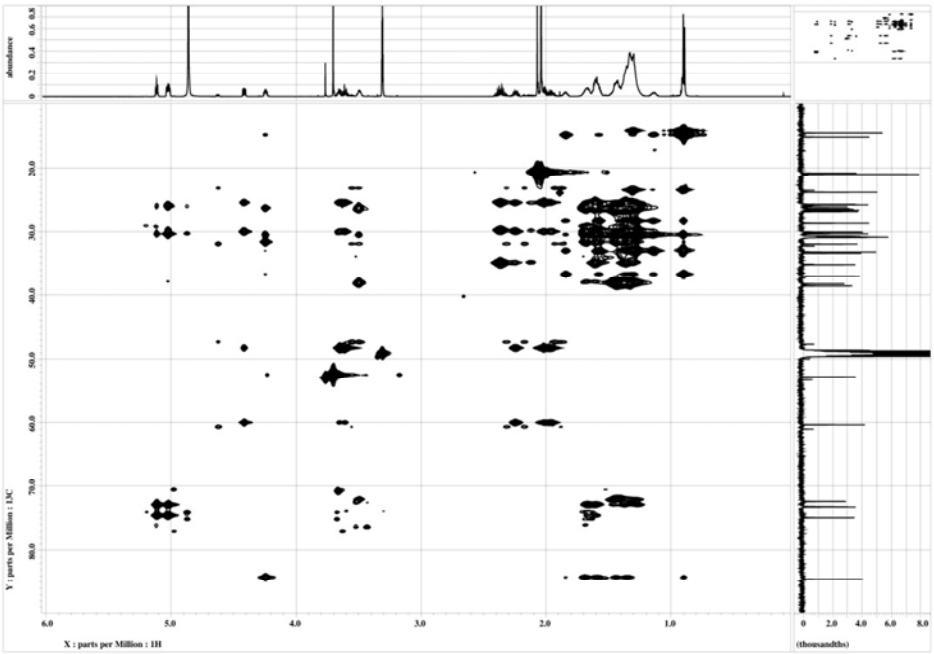

Figure S3-26. HSQC-TOCSY spectrum of compound C (**3-3**) in CD_3OD.

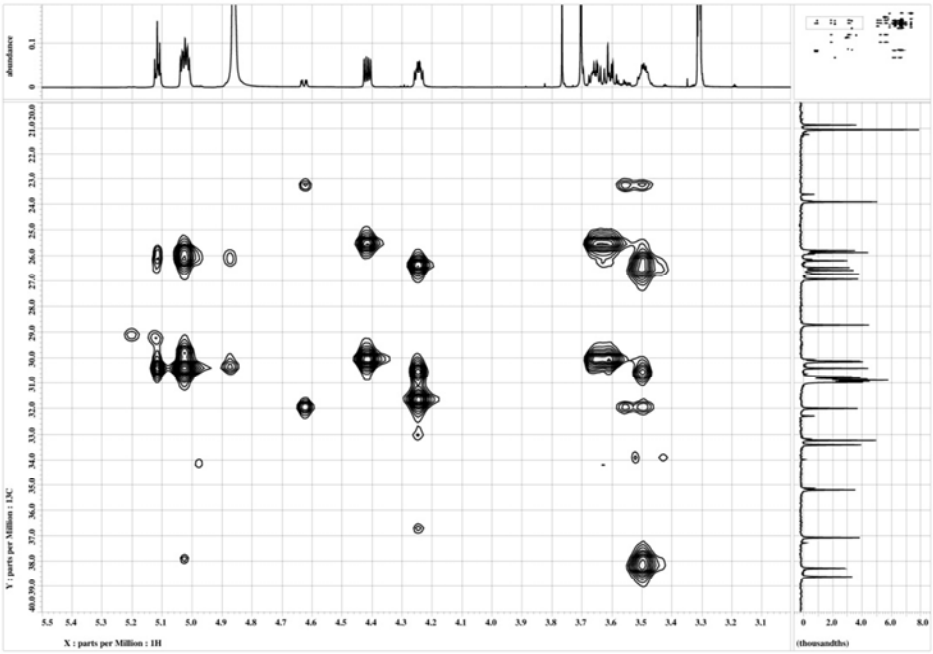

Figure S3-27. Partial HSQC-TOCSY spectrum of compound C (**3-3**) in CD_3OD.

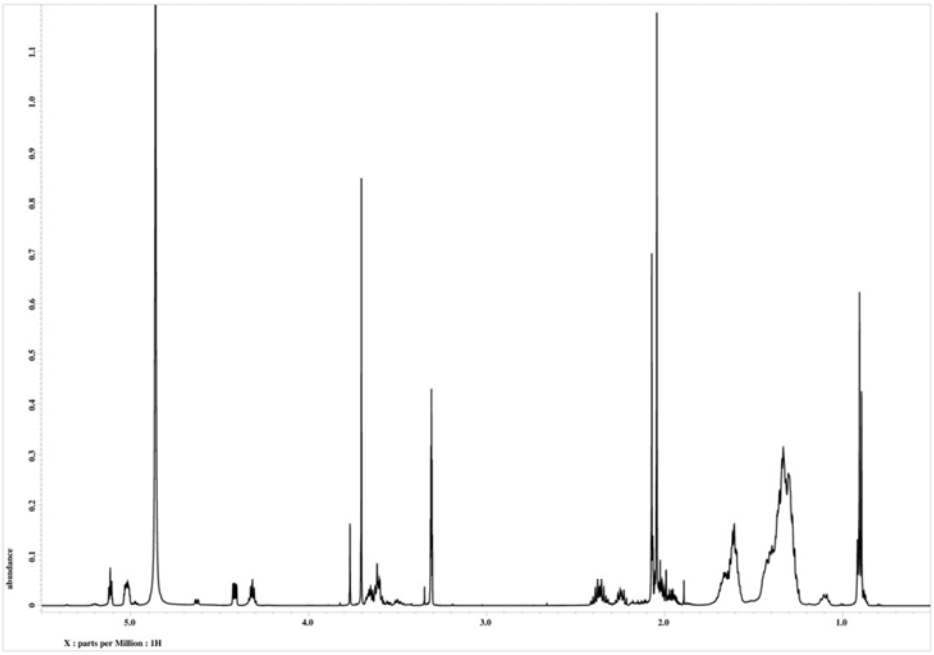

Figure S3-28. ^1H NMR spectrum of compound D (**3-4**) in CD_3OD.

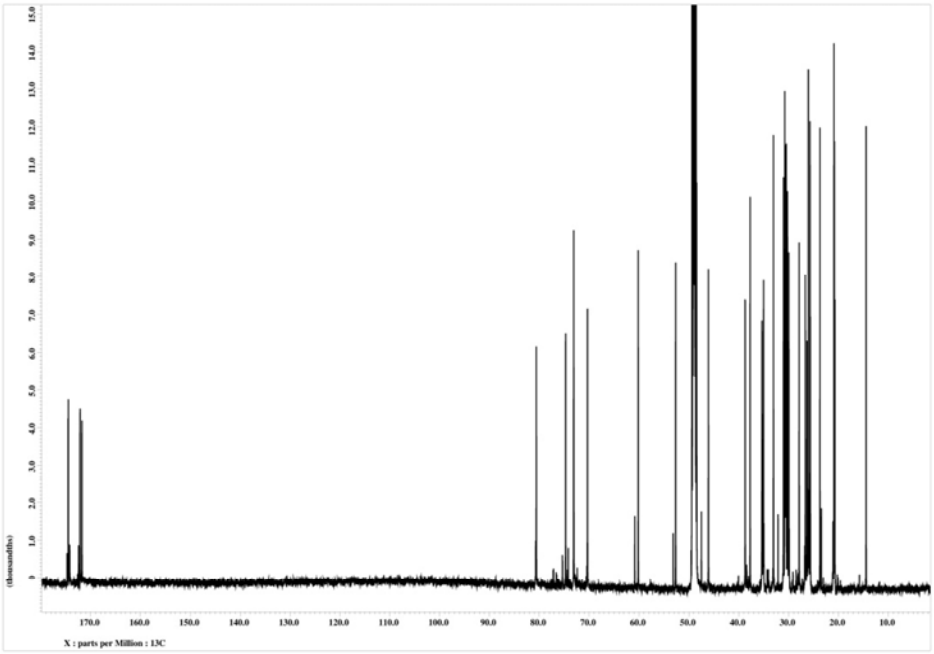

Figure S3-29. ^{13}C NMR spectrum of compound D (**3-4**) in CD_3OD.

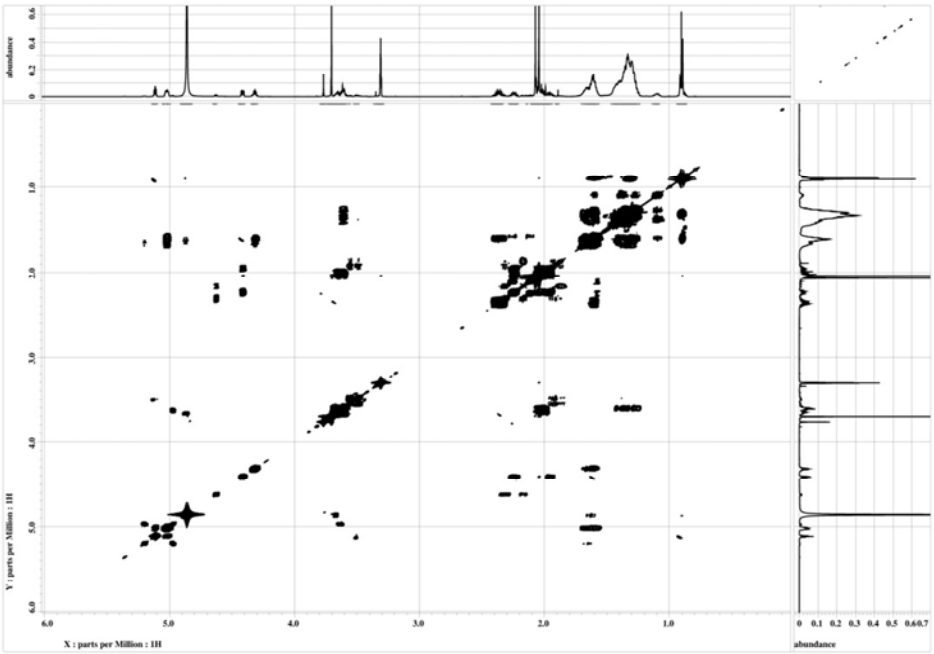

Figure S3-30. COSY spectrum of compound D (**3-4**) in CD_3OD.

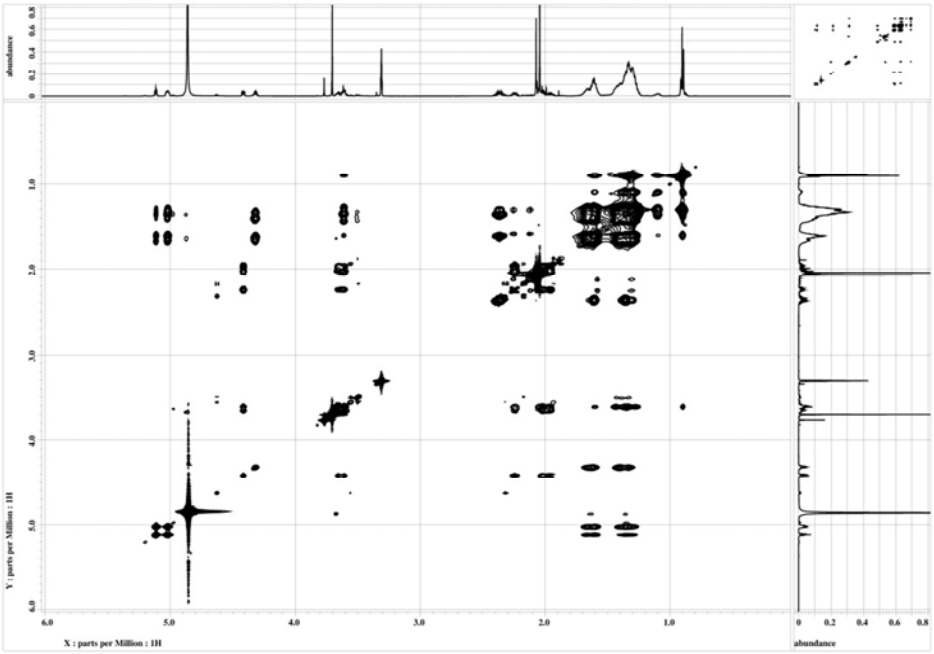

Figure S3-31. TOCSY spectrum of compound D (**3-4**) in CD_3OD.

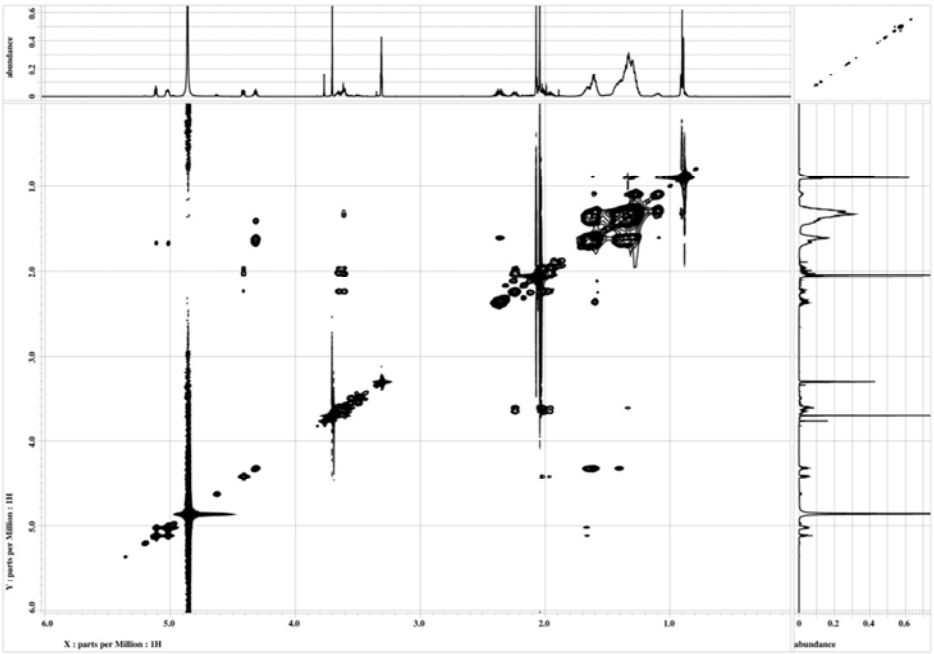

Figure S3-32. ROESY spectrum of compound D (**3-4**) in CD_3OD.

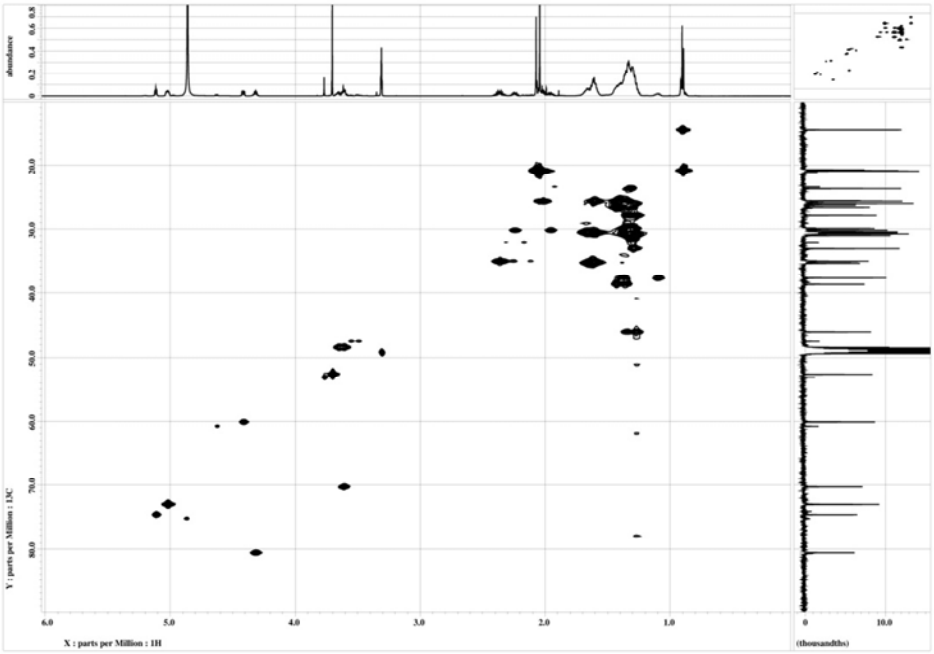

Figure S3-33. HSQC spectrum of compound D (**3-4**) in CD_3OD.

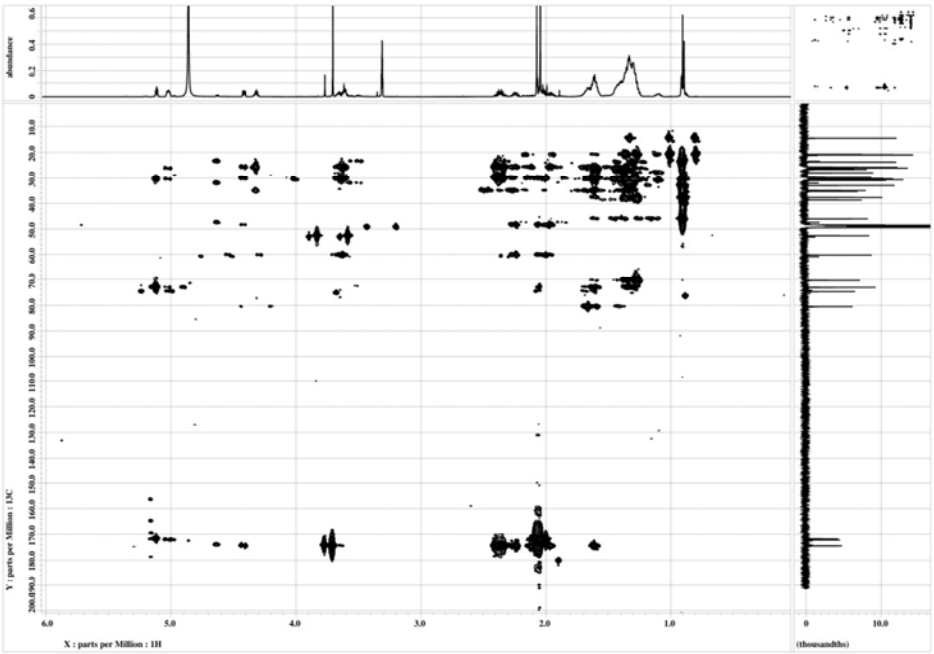

Figure S3-34. HMBC spectrum of compound D (**3-4**) in CD_3OD.

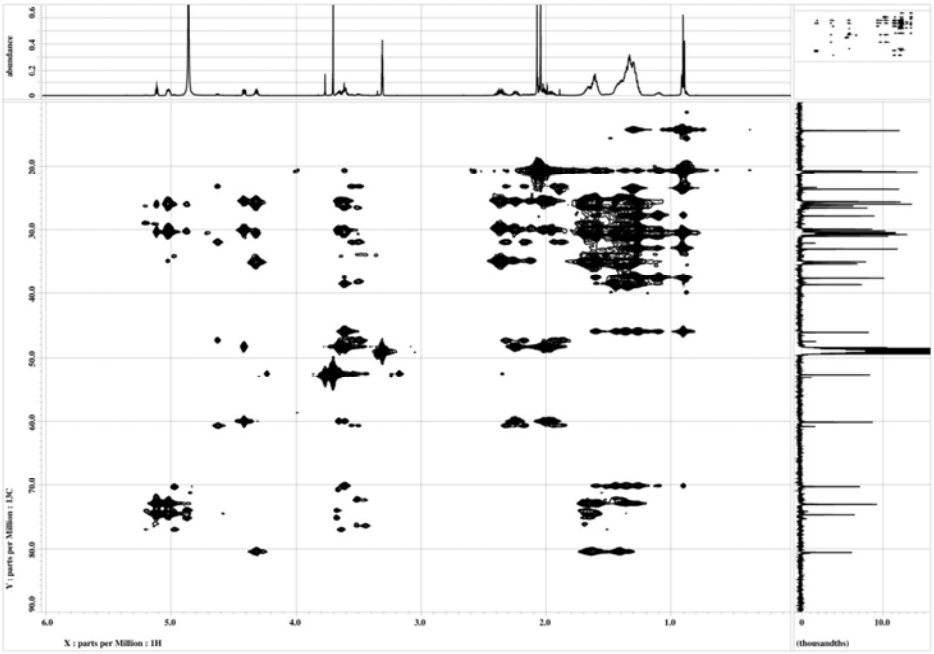

Figure S3-35. HSQC-TOCSY spectrum of compound D (**3-4**) in CD_3OD.

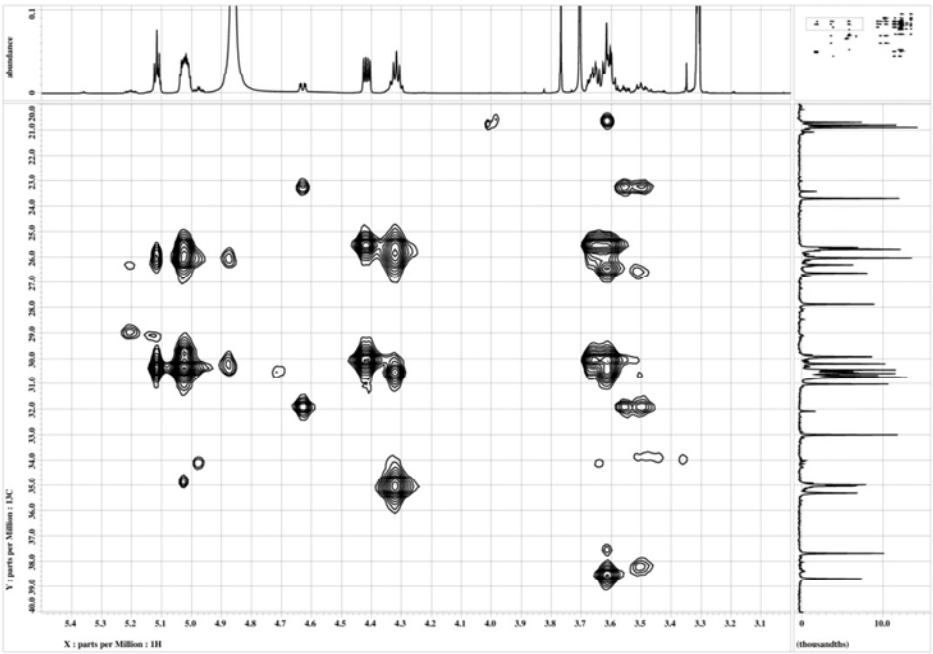

Figure S3-36. Partial HSQC-TOCSY spectrum of compound D (**3-4**) in CD_3OD.

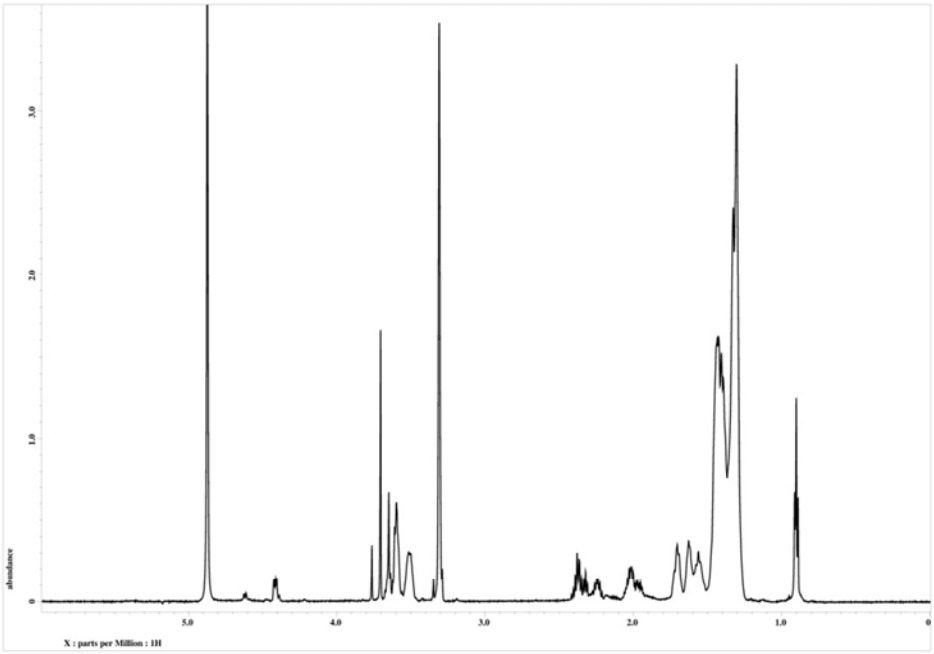

Figure S3-37. ^{1}H NMR spectrum of acid hydrolysate **3-5** in CD_3OD.

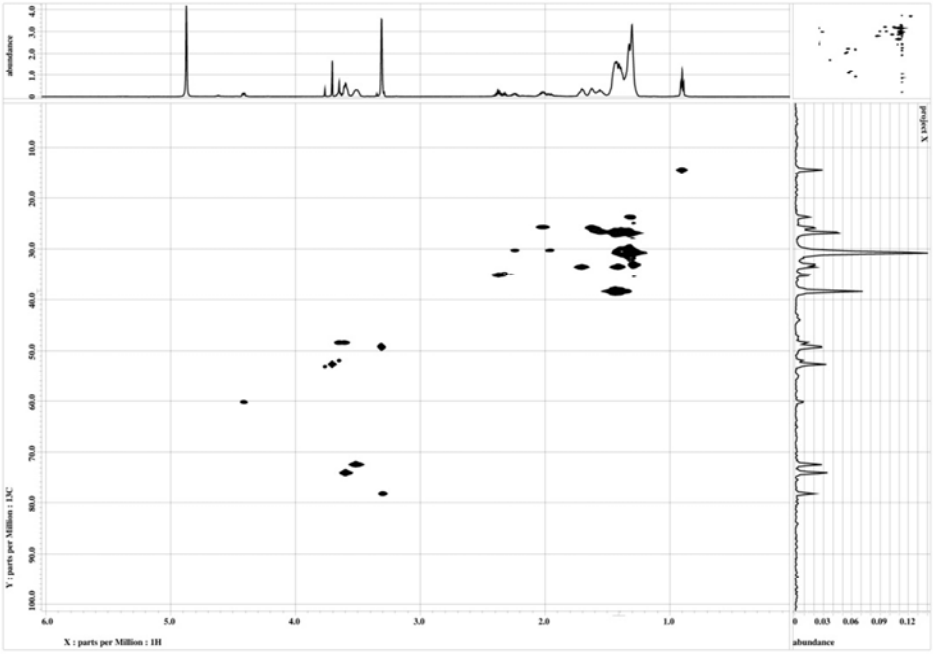

Figure S3-38. HSQC spectrum of acid hydrolysate **3-5** in CD_3OD.

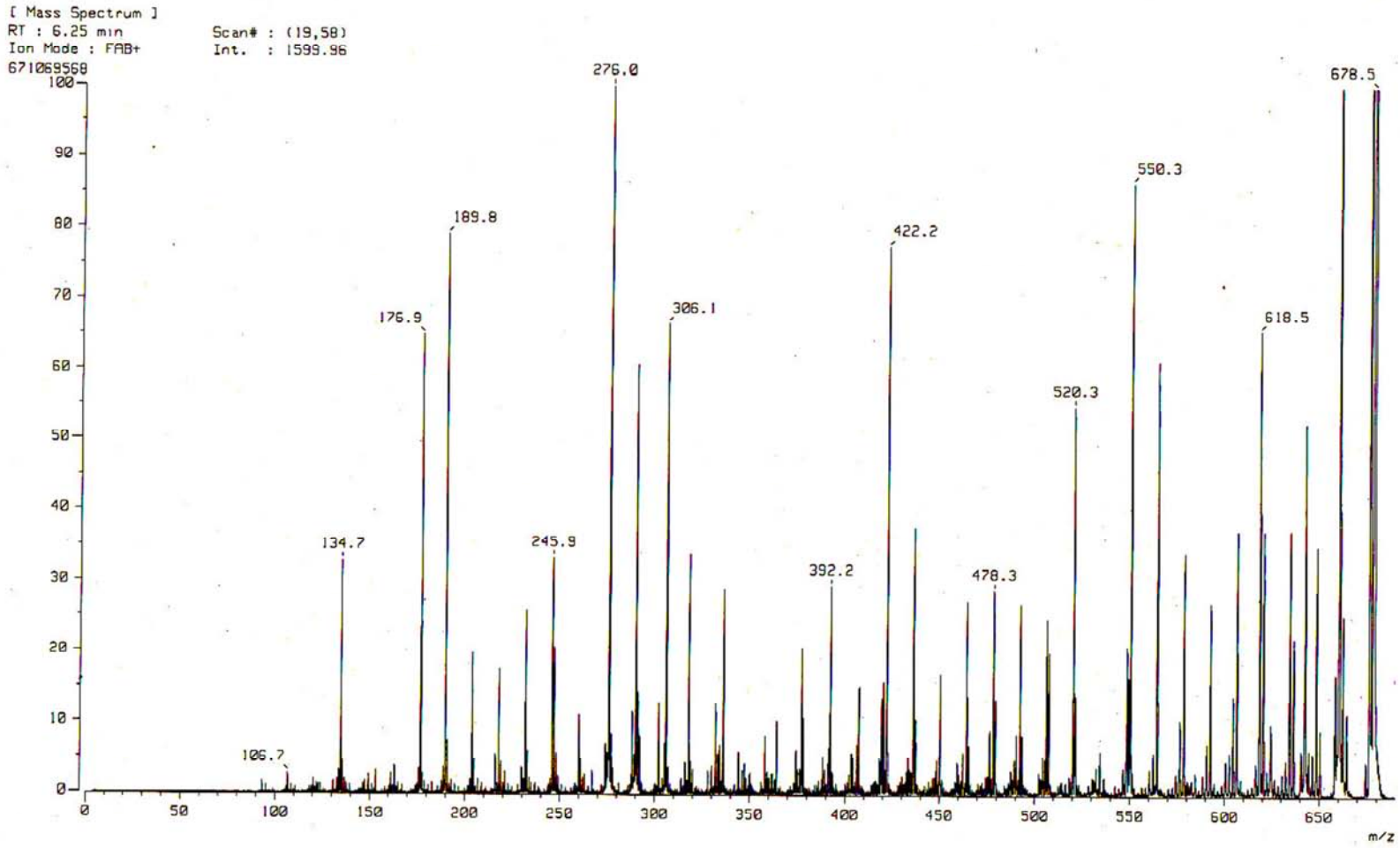

Figure S3-39. FAB-MS/MS data for **3-5**.

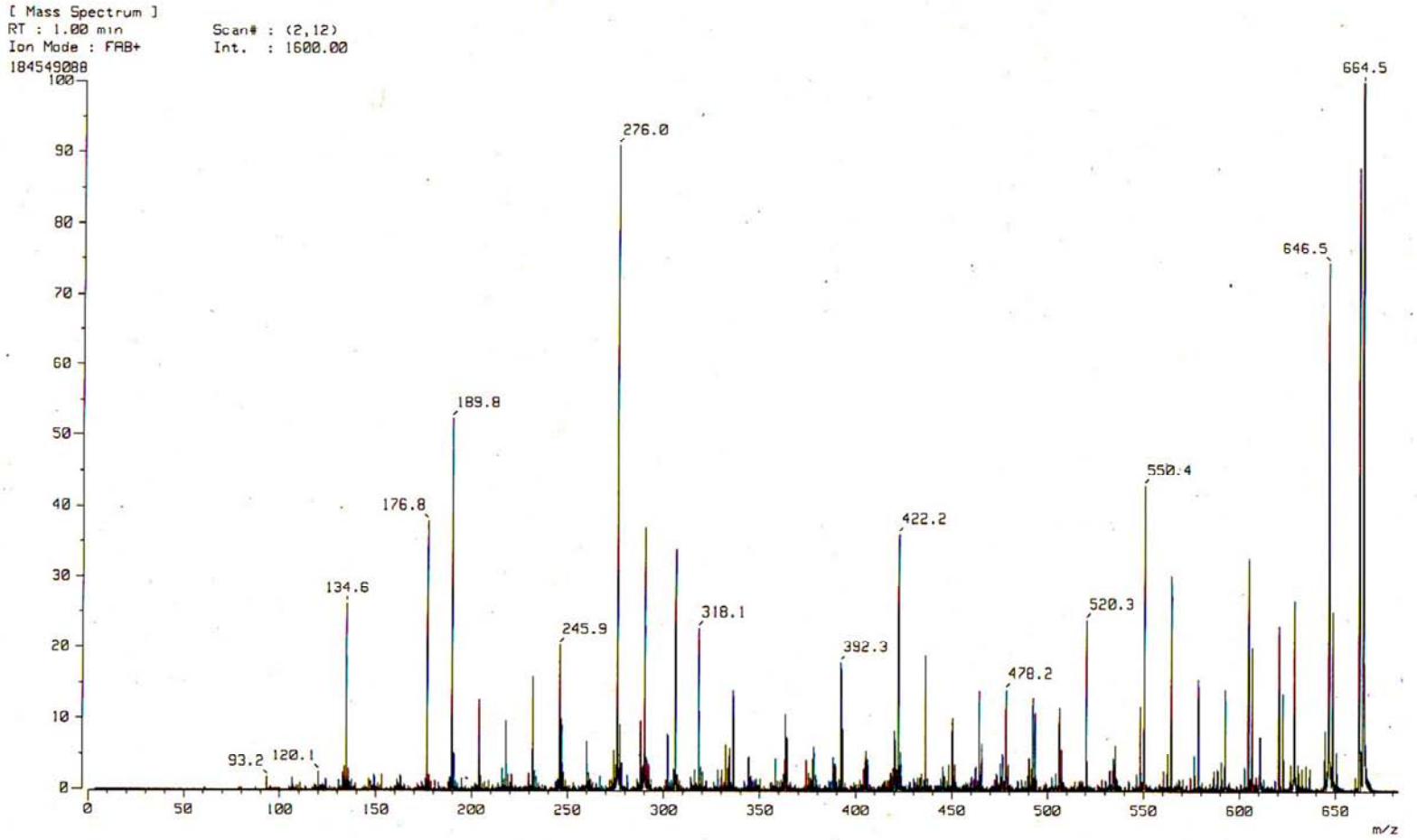

Figure S3-40. FAB-MS/MS data for **3-6**.

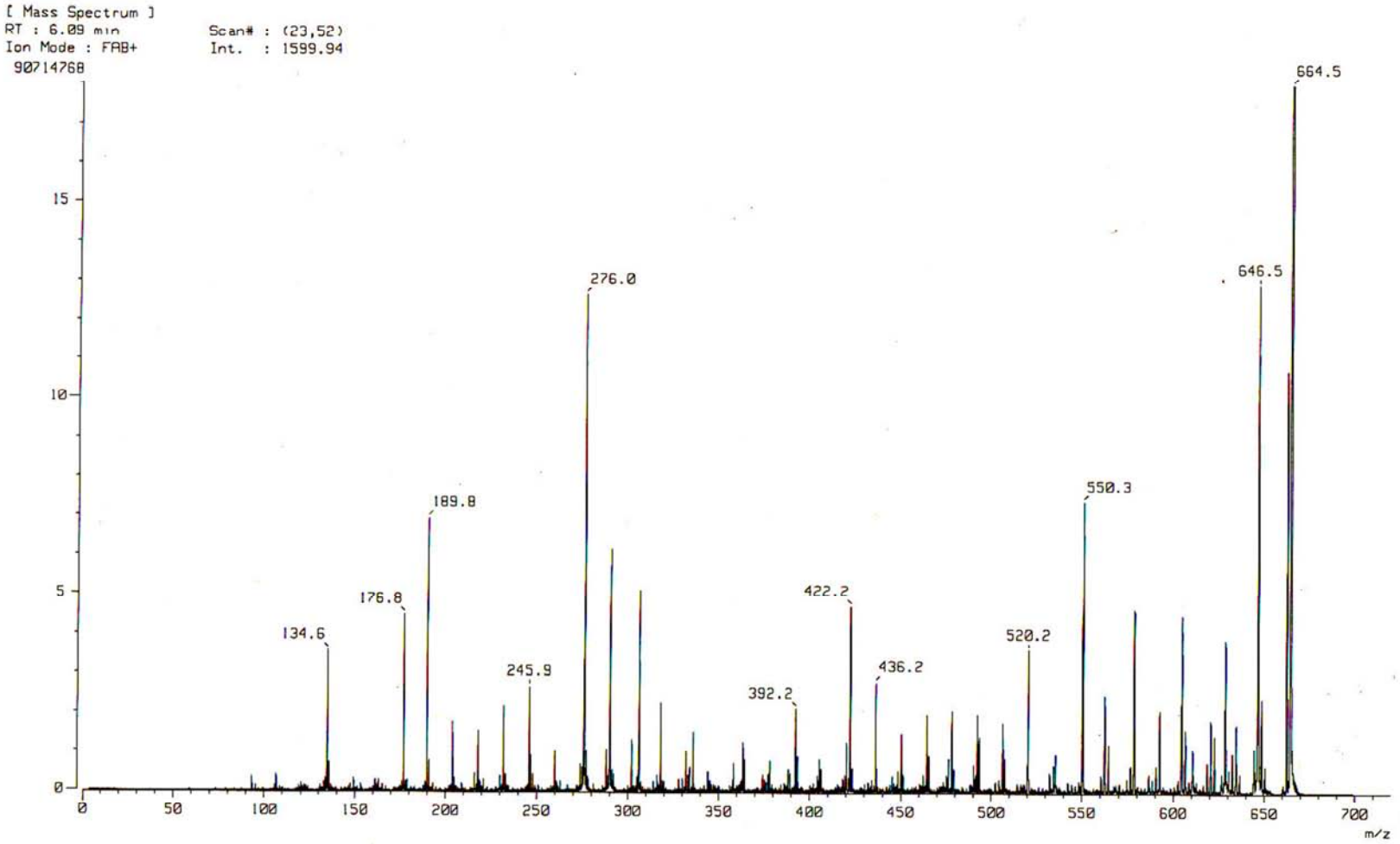

Figure S3-41. FAB-MS/MS data for **3-7**.

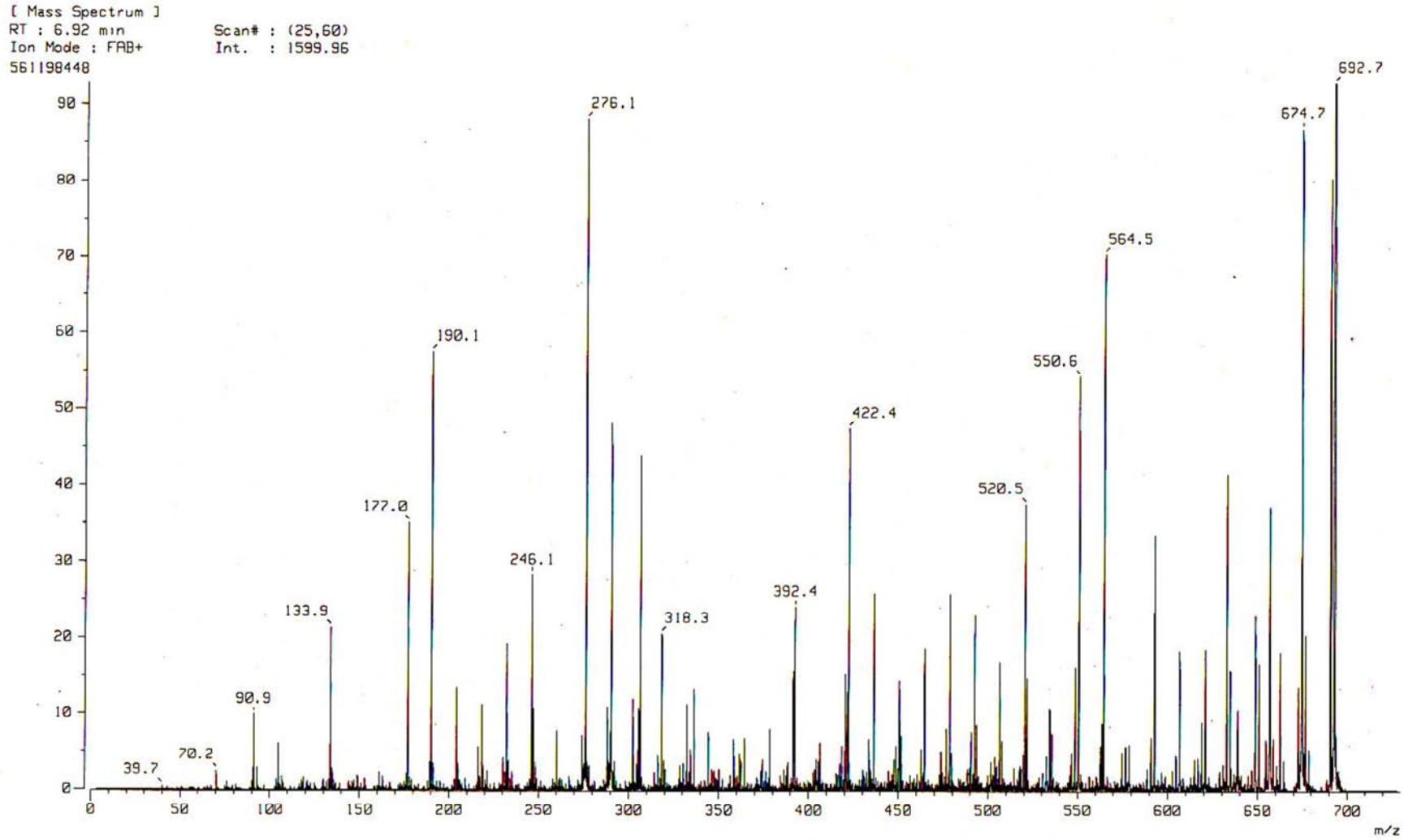

Figure S3-42. FAB-MS/MS data for **3-8**.

Table S3-1.[55] ^{13}C Chemical Shift Values of 1,5,6,7-Decanetetraol (**3-9a**–**3-9d**)

in CD_3OD

Position	**3–9a** ααα SS	**3–9b** αβα AA	**3–9c** ααβ SA	**3–9d** αββ AS
5	73.513	73.975	71.495	72.731
6	76.660	78.291	76.926	76.903
7	73.308	73.801	72.580	71.116

Table S3-2.[55] ^{1}H Chemical Shift Values of 1,5,6,7-Decanetetraol (**3-9a**–**3-9d**)

in CD_3OD

Position	**3–9a** ααα SS	**3–9b** αβα AA	**3–9c** ααβ SA	**3–9d** αββ AS
5	3.64	3.59	3.81	3.59
6	3.20	3.29	3.15	3.15
7	3.64	3.59	3.61	3.82

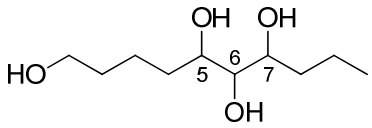

3-9

Conclusions

This study was set out to discover novel tumor-associated enzyme inhibitors from marine sponges and led to the isolation and structure elucidation of three types of the new compounds.

Chapter I described the isolation, structure elucidation, and cathepsin B inhibitory activity of novel isoquinolines, jasisoquinolines A (**1-1**) and B (**1-2**). Jasisoquinolines are the first examples of natural products containing the amide form of 5-(2-aminoethyl)resorcinol.

Chapter II dealt with the isolation and structure elucidation of a new lipopeptide ciliatamide D (**2-1**), and the detailed investigation of the absolute configuration of the known compound ciliatamide A (**2-2**).

Chapter III illustrates the isolation, planar structure elucidation, and HDAC1 inhibitory activity of four new compounds (**3-1**–**3-4**).

The isolated compounds in Chapter I and III are all sulfated. Sulfated compounds are often obtained from marine organisms.[58] Sulfated compounds may be architecturally interesting and therefore challenging to determine the structures, but usually considered to be "nuisance compounds" because they exhibit non-specific enzyme inhibitory activity;[59] schulzeines A (**1-3**) and C (**1-4**) showed inhibitory activities against cathepsin B as well as α-glucosidase.[39] In respect of seeking for specific enzyme inhibitors from marine organisms, avoiding the nuisance compounds is a future challenge to overcome.

The present study demonstrated that marine sponges are excellent sources of compounds with unprecedented structures and potent activities against tumor-associated enzymes. I hope that this study will lead to new antitumor drug development.

References

1. Newman, D. J.; Cragg, G. M. *J. Nat. Prod.* **2007**, *70*, 461–477.
2. Paterson, I.; Anderson, E. A. *Science* **2005**, *310*, 451–453.
3. Li, J. W.-H.; Vederas, J. C. *Science* **2009**, *325*, 161–165.
4. Koehn, F. E.; Carter G. T. *Nat. Rev. Drug Discov.* **2005**, *4*, 206–220.
5. (a) Mayer, A. M. S.; Glaser, K. B.; Cuevas, C.; Jacobs, R. S.; Kem, W.; Little, R. D.; McIntosh, J. M.; Newman, D. J.; Potts, B. C.; Shuster, D. E. *Trends In Pharmacol. Sci.* **2010**, *31*, 255–265. (b) Gerwick, W. H.; Moore, B. S. *Chem. Biol.* **2012**, *19*, 85–98.
6. Molinski, T. F.; Dalisay, D. S.; Lievens, S. L.; Saludes, J. P. *Nat. Rev. Drug Discov.* **2009**, *8*, 69–85.
7. Olivera, B. M. ω-Conotoxin MVIIA: from marine snail venom to analgesic drug. In *Drugs from the Sea*; Fusetani, N., Ed; Karger, 2000, pp. 75–85.
8. Olivera, B. M.; Cruz, L. J.; De Santos, V.; LeCheminant, G.; Griffin, D.; Zeikus, R.; McIntosh, J. M.; Galyean, R.; Varga, J. *Biochemistry* **1987**, *26*, 2086–2090.
9. Rinehart, K. L.; Holt, T. G.; Fregeau, N. L.; Stroh, J. G.; Keifer, P. A.; Sun, F.; Li, L. H.; Martin, D. G. *J. Org. Chem.* **1978**, *43*, 3454–3457.
10. Verweji, J. *J. Clin. Oncol.* **2009**, *27*, 3085–3087.
11. Zewail-Foote, M.; Hurley, L. H. *J. Am. Chem. Soc.* **2001**, *123*, 6485–6495.
12. Hirata, Y.; Uemura, D. *Pure & Appl. Chem.* **1986**, *58*, 701–710.
13. Yu, M. J.; Littlefield, B. A.; Kishi, Y. Discovery of E7389, a Fully Synthetic Macrocyclic Ketone Analog of Halichondrin B. In *Anticancer Agents from Natural*

Products; Cragg, G. M.; Kingstone, D. G. I.; Newman, D. J., Eds; CRC Press: Boca Raton, 2005, pp. 241–265.

14. Kuznetsov, G.; Towle, M. J.; Cheng, H.; Kawamura, T.; TenDyke, K.; Liu, D.; Kishi, Y.; Yu, M. J.; Littlefield, B. A. *Cancer Res*. **2004**, *64*, 5760–5766.
15. Rosa, D. D.; Ismael, G.; Lago, L. D.; Awada, A. *Cancer Treat*. *Rev*. **2008**, *34*, 61–80.
16. Sledge, G. W. *J*. *Clin*. *Oncol*. **2005**, *23*, 1614–1615.
17. Swinney, D. C.; Anthony, J. *Nat*. *Rev*. *Drug Discov*. **2011**, *10*, 507–519.
18. Manson, S. D.; Joyce, J. A. *Trends Cell Biol*. **2011**, *21*, 228–237.
19. (a) Jedeszko, C.; Sloane, B. F. *Biol*. *Chem*. **2004**, *385*, 1017–1027. (b) Mohamed, M. M.; Sloane, B. F. *Nat*. *Rev*. *Cancer* **2006**, *6*, 764–775. (c) Gocheva, V.; Joyce, J. A. *Cell Cycle* **2007**, *6*, 60–64.
20. Buck, M. R.; Karustis, D. G.; Day, N. A.; Honn, K. V.; Sloane, B. F. *Biochem*. *J*. **1992**, *282*, 273–278.
21. Gocheva, V.; Zeng, W.; Ke, D.; Klimstra, D.; Reinheckel, T.; Peters, C.; Hanahan, D. Joyce, J. A. *Genes Dev*. **2006**, *20*, 543–556.
22. Eeckhout, Y.; Vaes, G. *Biochem*. *J*. **1977**, *166*, 21–31.
23. Nalla, A. K.; Gorantla, B.; Gondi, C. S.; Lakka, S. S.; Rao, J. S. *Cancer Gene Ther*. **2010**, *17*, 599–613.
24. (a) Roth S. Y.; Denu, J. M.; Allis, C. D. *Annu*. *Rev*. *Biochem*. **2001**, *70*, 81–120. (b) Thiagalingam, S.; Cheng, K.-H.; Lee, H. J.; Mineva, N.; Thiagalingam, A.; Ponte, J. F. *Ann*. *NY Acad*. *Sci*. **2003**, *983*, 84–100.
25. (a) Witt, O.; Deubzer, H. E.; Milde, T.; Oehme, I. *Cancer Lett*. **2009**, *277*, 8–21. (b) Balasubramanian, S.; Verner, E.; Buggy, J. J. *Cancer Lett*. **2009**, *280*, 211–221.
26. Taunton, J.; Hassig, C. A.; Schreiber, S. L. *Science* **1996**, *272*, 408–411.

27. (a) Weichert, W.; Roske, A.; Gekeler, V.; Beckers, T.; Ebert, M. P.; Pross, M.; Dietel, M.; Denkert, C. *Lancet Oncol*. **2008**, *9*, 139–148. (b) Weichert, W.; Roske, A.; Gekeler, V.; Beckers, T.; Stephan, C.; Jung, K.; Fritzsche, F. R.; Niesporek, S.; Denkert, C.; Dietel, M.; Kristiansen, G. *Br*. *J*. *Cancer* **2008**, *98*, 604–610. (c) Weichert, W.; Roske, A; Niesporek, S.; Noske, A.; Buckendahl, A. C.; Dietel, M.; Gekeler, V.; Boehm, M.; Beckers, T; Denkert, C. *Clin*. *Cancer Res*. **2008**, *14*, 1669–1677.

28. Inoue, S.; Mai, A.; Dyer M. J.; Dohen, G. M. *Cancer Res*. **2006**, *66*, 6785–6792.

29. Keshelava, N.; Davicioni, E.; Wan, Z.; Ji, L.; Sposta, R.; Triche, T. J.; Reynolds, C. P. *J*. *Natl*. *Cancer Inst*. **2007**, *99*, 1107–1119.

30. Senese, S.; Zaragoza, K.; Minardi, S.; Muradore, I.; Ronzoni, S.; Passaforo, A.; Bernard, L.; Draetta, G. F.; Alcalay, M.; Setser, C.; Chiocca, S. *Mol*. *Cell Biol*. **2007**, *27*, 4784–4795.

31. Glaser, K. B.; Li, J.; Staver, M. J.; Wei, R. Q.; Albert, D. H.; Davidsen, S. K. *Biochem*. *Biophys*. *Res*. *Commun*. **2003**, *310*, 529–536.

32. (a) Minucci, S.; Pelicci, P. G. *Nat*. *Rev*. *Cancer* **2006**, *6*, 38–51. (b) Bolden, J. E.; Peart, M. J.; Johnstone, R. W. *Nat*. *Rev*. *Drug*. *Discov*. **2006**, 5, 769–784. (c) Smith, K. T.; Workman, J. L. *Int*. *J*. *Biochem*. *Cell Biol*. **2009**, *41*, 21–25. (d) Khan, O.; La Thangue, N. B. *Immunol*. *Cell Biol*. **2012**, *90*, 85–94.

33. Grant, S.; Easley, C.; Kirkpatrick, P. *Nature Rev*. *Drug Discov*. **2007**, *6*, 21–22.

34. Finnin, M. S.; Donigian, J. R.; Cohen, A.; Richon, V. M.; Rifkind, R. A.; Marks, P. A.; Breslow, R.; Pavletich, N. P. *Nature* **1999**, *401*, 188–193.

35. (a) Ueda, H.; Nakajima, H.; Hori, Y.; Fujita, T.; Nishimura, M.; Goto, T.; Okuhara, M. *J*. *Antibiot*. **1994**, *47*, 301–310. (b) Shigematsu, N.; Ueda, H.; Takase, S.; Tanaka,

H. *J. Antibiot*. **1994**, *47*, 311–314. (c) Ueda, H.; Manda, T.; Matsumoto, S.; Mukumoto, S.; Nishigaki, F.; Kawamura, I.; Shimomura, K. *J. Antibiot*. **1994**, *47*, 315–323.

36. Ueda, H.; Nakajima, H.; Hori, Y.; Goto, T.; Okuhara, M.; *Biosci*. *Biotechnol*. *Biochem*. **1994**, *58*, 1579–1583.
37. Furumai, R.; Matsuyama, A.; Kobashi, N.; Lee, K.-H.; Nishimura, M.; Nakajima, H.; Tanaka, A.; Komatsu, Y.; Nishino, N.; Yoshida, M.; Horinouchi, S. *Cancer Res*. **2002**, *62*, 4916–4921.
38. Shah, M. H.; Binkley, P.; Chan, K.; Xiao, J.; Arbogast, D.; Collamore, M.; Farra, Y.; Young, D.; Grever, M. *Clin*. *Cancer Res*. **2006**, *12*, 3997–4003.
39. Takada, K.; Uehara, T.; Nakao, Y.; Matsunaga, S.; van Soest, R. W. M.; Fusetani, N. *J*. *Am*. *Chem*. *Soc*. **2004**, *126*, 187–193.
40. Bowen, E. G.; Wardrop, D. J. *J*. *Am*. *Chem*. *Soc*. **2009**, *131*, 6062–6063.
41. (a) Kushi, Y.; Honda, S.; Ishizuka, I. *J*. *Biochem*. *(Tokyo)* **1985**, *97*, 419–428. (b) Murata, M.; Naoki, H.; Matsunaga, S.; Satake, M.; Yasumoto, T. *J*. *Am*. *Chem*. *Soc*. **1994**, *116*, 7098–7107.
42. Singh, S. B.; *Tetrahedron Lett*. **2000**, *41*, 6973–6976.
43. Ohtani, I.; Kusumi, T.; Kashman, Y.; Kakisawa, H. *J*. *Am*. *Chem*. *Soc*. **1991**, *113*, 4092–4096.
44. (a) Oikawa, H.; Matsuda, I.; Kagawa, T.; Ichikawa, A.; Kohmoto, K. *Tetrahedron* **1994**, *50*, 13347–13368. (b) Eguchi T.; Kobayashi, K.; Uesaka, H.; Ohashi, Y.; Mizoue, K. Matsushima, Y.; Kakinuma, K. *Org*. *Lett*. **2002**, *4*, 3383–3386.

45. Nakanishi, K.; Berova, N. In *Circular Dichroism, Principles and applications*; Nakanishi, K., Berova, N., Woody, R. W., Eds;VCH Publishers, Inc.: New York, 1994; Chapter 13.

46. (a) Snatzke, G.; Ho, P. C. *Tetrahedron* **1971**, *27*, 3645–3653. (b) Snatzke, G.; Kajtár M.; Werner-Zamojska, F. *Tetrahedron* **1972**, *28*, 281–288. (c) Snatzke, G.; Kajtár M.; Snatzke, F. In *Fundamental Aspects and Recent Developments in Optical Rotatory Dispersion and Circular Dichroism*; Ciardelli, F., Salvadori, P. Eds; Heyden: London, 1973; Chapter 3.4. (d) Toda, J.; Matsumoto, S.; Saitoh, T.; Sano, T. *Chem. Pharm. Bull*. **2000**, *48*, 91–98.

47. Kerti, G.; Kurtán, T.; Illyes, T.-Z.; Kövér, K. E., Sólyom, S.; Pescitelli, G.; Fujioka, N.; Berova, N.; Antus, S. *Eur*. *J*. *Org*. *Chem*. **2007**, *2007*, 296–305.

48. (a) Bringmann, G.; Wohlfarth, M.; Rischer, H.; Grüne, M.; Schlauer, J. *Angew*. *Chem*., *Int*. *Ed*. *Engl*. **2000**, *39*, 1464–1466. (b) Bringmann, G.; Irmer, A.; Feineis, D.; Gulder, T. A. M.; Fiedler, H.-P. *Phytochemistry* **2009**, *70*, 1776–1786.

49. Hiwasa, T.; Fujita-Yoshigaki, J.; Shirouzu, M.; Koide, H.; Sawada, T.; Sakiyama, S.; Yokokawa, S. *Cancer Lett*. **1993**, *69*, 161–165.

50. Nakao, Y.; Kawatsu, S.; Okamoto, C.; Okamoto, M.; Matsumoto, Y.; Matsunaga, S.; van Soest, R. W. M.; Fusetani, N. *J*. *Nat*. *Prod*. **2008**, *71*, 469–472.

51. Lewis, J. A.; Nathan Daniels, R.; Lindsley, C. W. *Org*. *Lett*. **2008**, *10*, 4545–4548.

52. (a) Harrigan, G. G.; Luesch, H.; Yoshida, W. Y.; Moore, R. E.; Nagle, D. G.; Paul, V. J. *J*. *Nat*. *Prod*. **1999**, *62*, 655–658. (b) Nogle, L. M.; Williamson, R. T.; Gerwick, W. H. *J*. *Nat*. *Prod*. **2001**, *64*, 716–719. (c) Matthew, S.; Ross, C.; Paul, V. J.; Luesch, H. *Tetrahedron* **2008**, *64*, 4081–4089.

53. (a) Marfey, P. *Carlsberg Res. Commun*. **1984**, *49*, 591–596. (b) Bhushan, R.; Brückner, H. *Amino Acids* **2004**, *27*, 231-247.

54. (a) Dorman, D. E.; Borvey, F. A. *J. Org. Chem*. **1973**, *38*, 1719–1722. (b) Dorman, D. E.; Borvey, F. A. *J. Org. Chem*. **1973**, *38*, 2379–2383. (c) Siemion, I. Z.; Wieland, T.; Pook, K. H. *Angew. Chem., Int. Ed. Engl*. **1975**, *14*, 702. (d) Whitson, E. L.; Ratnayake, A. S.; Bugni, T. S.; Harper, M. K.; Ireland, C. M. *J. Org. Chem*. **2009**, *74*, 1156–1162. (e) Williams, D. E.; Yu, K.; Behrisch, H. W.; van Soest, R. W. M., Andersen, R. J. *J. Nat. Prod*. **2009**, *72*, 1253–1257.

55. Higashibayashi, S.; Czechtizky, W.; Kobayashi, Y.; Kishi, Y. *J. Am. Chem. Soc*. **2003**, *125*, 14379–14393.

56. Nakao, Y.; Maki, T.; Matsunaga, S.; van Soest, R. W. M.; Fusetani, N. *Tetrahedron* **2000**, *56*, 8977–8987.

57. Nakao, Y.; Maki, T.; Matsunaga, S.; van Soest, R. W. M.; Fusetani, N. *J. Nat. Prod*. **2004**, *67*, 1346–1350.

58. Kornprobst, J. -M.; Sallenave, C.; Barnathan, G. *Comp. Biochem. Physiol. B* **1998**, *119*, 1–51.

59. Nakao, Y.; Fusetani, N. *J. Nat. Prod*. **2007**, *70*, 689–710.